MASS TRANSFER AND SOLVENT EFFECTS IN HETEROGENEOUSLY CATALYZED HYDROGENATIONS IN SOLUTIONS

by

Pushpinder Singh PURI

A thesis submitted to the School of Graduate Studies in partial fulfillment of the requirements for the degree of

DOCTOR OF PHILOSOPHY

in the

Department of Chemical Engineering
University of Ottawa

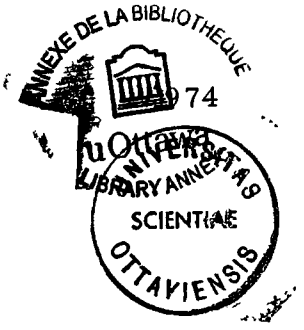

ABSTRACT

The effects of external and internal particle mass transfer resistance, and of solvents on the rate of hydrogenations carried out on finely divided catalysts in slurry reactors are treated.

A method is developed for estimating external particle mass transfer resistance from rate measurements and is demonstrated experimentally. The magnitude of mass transfer resistance of the reactants is determined by calculating the transport factors for the reactions. It is shown that systems that exhibit superficially similar behavior may have their rates controlled by different combinations of diffusion and kinetic resistance. The existence of reactions with negligible internal diffusion and significant external diffusion resistance in slurry reactors is modelled theoretically and demonstrated experimentally.

The heterogeneous hydrogenation of acetone on Raney nickel in the solvents benzene, cyclohexane, and isopropanol is studied at 25°C. It is observed that both the rate and acetone surface concentration increase with the acetone activity coefficient, in comparing the three systems. Neither rate nor the acetone surface concentration could be correlated with the acetone activity coefficient for the three systems, however. The finding that the rank of the "rate" is the same as that of the "acetone adsorbed" tests experimentally the qualitative notion of Wauquier and Jungers that the differences of hydrogenation rates in different solvents are due to differences in adsorption.

ACKNOWLEDGMENTS

The author wishes to express his sincere thanks to Dr. J.A. Ruether for giving generously of his time, advice, guidance and encouragement throughout this investigation. Also discussions with Drs. B.C.-Y. Lu and W. Hayduk are gratefully acknowledged.

Thanks are due to the National Research Council of Canada for providing Post Graduate Scholarship and to the Department of Chemical Engineering for financial and laboratory assistance.

Sincere appreciation is expressed to Mr. G. Gasperetti for assistance in constructing the experimental apparatus and to Mr. H. A. Laudie for assistance in computer programming.

Finally the author wishes to thank all those closest to him for their help and encouragement.

TABLE OF CONTENTS

Page

Page

Page

Page

LIST OF FIGURES

LIST OF TABLES

NOMENCLATURE

NOTATION

a	gas-liquid interfacial area per unit volume of liquid, cm^2/cm^3.
a_p	external particle surface area per unit mass of catalyst, cm^2/g.
A	total interfacial area, cm^2.
A_p	external surface area per particle, cm^2.
$A_{i,j}$, $B_{i,j}$	Van Laar constants in equations (IV-8) and (IV-9).
A, B, C	constants in equation (IV-1).
b	distribution coefficient used in equation (2-5).
b_1	constant defined by equation (III-4).
$B_{i,j}$	Porter equation constant used in equations (IV-4) and (IV-5).
$B_{i,j}$, $C_{i,j}$	Margules equation constants in equation (IV-6) and (IV-7).
C	concentration, mol/l.
C_1, C_2, C_3	constants in equation (IV-2).
C_t	total number of catalyst active sites.
d_p	particle diameter, microns.
D	bulk diffusivity, cm^2/sec.
D_e	effective diffusivity within catalyst particle, cm^2/sec.
f	function of.

$f(\theta)$	defined by equation (II-7.1).
g	accleration due to gravity, cm/sec^2.
$g^E_{i,j}$	excess Gibbs free energy for a mixture of components i and j.
h	Thiele diffusion modulus.
$\hat{h}_n$	normalized Thiele diffusion modulus defined by equation (3-16).
$\bar{h}_n$	Thiele parameter defined by equation (3-25).
H	Henry's law constant, atm^{-1}.
H'	Henry's law constant defined by equation (II-1.2).
k	kinetic rate constant.
K	equilibrium constant.
k_L	gas-liquid mass transfer coefficient, cm/sec.
k_p	particle-liquid mass transfer coefficient, cm/sec.
K'_V	zero order reaction constant based on volume.
m	constant defined by equation (III-11).
M	molecular weight.
n	constant defined by equation (III-10).
N	molar flux, $mol/(sec)\ (cm^2)$.
N_{Gr}	Grashof number, $L^3 \rho^2 \beta g Dt/\mu^2$.
N_{Re}	Reynolds number, $Du\rho/\mu$.
N_{Sc}	Schmidt number, $\mu/\rho D$.

N_{Sh}	Sherwood number, $k_p d_p/D$.
P	pressure, mm Hg, atm.
r	rate of reaction per unit mass of catalyst, mol/(sec) (g Ni).
r_p	rate of reaction per particle, mol/sec.
r_v	rate of reaction per unit volume of liquid, mol/(sec)(l).
r_e	normalized extinction length, used in Appendix I.
R	universal gas constant.
R	mean particle radius, microns.
$\mathscr{R}$	intrinsic reaction rate per unit internal area of catalyst, mol/(sec)(cm^2).
R_D	rate per unit volume of catalyst, mol/(sec) (cm^3).
S	specific surface area per unit mass of catalysts, cm^2/g.
t	time, sec, min, hr.
T	absolute temperature, °K.
u	a constant used in equation (3-7).
U_E	effective velocity arising from velocity gradients in the neighbourhood of particle surface, cm/sec.
U_S	slip velocity arising from the differences in inertia between the particles and the fluid, cm/sec.
U_t	terminal velocity of the particles, cm/sec.
v	slip velocity defined by equation (II-6.2).

V	volume, cm^3, l.
V^o	initial volume of hydrogen read on the burets, cm^3.
$V_{g,s}$	volume of gas dissolved to saturation, cm^3.
W	mass of the catalyst, g. Ni.
x	mole fraction in the liquid phase.

GREEK LETTERS

α	$Sh/12\ \theta\ \bar{h}_o$.
α	defined by equation (III-13).
β	defined by equation (III-14).
γ	activity coefficient in the liquid phase.
η	internal effectiveness factor.
η_D	refractive index.
θ	internal void fraction of catalyst.
μ	viscosity, poise.
ρ	density, g/cm^3.
ρ_p	apparent density of a single catalyst particle.
τ	tortuosity factor
$\mathcal{J}$	transport factor

SUBSCRIPTS

A	substrate, acetone.
A-*	adsorbed acetone.

A-H-*	adsorbed surface complex.
A-2H	product of acetone hydrogenation, isopropanol.
b	bulk liquid or bulk gas.
H	hydrogen.
H-*	adsorbed hydrogen
i	component i.
j	component j.
L	liquid phase.
m	number of components.
M	mixture property.
n	n-th order reaction.
p	particle.
s	particle external surface; solvent; solution.
S-*	adsorbed solvent.
O	zero-order reaction; initial value in case of concentrations.
1	first order reaction; component 1.
*	equilibrium value for concentrations, active catalyst site.

SUMMARY

Objectives of this Study

There are two main objectives of this work. First, to study the mass transfer effects during the heterogeneously catalysed hydrogenation reactions in the liquid phase and to develop and apply the theory of a new technique to measure the particle-liquid mass transfer coefficients. The second, to study the kinetics of the liquid phase hydrogenation of acetone in different solvents and to investigate the causes of solvent effects on the reaction rates.

Mass Transfer Effects

In a three phase reaction system, such as a slurry reactor, the rate of transfer of gas from gas phase to the bulk liquid is governed by the product of the gas absorption coefficient and the gas-liquid interfacial area. The reactants dissolved in the liquid phase must overcome fluid-particle mass transfer resistance arising from the boundary layer surrounding the particle. Finally, within a porous catalyst particle there is a kinetic resistance and intraparticle diffusion resistance. To obtain an appropriate kinetic rate expression for a reactor design, the kinetic and intraparticle diffusion resistances cannot be ignored. The particle surface concentration of the reactants, needed to develop a kinetic expression, can be calculated only if the quantity $k_{p,A}\, a_p$ is known. Numerical values of the fluid particle mass transfer coefficients can be calculated by using the terminal velocity for unhindered settling of the catalyst particles. Several more sophisticated correlations have been advanced. These correlations have several shortcomings such as a they are mostly useful for reactors of standard configurations, b the average particle diameter is needed to calculate the effective particle-fluid slip velocity and to compute the

external surface area of the particles, c particles tend to agglomerate in liquids to an unknown degree, and d none of the methods accounts for the intraparticle diffusion resistances. Because of these reasons the available methods in the literature are not precise for obtaining particle-liquid mass transfer coefficients for situations such as reactions in slurries.

Theory of a method is developed for estimating the external particle mass transfer resistance from rate measurements and is demonstrated experimentally.

The hydrogenation of allyl alcohol and fumaric acid over a Raney nickel catalyst in the solvents water and ethanol are chosen as model reactions. Reactions are conducted in a slurry reactor developed in these laboratories. The apparatus is found to be excellent for obtaining precise experimental data for liquid phase hydrogenations. The reactions are conducted in the temperature range 24.5°C to 35.3° C, most runs being at 25°C. The partial pressure of hydrogen ranged from 100 - 730 mm Hg.

The hydrogenation reaction rates obtained from the hydrogen absorption rates, are found to be first order in hydrogen for allyl alcohol in water and approximately one half order for allyl alcohol and for fumaric acid in ethanol. In all the three cases, the rate is approximately zero order in substrate at high substrate concentrations and first order at very low substrate concentrations.

The experimental values of the particle-liquid mass transfer coefficients obtained are 20.0 and 13.3 $cm^3/sec\text{-}g$, for the systems allyl alcohol in water and allyl alcohol in ethanol, respectively. These values agree closely with values calculated using a published correlation.

The transport factors for the reactions are calculated and are used to determine whether or not the measured rate is given by the intrinsic rate expression, and to determine the magnitude of mass transfer resistance of each reactant. It is shown that the three systems that exhibit superficially similar behavior -- zero order in substrate at high concentrations, first order at low concentrations -- are seen to be rate controlled by different combinations of diffusion and kinetic resistance. For the system allyl alcohol - water, there is significant mass transfer resistance over the entire concentration range. For the system allyl alcohol in ethanol, mass transfer effects are negligible for $C_{A,b}$ greater than about 0.04 mol/l. For fumaric acid system, the measured rate is given by the intrinsic rate expression over the entire concentration range.

A rate expression is obtained in the case of a constant volume batch reactor in which a zero order reaction is taking place with external and internal diffusion resistances. This is done for the asymptotic region and the calculated values for the system allyl alcohol in ethanol are compared with experimental data. The results show that an apparent change from zero order to first order kinetics may be due to a zero-order reaction passing from negligible external resistance to external diffusion controlling.

The existence of reactions with negligible internal diffusion and significant external diffusion resistance in slurry reactors is modelled theoretically and demonstrated experimentally.

Solvent Effects

The importance of solvents in the liquid phase hydrogenation reactions has been recognized for a long time but the actual role played by them during the reaction is not very well understood. Very few investigations are available where the main emphasis was to assess the solvent effects.

Waquier and Jungers found that the differences of hydrogenation rates in different solvents were due to differences in adsorption, not in the kinetic constants. They suggested qualitatively that the differences in adsorption could be explained by degree of non-ideality of acetone in the solvent. In this work the qualitative notion of Waquier and Jungers on the effects of substrate activity in the solvent are tested quantitatively.

Heterogeneous hydrogenations of acetone at 25°C in solvents benzene, cyclohexane, and isopropanol are studied over Raney nickel catalyst. Hydrogen solubility data for the pure components and the solvent-acetone binary systems are obtained experimentally. These data are needed to calculate both gas absorption resistance and the liquid phase concentration of hydrogen. The binary solubility data are correlated by thermodynamic models for predicting mixed solvents Henry's law constants. The Van Laar model fits the data best and is used to interpolate the solubility data. The vapor pressure - composition data for the binaries acetone - cyclohexane and acetone - isopropanol are obtained at 25°C ; data for acetone - benzene binary are taken from the literature. These data are needed to establish acetone activity as a function of concentration for purposes of investigating adsorption isotherms and reaction rates in different solvents as a function of acetone activity, and to obtain hydrogen partial pressures from the total system pressures.

The rate of hydrogenation is zero order in acetone at high acetone concentrations and first order at low acetone concentrations. The order of reaction with respect to hydrogen pressure is approximately one half in all the three systems. The activation energies obtained in the zero order region are approximately 5 K cal/g mol for all the three systems.

The steady state hydrogenation reaction rates are obtained in all the three solvents over a composition of acetone from 0 to 100 percent. A mechanism for the liquid phase hydrogenation of acetone is postulated and rate equations are developed for the kinetic controlled steps. It is observed that the rate determining step is probably the reaction of adsorbed acetone with atomic hydrogen.

The effect of solvent on the reaction rates is studied in the first order region. The reason for choosing this low concentration of acetone is that the quantities of acetone involved in the liquid phase are very small and the amount of acetone adsorbed on the catalyst is sufficient to cause a measurable change in the bulk concentration. Thus by knowing the total quantity of acetone introduced in the system and analysing the quantity in the solution, the amount of acetone adsorbed can be calculated by simple mass balance. A gas chromatographic technique is used for the liquid phase analysis.

Before proceeding to the kinetic studies, it is first established that the experimental rates obtained in the first order region are only kinetically controlled. This is done by two methods. One is by extrapolating the value of $k_p a_p$ obtained in the previous section and calculating the surface concentrations of the reactants. The ratios of surface concentrations to bulk concentrations were found to be more than 0.9 for both acetone and hydrogen. In the other method the effect of hydrogen pressure on the reaction in the first order region

is studied and the theory developed in the previous section is used to check the absence of mass transfer resistances.

Experimental data are obtained for the acetone concentration on the catalyst surface when the reaction is in progress. These data give the distribution of acetone between the liquid phase and the catalyst phase. For these experiments both rate and acetone surface coverage increased with the acetone activity coefficient, in comparing the three systems. Neither rate nor acetone surface concentration could be correlated with the acetone activity coefficient for the three systems, however.

It is observed in this work that the rank of the "rate" is the same as that of "acetone adsorbed". The similarities in the activation energies obtained for the hydrogenation reaction in the three solvents tend to show that the turnover frequency is independent of the solvent.

Published Work

"Mass Transfer Effects in Hydrogenations in Slurry Reactors", Can. J. Chem. Eng., 51, 345 (1973). (with J.A. Ruether).

"Vapor-Liquid Equilibria of Acetone - Cyclohexane and Acetone - Isopropanol Systems at 25°C" J. Chem. Eng. Data, 19 (1), 87 (1974). (with J. Polak and J.A. Ruether).

"Additive Excess Free Energy Models for Predicting Gas Solubilities in Mixed Solvents", Can. J. Chem. Eng., in press. (with J.A. Ruether).

I. INTRODUCTION

1.1 Slurry Reactors

Industrial chemical processes involving heterogeneous catalysis in the liquid phase often employ several different types of operations in order to obtain the desired contact between the three phases. They may be grouped into two main classes: the fixed beds of the catalyst pellets and the suspended catalyst particles in liquids. Slurry reactors fall in the second category. Reactions like polymerization and hydrogenation are carried out in stirred autoclaves. Recently, interest has been shown in other types of slurry reactors employing mixing by gas lift, circulation of the liquid phase through an external heat exchanger etc., for wider applications, such as, removal by adsorption and absorption with chemical reactions of gaseous pollutants (SO_2, NO_2, H_2S, and hydrocarbons), hydrogenation and hydrodesulfurization of the petroleum fractions. Slurry reactors have also been applied to the continuous operations of the Fisher-Tropsch reactions and for various other processes of possible commercial interest (1-4).

Slurry reactors have several potential advantages over fixed beds, particularly for the large scale petroleum and petrochemical processes, where their use is not presently widespread. A stirred slurry reactor can be kept at a uniform temperature throughout, eliminating the "hot spots" that hinder the possible attainment of high selectivity of catalyst in three phase fixed bed operations. In slurry reactors, the exothermic reactions are more easily controlled, and heat recovery is possible with good coefficients of heat transfer. For the same reaction rates, the reactor volume required by a slurry reactor may be much smaller than the one required by a fixed or trickle bed, provided the conditions for the reaction are such that a low effectiveness factor is encountered in the

latter case. Catalyst can be regenerated continuously by removing small parts of slurry, regenerating, and returning to the reactor.

In spite of these merits, the overall use of the slurry reactors is limited by the inadequate published data for the design purposes, for example, data on allowable space velocity are very limited [4]. Easy and efficient techniques for handling the catalyst suspensions have not been developed as yet. In many cases it is very difficult to select a solvent in which the reactants are soluble, which does not adversely affect the reaction rates, and is stable at the conditions of the r eaction.

1.2 Mass Transfer Effects in Hydrogenations in Slurry Reactors

A slurry reactor used for the hydrogenation reactions consists of solid catalyst particles suspended in the liquid to be hydrogenated either as such or dissolved in some inert solvent. Gaseous hydrogen used is bubbled in the slurry to provide stirring in addition to the mechanical stirrers. The rate of transfer of hydrogen from the gas phase to the bulk liquid phase is governed by the product of gas absorption coefficient and gas-liquid interfacial area, $k_L a$. To reach the exterior surface of a catalyst particle, reactants dissolved in the liquid phase must overcome fluid-particle mass transfer resistance arising from the boundary layer surrounding the particles. Finally, within a porous catalyst particle there is a kinetic resistance, and an intraparticle diffusion resistance.

For a sufficiently slow reaction, it can readily be verified that the reactant concentrations throughout the interior of the catalyst are the saturation value for hydrogen, and the bulk value for the substrate. In this case the measured rate gives the kinetic rate directly. The situation is more complicated in cases which are intermediate between negligible kinetic resistance and complete kinetic control. If the

contents of the reactor are well mixed and the quantity $k_L a$ is known, the bulk hydrogen concentration can be calculated from the measured reaction rates. However, in practice the surface concentration of hydrogen needed to develop a kinetic expression can be calculated only if the fluid-particle mass transfer coefficient, $k_{p,H} a_p$, is known.

A conservative value for the fluid particle mass transfer coefficient can be calculated using the terminal velocity for unhindered settling of the catalyst particle. More accurate correlations have been advanced for particles in an agitated system [5-7]. The correlations require knowledge of agitation power delivered to the liquid, which is frequently difficult to measure. It is necessary to estimate an average particle diameter to calculate the effective particle-fluid slip velocity and to compute the external surface area per unit mass of catalyst. Since finely divided catalyst particles tend to agglomerate in liquids to an unknown degree, any average diameter used is likely to introduce errors in the values of mass transfer coefficients and external surface areas obtained.

It would be useful in kinetic studies with finely divided catalyst particles in solution to be able to determine $k_p a_p$ for the catalyst in the state of agglomeration it exhibits during reaction.

1.3 Solvent Effects in Hydrogenations in Slurry Reactors

Solvents are widely used in liquid phase catalytic hydrogenation reactions. The rate, products of reaction, and sometimes extent of reaction depend on the proper choice of solvent. In highly exothermic reactions, solvent is useful for controlling the temperature rise resulting from the reaction. It has been experimentally established by several authors [8-11] that the rate of a catalytic reduction depends on the solvents, but it has not been fully ascertained why. Very few generalities are

available in the literature which could be used as a guide in choosing solvents.

A solvent may influence the course of reduction in some subtle way, the details of which can usually be only inferred. These ways may be competition between the reactants and the solvents for the active catalyst sites [9,12], complex formation between solvents and intermediates [13], and controlling diffusion of hydrogen to the catalyst surface [14-15].

The model of competitive adsorption has been used in several studies [9,16] because it leads to a Langmuir-Hinshelwood type of equation which is known to be applicable to liquid phase catalytic hydrogenations [17]. The concept of complex formation is used to explain different products arising from the hydrogenation of a single substance[18]. The availability of hydrogen on the catalyst surface has been linked to the selectivity in the natural fats hydrogenations. The role of solvent in the last case is mostly in hydrogen transport.

For reaction systems where single hydrogenation product is formed and where transport effects are totally absent, a solvent may show its effect by altering the distribution of the substrate between the catalyst and the liquid phase and by affecting the reactivities of the adsorbed species on the catalyst surface. Wauquier and Jungers [8] concluded from their study of solvent effects on hydrogenation of a mixture of acetone and cyclohexene and Raney nickel catalyst that the solvent affects only the distribution of substrates between the catalyst and solvent phases and has no effect on the reaction rate constants. Eckert [10] misapplied their data in attempting to show that the effect was mostly on the reaction rate constants. Balandin [17] observed the effect on

both the distribution coefficient and the reaction rate constant and pointed out that in certain situations these effects may be in opposite directions and thereby the effect of solvent may even not be observed.

It will be worthwhile to study a simple hydrogenation reaction in different solvents and to study the effect of solvent on reaction rates to see if it affects the distribution coefficients or the reactivities of the adsorbed species or both. It will also be of interest to study the influence of bulk activities of substrate on the reaction rates and on the distribution coefficients. Such a study will be of interest not only from theoretical point of view but may also be useful in predicting reaction rates in different solvents.

1.4 Objectives of the Study

Based on this background, a research program for this work was pursued. The main objectives of the work are two-fold. The first is to develop and apply the theory of a new technique to measure mass transfer coefficients between the liquid and catalyst particles. Such a technique must have sound theoretical foundations, and yet it must be simple enough to permit easy determination of mass transfer coefficients. The second objective is to study the kinetics of liquid phase hydrogenation of a simple reaction in different solvents, to forward reaction mechanism and rate equations, and to establish from experimental observations the causes for the effect of solvent on the reaction rates. In this part of the study it is necessary to be assured that external and internal mass transfer effects are negligible; therefore, it has to follow the first part, namely, the mass transfer study.

These objectives have been accomplished by designing an apparatus to study the hydrogenation reactions using a stirred slurry

reactor, and studying the hydrogenation reactions of fumaric acid, allyl alcohol, and acetone, in different solvents over Raney nickel catalyst. Theoretical models developed have been demonstrated experimentally.

2. PREVIOUS WORK

2.1 Particle-Liquid Mass Transfer

Mass transfer can occur from liquid to suspended particles by any of the three modes--- forced convection, free convection, and radial diffusion. When a difference in motion or velocity exists between the solid and the fluid phases, it produces a laminar boundary layer in the fluid at the phase interface. The effective thickness of this film depends on the magnitude of velocity difference or slip velocity. It is this laminar film which offers a major resistance to mass transfer. The rate of mass transfer depends on the molecular diffusivity of the solute and the laminar film thickness.

In a slurry reactor, usually a slip between the solid particles and the circulating liquid is encountered. For given agitation conditions and fluid properties, the Sherwood number, $\frac{k_p d_p}{D}$, approaches 2 as the particle diameter decreases. There are several correlations in the literature which relate mass transfer coefficients with different process variables and solution properties. Harriott [19] has given an excellent review of such correlations up to 1961. Reviews by Miller [7] and by Levins and Glastonbury [5] deal with later developments. No attempt is being made here to discuss the individual contributions. However, it will be of interest to briefly look at the basic approach adopted by several authors.

Friedlander [20] showed that for Stokes law flow, Sherwood number is a function of Schmidt number. Under the convective conditions, either natural or forced, the following relation may be obtained theoretically from the equation of motion.

$$N_{Sh} = f(N_{Re}, N_{Gr}, N_{Sc}) \qquad (2.1)$$

The definitions of the dimensionless numbers used in equation (2.1) are given in the Nomenclature section.

Under forced convection currents, where N_{Gr} is unimportant, equation (2.1) becomes

$$N_{Sh} = f(N_{Re}, N_{Sc}) \qquad (2.2)$$

This is the starting equation for most of the expressions available in the literature.

Equations of Frossling [21], Garner [22], Ranz and Marshall [23], and Miller [7] are representative of the various expressions available in the literature. The general form of the expression is

$$N_{Sh} = 2 + B\, N_{Re}^{0.5}\, N_{Sc}^{0.33} \qquad (2.3)$$

Different values of B have been reported by the authors for the conditions of their experiments.

The velocity used for calculating Reynolds number is the slip velocity, which can be calculated in several different ways. Levins and Glastonbury [5] considered it to consist of three types of velocities. They were a velocity U_e arising from velocity gradients in the neighbourhood of the particle surface, terminal velocity U_t, and a velocity U_s arising from the differences in inertia between the particles and the fluid. The resultant velocity was represented to an approximation by the rule of addition of orthogonal vectors, resulting in

$$v = (U_e^2 + U_t^2 + U_s^2)^{\frac{1}{2}} \qquad (2.4)$$

A similar equation was suggested by Brian et al. [24]. Harriott [19] suggested the use of the terminal velocity to calculate the minimum value of the coefficient.

Harriott [19] observed that the scatter in the data and large differences in effects reported make published correlations uncertain. Levins and Glastonbury [5] pointed out that the lack of agreement in different publications may be to some extent because of using dimensionless numbers consisting of variables which may have theoretical objections. One such example can be the use of stirrer diameter instead of particle diameter in both Sherwood number and Reynolds number. There has not been a unanimous agreement on the use of the exponent of Schmidt number. Some correlations require the knowledge of the power delivered to the liquid as power input per unit mass or volume, which is frequently difficult to measure. Correlations by which agitation power can be calculated from reactor and agitator geometry, fluid properties, and agitator speed are available for some standard configurations. The utility of these correlations is reduced if mixers of non standard configurations are used.

All the correlations described above use an average particle diameter to calculate effective particle fluid velocity and to compute the external surface area per unit mass of the solid particles. In practice, slurries consist of particles over a wide range of sizes. Use of an average diameter introduces inaccuracies in measuring both the specific area and the mass transfer coefficients. Further, finely divided catalyst particles tend to agglomerate in liquids to an unknown degree. Sherwood and Farkas [3] have pointed out that there is probably more uncertainity in determining the particle diameter to use than in calculating the mass transfer coefficients for a particle of a given size.

Furusawa and Smith [25] studied adsorption of benzene in aqueous slurries of activated carbon. They interpreted their experimental data by supposing a three step model involving mass transfer of benzene from bulk liquid to particle surface, intraparticle diffusion, and adsorption at an interior site. They found their results to be in agreement with those obtained from dissolution data [24]. It was pointed out that a significant intraparticle diffusion resistance in slurries was observed, even for the smallest particles of 161 microns.

A method of obtaining mass transfer coefficients under reaction conditions where both particle agglomeration and intraparticle resistances could be accounted for would be of interest to the engineers engaged in the designing of slurry reactors.

2.2 Effects of Solvents on Heterogeneous Hydrogenation Reactions

The effect of solvent on homogeneous reaction rates has been given extensive treatment in the literature [10, 26-28]. Much less attention has been given to the area of heterogeneous reactions. In general, it is believed that in case of heterogeneous reactions, solvent may affect the reaction rates by competing for the active sites on the catalyst surface and thereby changing the surface coverage by the reactants on the catalyst surface. Some workers have suggested that a solvent may interact significantly with the reactants both in the solution and in the adsorbed phases, in addition to adsorbing on the catalyst. Extent of different interactions in a particular system depends on the nature of the substrate, solvent, and the catalyst.

Much of the literature on reactions in organic solvents deals with studying the effect of a number of solvents on a particular hydrogenation

reaction and listing the solvents in the order of rates observed. Physical or structural properties of the solvents giving higher reaction rates are given as parameters in selecting solvents, which are used as guides for choosing solvents for other substrates.

Some of the important work reported in the literature which leads to a better understanding of solvent effects in heterogeneous hydrogenations in non-electrolyte solutions is discussed here briefly.

2.2.1 Solvent Selection for Heterogeneous Hydrogenations

A solvent for liquid phase heterogeneously catalyzed hydrogenation is often chosen for its ability to dissolve the compound to be reduced and/or reduction product. Any solvent that is available in pure form may be considered if it is known that it will not react with the substrate or product, and will not itself react under the conditions of reaction. Other desired properties of a solvent are low vapor-pressure, high boiling point, stability at high temperature, and low viscosity.

Eckert [10] pointed out that the analysis of a reacting system shows that the best solvent for a given case is one which is as highly polar as possible, or perhaps one with the lowest possible cohesive energy density. However, for heterogeneous reactions Shutt and Winterbottom[29] gave another point of view. They pointed out that solvents with electron rich groups can interact with the metal and retard reaction rates. The dielectric constant or polarity of a solvent seems to influence the rate attained in a solvent. This they attribute to the influence of solvent polarity on the formation and dissociation of metal carbon bond. Sometimes it is advisable to use solvent mixtures which have better properties than the pure solvents [28].

Way and Satterfield [30] made the generalization that polar compounds are more strongly adsorbed than the non-polar compounds by polar solids and vice-versa. An adsorbing solvent competes with the substrate for the active sites on the catalyst surface and thus causes reduction in reaction rates.

Catalyst particles should show a low degree of agglomeration in the chosen solvent. A highly agglomerating catalyst can reduce reaction rates by reducing the effective surface area of the catalyst. The importance of the state of aggregation in the kinetics of the reacting slurries has been discussed by Polinskii and Huang [31].

A solvent should not have very different characteristics than the substrate, as in those cases, Fasman and Sokol'skii [32] pointed out that sometimes poisoning of the catalyst may occur. This is one of the reasons that in certain cases, the specific reaction rate passes through a maximum when the concentration of unsaturated compound is varied.

Shutt and Winterbottom [29] ruled out the difference of hydrogen solubility as the cause of the rate differences in different solvents, since low reaction rates are often observed in solvents that have the largest amount of hydrogen dissolved in them.

2.2.2 Heterogeneous Hydrogenation of Acetone in Solutions

Effects of solvents on the heterogeneous hydrogenations of acetone has been a subject of interest to several authors. Ruiter and Jungers [33] studied hydrogenation of acetone over nickel catalyst. They observed that methanol inhibits the reaction, ethanol is satisfactory, and saturated hydrocarbons are the best. Orito et al. [34] found that saturated hydrocarbons promote the reaction, but primary alcohols

and amines inhibit the reaction. Kishida and Teranishi [9] interpreted their results obtained in several solvents by a rate equation based on Langmuir-Hinshelwood mechanism. It was assumed that hydrogen, acetone, and solvent were adsorbed competitively on the catalyst surface. They pointed out that the scheme of competitive adsorption does not hold for all cases. The difference between rates in various solvents was explained on the basis of different adsorption strengths. Iwamoto et al. [16] proposed a reaction mechanism of acetone hydrogenation and developed rate equations for the reaction steps to be rate controlling. They concluded that solvent had no effect on the adsorption of hydrogen and that the variations in the initial rates in different solvents were not caused by competitive adsorption of the solvent but by the change in the rate constants.

In the presence of non-reacting substances, Wauquier and Jungers [8] started with the following general expression for calculating the effect of substrate concentration on the rate constant and the ratio of distribution coefficients.

$$r = k \frac{b C}{\Sigma b_i C_i} \qquad (2.5)$$

Here C's are the concentrations of various components in the solution and b's are their distribution coefficients, respectively. The distribution coefficient determines the distribution of reactant between the liquid and the adsorbed phases.

For a mixture of two reactants A and B, they obtained

$$\frac{r_A}{r_B} = \frac{dC_A}{dC_B} = \frac{k_A b_A C_A}{k_B b_B C_B} \qquad (2.6)$$

which was integrated to give

$$\frac{k_A b_A}{k_B b_B} = \frac{\log C_{A,O} - \log C_A}{\log C_{B,O} - \log C_B} \qquad (2.7)$$

Here $C_{A,O}$ and $C_{B,O}$ are the initial concentrations and C_A and C_B are the concentrations at any time of sampling of reactants A and B, respectively. The left hand side of equation (2.7) called the reactivity ratio, is determined by the corresponding rate constants and distribution coefficients. The ratio of distribution coefficients could be calculated when the rate constants or their ratio was known. It may be pointed out here that the distribution coefficients obtained from kinetic experiments bear no direct relation to the coefficients of physical adsorption.

Wauquier and Jungers [8] used equation (2.7) to determine the effect of solvent on the rate and selectivity of hydrogenation of a mixture of acetone and cyclohexene in several solvents over Raney nickel catalyst. The solvents chosen were the ones which do not react with either the reactant or the catalyst. Wide variations (from 1.3 to 18) were observed in the value of the reactivity ratio for different solvents. It was suggested that the effect of a solvent on the reactivity ratio may be due to its effect on the adsorption coefficient, as well as to the change in the reaction rate constant. In their study, they observed that the change in the reactivity ratio in different solvents was due to the effect of solvent on the distribution coefficients of the reactants. To prove this they studied the hydrogenation of pure cyclohexene and of its solutions with benzene, isopropanol, and cyclohexane and of acetone in the last two solvents. Almost identical reaction rates were obtained in all solutions of cyclohexene. The maximum deviation in the value of the rate

was 10 percent for 30 measurements made at different compositions of cyclohexene. It was thus concluded that these solvents are not the adsorbing type and do not affect the rate constant. The ratio of rate constants, $k_{acetone}/k_{cyclohexene}$, was estimated to be 0.4.

It was noted by Wauquier and Jungers that the effect of solvents on the reactivity of cyclohexene and acetone varies inversely as their affinity for these compounds. This can be found from the thermodynamic behavior of the solvent-substrate binary. For example, acetone forms a highly non ideal solution with cyclohexane, while cyclohexane and cyclohexene form an ideal solution. Consequently, acetone is attracted to the catalyst and cyclohexene is retained in the solutions so that the reactivity of cyclohexene is diminished and that of acetone increases. The reverse is observed when dioxane is used as a solvent. This means that solvent changes the reactivity by changing the distribution coefficients. It was argued that if solvent is capable of changing the adsorption of the reactants, it should also change the adsorption of inhibitors. To prove this statement, the effect of inhibitors like aniline, methylaniline and dimethylaniline in cyclohexane or isopropanol on the hydrogenation of cyclohexane was studied. The adsorption coefficients of all the investigated amines were higher in cyclohexane than in isopropanol, thus confirming the above observation made about the solvent effects in heterogeneous hydrogenations in solutions.

Sokol'skii [17] pointed out that Wauquier and Jungers ignored the adsorption of hydrogen on the catalyst surface and did not discuss the effect of solvent on the amount of hydrogen on the surface, the energy of its bond with the surface, and the rate of its replenishment. He reported the effect of solvent on the amount of hydrogen adsorbed on the catalyst surface in different cases. For example, in the case of

PtO_2, the amount of hydrogen adsorbed on the surface varied with the pH of the medium. A similar behavior was observed in the case of nickel catalyst.

From the results of Balandin [17], it seems that the conclusions of Wauquier and Jungers are applicable only for substances of similar chemical nature, so that the effect of solvent on the rate constants of both the reactants is identical, leaving their ratio almost constant. Balandin pointed out that for mixtures containing substances of dissimilar unsaturated groups e. g. acetylene and ethylene, the solvent may have opposite effects on the rate constants in different cases. Thus the ratio of the rate constants may also vary with the nature of the solvent.

In spite of these discrepancies arising from the works of Sokol'skii and Balandin, the work of Wauquier and Jungers is not without value. Their work was the first attempt to explain the solvent effect on the basis of surface coverage by the substrates and they explained the phenomenon from the liquid phase interactions between solvent and substrate. Furthermore, in practice situations are usually encountered where hydrogen adsorption is nearly independent of the medium [16].

In summary, Wauquier and Jungers found that the differences of hydrogenation rates in different solvents were due to differences in adsorption, not in kinetic constants. They suggested qualitatively that the differences in adsorption could be explained by the degree of non ideality of acetone in the solvent, for non-ideal solvents. In this work, the notions of Wauquier and Jungers were examined more quantitatively through knowledge of the activity of acetone in the solvents.

3. THEORETICAL

3.1 Mass Transfer in Slurry Reactors

Consider a simple hydrogenation reaction, $A + H_2 \rightarrow P$, being carried out in a slurry reactor. The two external diffusion steps, namely, gas-liquid and liquid-particle mass transfer of hydrogen, act in series with the diffusion and reaction step within the catalyst. The rates of the three steps must be equal under steady state conditions and can be written as

$$\begin{aligned} r_v &= k_L\, a.\, (C_{H,*} - C_{H,b}) \\ &= k_{p,H}\, a_p \cdot (C_{H,b} - C_{H,S})\, W \\ &= S\, \eta\, \mathcal{R}(C_{H,S}, C_{A,S})\, W \end{aligned} \qquad (3.1)$$

Here $\mathcal{R}(C_{H,S}, C_{A,S})$ is the intrinsic reaction rate when both reactants are at the concentrations existing at the outer surface of the catalyst particle.

For an active catalyst it is frequently observed that the particle surface concentration of hydrogen is nearly zero, or more precisely, $C_{H,b} >> C_{H,S}$. In this case the rate is controlled by the two external diffusion steps. Since the rates of both steps are linear in the concentration driving force, the specific rate is given by

$$C_{H,*}/r_v = \frac{1}{(k_{p,H}\, a_p\, W)} + \frac{1}{(k_L\, a)} \qquad (3.2)$$

The saturated hydrogen concentration, $C_{H,*}$, is usually calculated using a Henry's law constant and the hydrogen partial pressure. It

has long been known that under these conditions a plot of $1/r_v$ versus $1/W$ where only catalyst loading is changing gives a straight line. Sherwood and Farkas in their slurry reactor studies calculated $k_L a$ in this manner [3].

In the more general case the kinetic and intraparticle diffusion resistances cannot be ignored, and knowledge of an appropriate kinetic rate expression is required for reactor design. For sufficiently slow reactions, the reactant concentration throughout the interior of the catalyst are the saturation value for hydrogen, and the bulk liquid value for the substrate. In this case the measured rate gives the kinetic rate directly.

In the cases which are intermediate between negligible kinetic resistance and complete kinetic control, the particle surface concentration of hydrogen needed to develop a kinetic expression can be calculated only if quantity $k_{p,H} a_p$ is known. No information about the relative resistances to reaction due to fluid particle diffusion, and the intraparticle processes of diffusion and reaction, can be gained by changing the mass of the catalyst as can be seen from equation (3.1).

In the following pages a method for estimating $k_p a_p$ from reaction rate data is presented.

3.1.1 Calculation of Fluid Particle Mass Transfer Coefficients from Reaction Rates

Satterfield et al. have considered internal diffusion resistance in heterogeneously catalyzed hydrogenation reactions in solution [35]. They show that it is necessary in general to consider effectiveness factors for both reactants. Because the concentration of the substrate

is usually much greater than the dissolved hydrogen concentration, often both external and internal diffusion resistance for the liquid reactant is negligible. In that case the concentration of the substrate is the same in the bulk liquid, at the outer surface of the catalyst particle, and within the particle. To calculate diffusion resistance for hydrogen, the substrate concentration that appears in the kinetic rate expression may be combined with the kinetic rate constant to give a rate expression having dependence only on hydrogen concentration. This pseudo-one component kinetic rate expression is used to calculate the effectiveness factor for hydrogen in the conventional manner.

In this study, a case opposite from that just described for the relative magnitudes of the concentrations of substrate and dissolved hydrogen is considered. By making the concentration of substrate sufficiently small, the concentration of dissolved hydrogen can be made essentially constant in the bulk liquid and at the surface of and within the catalyst particle. In this case any external or internal diffusion resistance that occurs is due to the substrate. A pseudo-one component kinetic rate expression can be developed for the substrate, by combining the kinetic dependence on hydrogen concentration with the kinetic rate constant.

An expression similar to equation (3.1) can be written considering the concentration of the substrate as the driving force for reaction. The rate per catalyst particle is:

$$r_p = k_{p,A} A_p \cdot (C_{A,b} - C_{A,s}) = V_p \rho_p S \eta \mathcal{R}(C_{H,s}, C_{A,s}) \qquad (3.3)$$

Equation (3.3) is rearranged to get an expression of the form of equation (3.2), since this would permit the determination of $k_{p,A} A_p$. To do this it is necessary that the expressions for the rate in equation (3.3) have a linear dependence on the concentration driving force of the substrate. Two possibilities present themselves. If $C_{A,b} >> C_{A,s}$, then the term involving the intrinsic reaction rate in equation (3.3) need not be considered, since it offers a negligible resistance to reaction. This is the case of external diffusion control, and the rate would be given by $r_p = k_{p,A} A_p C_{A,b}$.

The other possibility is that the kinetic resistance cannot be neglected. Then to get an expression of the form of equation (3.2) it is necessary that the rate show a linear dependence on the concentration of substrate at the catalyst particle surface, $C_{A,s}$. The case with appreciable kinetic resistance is considered first.

I. Conditions for the Reaction Rate to be a Linear Function of $C_{A,s}$

Frequently the dependence of the intrinsic reaction rate on hydrogen concentration can be written as a power law expression.

$$\mathcal{R} = k C_H^{\,m} f(C_A) \qquad (3.4)$$

At a sufficiently slow reaction rate, the hydrogen concentration everywhere within a catalyst particle would approach the value of $C_{H,b}$. This state could be achieved, at least in principle, by using a sufficiently small value of $C_{A,b}$ to make the rate as small as required. The external and internal diffusion resistances of hydrogen would be negligible, but in general the same would not be true of the substrate. With the assumption that equation (3.4) applies, the reaction term in equation (3.3) can be written

$$r_p = V_p \rho_p S k C_{H,b}^{m} \eta (C_{A,s}) f (C_{A,s}) \qquad (3.5)$$

Here it is assumed that the effectiveness factor for hydrogen is unity. The term $\eta (C_{A,s})$ is the effectiveness factor for substrate, and in general its value is a function $C_{A,s}$.

In order for the rate to be linear in $C_{A,s}$, it is necessary that in equation (3.5),

$$\eta (C_{A,s}) f (C_{A,s}) = C_{A,s} \qquad (3.6)$$

Conditions under which Equation (3.6) holds are now considered.

Irreversible heterogeneously catalyzed reactions often exhibit rate expressions of the Langmuir-Hinshelwood form

$$\mathcal{R} = k \prod_i C_i^{\alpha i} / (1 + \sum_i K_i^{n} C_i^{n})^{u} \qquad (3.7)$$

The exponents u and n in equation (3.7) are always positive numbers. In rate expressions of this form, for a sufficiently small reactant concentration, terms in which it appears make a negligibly small contribution to the denominator. As mentioned earlier, the concentration of substrate must be kept low if the diffusion resistance of hydrogen is to be made negligible. Under these conditions, equations (3.4) and (3.7) simplify to a power law expression for the intrinsic reaction rate.

$$\mathcal{R} = k C_H^{m} C_A^{n} \qquad (3.8)$$

The criterion for the rate to be linear in $C_{A,s}$, as expressed in equation (3.6) is simplified to

$$\eta (C_{A,s}) C_{A,s}^{n} = C_{A,s} \qquad (3.9)$$

Equation (3.9) applies for reactions first-order in substrate concentration. The exponent n = 1, and the effectiveness factor is independent of $C_{A,s}$. Assuming hydrogen diffusion resistance is negligible, the intrinsic rate expression is

$$\mathcal{R} = k\, C_{H,b}^{\,m}\, C_A \tag{3.10}$$

To calculate the effectiveness factor for substrate, a pseudo-first-order rate constant is defined

$$k_1' = k\, C_{H,b}^{\,m} \tag{3.11}$$

If the catalyst particles are considered to be spheres, the expression for the effectiveness factor for a first-order reaction is [4]

$$\eta_A = 3/h_1 \left[\frac{1}{\tanh h_1} - \frac{1}{h_1} \right] \tag{3.12}$$

where the Thiele modules h_1 is

$$h_1 = R \sqrt{\frac{\rho_p S k_1'}{D_e}} \tag{3.13}$$

The effectiveness factor increases with decreasing h_1, being equal to 0.95 at $h_1 = 1.0$. For $h_1 < 1.0$, equation (3.5) is closely given by

$$r_p = V_p \rho_p S k\, C_{H,b}^{\,m}\, C_{A,s} \tag{3.14}$$

For large h_1, η_A approaches the asymptotic relation $\eta_A = 3/h_1$, the agreement being within 10 percent at $h_1 = 10$. In this case equation (3.5) becomes

$$r_p = V_p \sqrt{D_e \rho_p S k C_{H,b}^{m} C_{A,s}} \qquad (3.15)$$

When equation (3.15) applies, r_p is proportional to $C_{H,b}^{m/2}$. For values of h_1 between 1.0 and 10 there is no simple relation giving the dependence of rate on $C_{H,b}$, but this is a relatively small interval in the range of all possible values of h_1.

II. Conditions for the Reaction Rate to be External Diffusion Controlled in Substrate

The case where for sufficiently small values of $C_{A,b}$ the rate becomes external diffusion controlled in substrate is now considered. This situation is sought in systems with kinetics given by equation (3.8) where $n \neq 1$. It is again assumed that the rate can be made sufficiently small that diffusion effects for hydrogen can be neglected. It is then possible to define a pseudo-n'^{th} order rate constant in substrate concentration, k_n', similar to that given in equation (3.11) for $n = 1$. For the purposes of analyzing diffusion effects of the substrate the kinetic expression used is $\mathcal{R} = k_n' C^n$.

Petersen has shown for power law kinetics of this form that when the following expression is used for the Thiele modulus h, to a good approximation the effectiveness factor is the same function of h regardless of particle shape or reaction order [36].

$$\hat{h}_n = \frac{V_p}{A_p} \sqrt{\frac{(n+1)\, \rho_p S k'_n C_s^{n-1}}{2 D_e}} \qquad (3.16)$$

This definition has the additional convenience of yielding the asymptotic relation $\eta = 1/\hat{h}_n$ for large $\hat{h}_n$ ($\hat{h}_n > \sim 3$), without a proportionality factor. In the asymptotic region, essentially all reaction occurs in a

thin shell near the catalyst surface. The depth of the shell is small compared to the radius of curvature of the particle, so the catalyst particle can be treated like a flat plate regardless of its shape.

A transport parameter $\mathcal{J}$ for substrate A is also defined,

$$\mathcal{J}_A = C_{A,s}/C_{A,b} \tag{3.17}$$

For $\mathcal{J}_A$ approaching zero, the rate is external diffusion controlled in A. For a reaction in the asymptotic region it is possible to develop an analysis originally suggested by Frank-Kamenetskii to evaluate the transport factor, $\mathcal{J}_A$ [37]. The object is to express $\mathcal{J}_A$ in terms of constants and the bulk concentration, $C_{A,b}$. The catalyst particles will be assumed to be spherical, so the Sherwood number is

$$Sh = 2\, k_p\, R/D \tag{3.18}$$

The rate of reaction per particle can then be expressed as

$$r_p = \frac{Sh\, D}{2\, R}\; A_p\, C_{A,b} \cdot (1 - \mathcal{J}_A) \tag{3.19}$$

Since reaction is assumed to be in the asymptotic region with respect to η_A, the rate can also be expressed as

$$r_p = V_p\, \rho_p\, S\, k_n'\, C_{A,b}^{\,n}\, \mathcal{J}_A^{\,n}/\hat{h}_n \tag{3.20}$$

Equations (3.19) and (3.20) are combined to yield an expression for $\mathcal{J}_A$.

$$Sh\,(1 - \mathcal{J}_A) = \frac{2R}{D}\sqrt{\frac{2\, De\, \rho_p\, S\, k_n'}{n+1}}\; C_{A,b}^{\,(n-1)/2}\, \mathcal{J}_A^{\,(n+1)/2} \tag{3.21}$$

Equation (3.21) cannot be solved for $\mathcal{J}_A$ for arbitrary power n, but one can show that the dependence of $\mathcal{J}_A$ on $C_{A,b}$ as $C_{A,b}$ approaches zero is of three different types depending on whether n is equal to, greater than, or less than unity.

For reaction in the liquid phase the effective diffusivity D_e within a catalyst particle appearing in equation (3.16) is related to the bulk diffusion coefficient D in equation (3.18) as $D_e=(\theta/\tau)\,D$. For first-order reaction, equation (3.21) can be simplified and solved for $\mathcal{J}_A$.

$$\mathcal{J}_A = \frac{Sh}{Sh + \dfrac{6\,\theta\,\hat{h}_1}{\tau}} \qquad (n = 1) \tag{3.22}$$

The right hand side of equation (3.22) is independent of $C_{A,b}$, so for first-order reaction the relative magnitudes of internal and external resistances in the asymptotic region are also independent of $C_{A,b}$.

For the case of reaction order greater than one a more general relation for $\mathcal{J}_A$ that does not assume the asymptotic relation of η_A to $\hat{h}_n$ can be written.

$$1 - \mathcal{J}_A = \frac{2\,R^2\,\rho_p\,S\,k_n'}{3\,D\,Sh}\;\eta_A\,C_{A,b}^{\,n-1}\,\mathcal{J}_A^{\,n} \tag{3.23}$$

For $C_{A,b}$ sufficiently small the right hand side of equation (3.23) tends to zero, so that

$$\lim_{C_{A,b}\to 0} \mathcal{J}_A = 1 \qquad (n > 1) \tag{3.24}$$

for reaction orders greater than unity. From equation (3.16) it is seen that $\hat{h}_n$ also decreases with decreasing $C_{A,b}$, so that η_A tends toward unity. Thus as $C_{A,b}$ approaches zero the reaction becomes kinetically controlled. It is not possible to determine $k_p A_p$ by measuring the dependence of rate on $C_{A,b}$ when the order with respect to A is greater than one.

For the reaction order n less than unity, as $C_{A,b}$ is reduced sufficiently the reaction becomes external diffusion controlled. It is noted first that in this case, for $C_{A,b}$ sufficiently small the reaction will be in the asymptotic region with respect to internal resistance, as can be seen from equation (3.16). Equation (3.21) is therefore applicable. Incorporate $C_{A,b}$ in a parameter $\bar{h}_n$ defined analogously to the Thiele parameter.

$$\bar{h}_n = \frac{V_p}{A_p} \sqrt{\frac{(n+1)\,\rho_p\, k_n'\, C_{A,b}^{\,n-1}}{2\,D_e}} \qquad (3.25)$$

Equation (3.21) becomes

$$Sh\,(1 - \mathcal{J}_A) = \frac{12\,\theta}{(n+1)\tau}\,\bar{h}_n\,\mathcal{J}_A^{\,(n+1)/2} \qquad (3.26)$$

For order n = 0, this gives a quadratic equation in $\mathcal{J}_A$,

$$\left[\frac{\tau\, Sh}{12\,\theta\,\bar{h}_o}\right]^2 \mathcal{J}_A^{\,2} - \left[2\left(\frac{\tau\, Sh}{12\,\theta\,\bar{h}_o}\right)^2 + 1\right] \mathcal{J}_A + \left[\frac{\tau\, Sh}{12\,\theta\,\bar{h}_o}\right]^2 = 0 \qquad (3.27)$$

Let $a = \frac{\tau\, Sh}{12\,\theta\,\bar{h}_o}$. Solving for $\mathcal{J}_A$, and taking the smaller root since $\mathcal{J}_A < 1$,

$$\mathcal{J}_A = \frac{2\alpha^2 + 1 - \sqrt{4\alpha^2 + 1}}{2\alpha^2} \tag{3.28}$$

The quantity α approaches zero as $C_{A,b}$ approaches zero. By use of L'Hopital's rule $\mathcal{J}_A$ is evaluated in the limit of vanishing α. The result is

$$\lim \mathcal{J}_A = 0 \quad (n < 1)$$
$$C_{A,b} \rightarrow 0 \tag{3.29}$$

In this case as $C_{A,b}$ approaches zero the rate becomes external diffusion controlled, and the quantity $k_p A_p$ can be determined.

Equation (3.3) is now rearranged to put it in the form of equation (3.2). Assuming the intrinsic rate is given by equation (3.8) and mass transfer resistances for hydrogen are negligible, the result is

$$C_{A,b}/r_p = 1/(k_{p,A} A_p) + 1/(V_p \rho_p S \eta_A k C_{H,b}^{m}) \tag{3.30}$$

To utilize equation (3.30) to determine $k_{p,A} A_p$, the left hand side is plotted as ordinate with the reciprocal bulk hydrogen concentration to some power as abscissa. The intercept of such a plot would be $(k_{p,A} A_p)^{-1}$.

To summarize the cases in which equation (3.30) can be used:

Intrinsic rate first-order in A; kinetic control

Here $\eta_A = 1$, and the ordinate is $C_{H,b}^{-m}$.

Intrinsic rate first-order in A; η_A given by asymptotic relation

In this case, it is seen from equation (3.15) that the denominator of the second term on the right hand side of equation (3.30) is

$V_p \sqrt{D_e \rho_p S k C_{H,b}^{\ m}}$. Thus the ordinate is $C_{H,b}^{\ -m/2}$

Intrinsic rate of order less than unity in A; $C_{A,b}$ approaching zero

Here, the left hand side of equation (3.30) is independent of $C_{H,b}$, so the ordinate will have a constant value regardless of the function of bulk hydrogen concentration used as the abscissa.

Equation (3.30) was developed by considering the flux of the substrate to a particle catalyzing reaction at the steady state. An analogous development considering hydrogen flux leads to the equation

$$C_{H,b}/r_p = 1/(k_{p,H} A_p) + 1/(V_p \rho_p S \eta_H k C_{A,b}^{\ n}) \qquad (3.31)$$

provided that $C_{A,b} = C_A$ throughout the particle, and that the rate is linear in $C_{H,s}$.

Equation (3.30) is thought to be more useful than equation (3.31) for two main reasons. It has been observed experimentally for a number of compounds that the hydrogen dependence in the intrinsic rate expression is to the one-half power, making equation (3.31) unusable for these compounds when the rate is kinetically controlled. The one-half order is likely due to hydrogen molecules dissociating on the catalyst surface, a phenomenon that does not occur with the substrate. The other reason for preferring equation (3.30) is one of experimental convenience. When the reaction is carried out in a constant volume batch reactor, the rate is measurable from the decrease in substrate concentration with time. The left hand side of equation (3.30) can thus be evaluated with a semi-log plot of $C_{A,b}$ versus time as $C_{A,b}$ approaches zero. The quantity $C_{H,b}$ appearing on the right hand side of equation (3.30) is conveniently controlled by varying hydrogen partial pressure.

3.1.2 External and Internal Resistance with Zero-Order Reaction

Petersen has studied the problem of the relative sizes of external and internal resistances to reaction in a catalyst particle. He showed that for a first-order reaction, $\eta < \mathcal{J}$ always, and by extension this result applied to other reaction orders for gas-solid reactions [36]. Thus his finding was that it is possible to encounter the situation where external diffusion resistance is negligible and internal resistance is appreciable, but the converse would not occur. The dependence of $\mathcal{J}_A$ on reaction order in the region where $C_{A,b}$ is small enough that $\hat{h} << 1$ for $n > 1$, and $\hat{h}_n >> 1$ for $n < 1$ was noted in the previous Section. It is worthwhile to investigate if Petersen's finding is valid for zero-order reaction under conditions that obtain for hydrogenation in solution on finely divided catalyst.

Considering the catalyst particles as spheres, it is once again noted that the rate of reaction per particle can be expressed by equation (3.19) and for a zero-order reaction by

$$r_p = \eta \; V_p \; \rho_p \; S \; k_o \tag{3.32}$$

Equations (3.19) and (3.32) are combined and simplified. The result, when solved for $\mathcal{J}$, is

$$\mathcal{J} = \frac{1}{1 + 12 \left(\frac{\theta}{\tau} \right) \left(\frac{1}{Sh.} \right) \eta \hat{h}^2_o} \tag{3.33}$$

If the two parameters θ / τ and Sh are fixed, equation (3.33) gives $\mathcal{J}$ as a function of the Thiele parameter $\hat{h}_o$, since η is also fixed by $\hat{h}_o$.

For large $\hat{h}_o$, the effectiveness factor is given by $\eta = 1/\hat{h}_o$. Therefore the asymptotic values of $\mathcal{J}$ and η are equal for

$$(\theta/\tau)(1/Sh) = 1/12 \tag{3.34}$$

For values of the parameters such that the product in equation (3.34) is greater than 1/12, $\mathcal{J}$ will be less than η for all $\hat{h}_o$. The maximum possible value of the product is obtained when the Sherwood number has a value of 2, corresponding to diffusion in a stagnant medium. The quantity θ/τ covers a considerable range for various catalysts, but a value close to the maximum to be expected is 0.5/2 = 1/4. Plots of $\mathcal{J}$ and η for a spherical particle with zero-order reaction are given in figure 3-1.

For given agitation condition and fluid properties, the Sherwood number approaches 2 as the particle diameter decreases. Levins and Glastonbury measured Sherwood numbers for solid copper spheres of 61.2 microns diameter in an agitated vessel and found some values less than 4 [5]. Since catalyst particles used in slurry reactors are often smaller and less dense than the copper spheres used, the region between the graphs of $\mathcal{J}$ for $(\theta/\tau)(1/Sh) = 1/8$ and 1/16 represents realizable conditions in a slurry reactor.

3.1.3 Experimental Program

Based on the theoretical developments in this section an experimental program can be developed. The model reactions chosen here are the hydrogenation of allyl alcohol and fumaric acid in aqueous and alcoholic solutions. The hydrogenation reactions are:

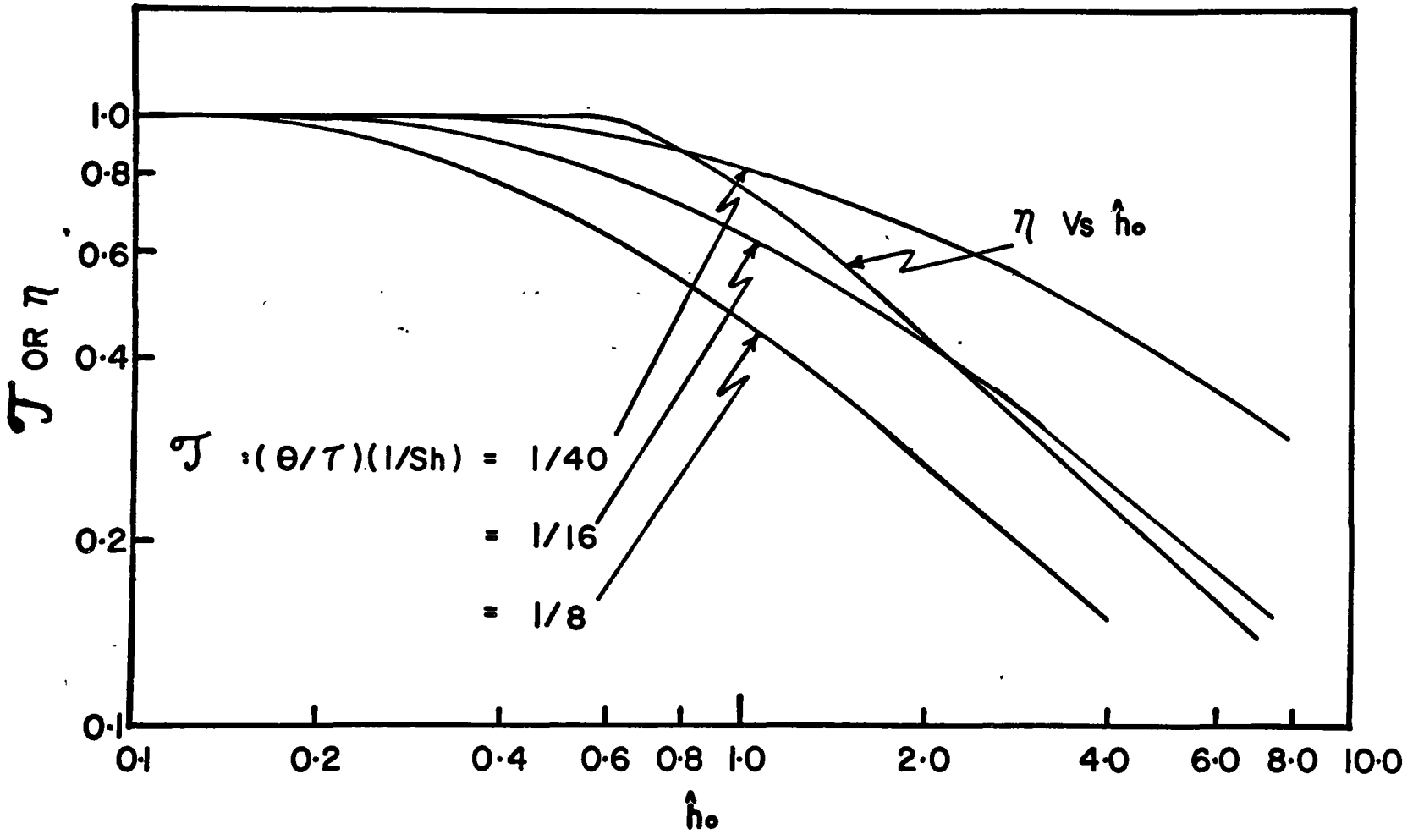

Fig. 3.1 Effectiveness factor and transport factor for a zero-order reaction in a spherical porous catalyst particle.

$$CH_2 : CH.\ CH_2\ OH + H_2 \xrightarrow{cat.} CH_3\ .\ CH_2.\ CH_2.\ OH$$

allyl alcohol — 1- propanol

$$HOOC - CH \overset{\|}{} HC - COOH + H_2 \xrightarrow{cat.} \begin{matrix} CH_2 - COOH \\ | \\ CH_2 - COOH \end{matrix}$$

fumaric acid — succinic acid

These reactions have previously been studied and the basic properties of them are listed below [38,39].

(i) There are no measurable side reactions when pure chemicals are used.

(ii) The reactions are irreversible at a temperature in the vicinity of 25°C.

(iii) No reaction takes place in the absence of catalyst.

(iv) The reaction rates are easily measurable at 25°C and one atmosphere hydrogen pressure.

(v) The rate of hydrogenation of allyl alcohol is several times that of fumaric acid [17].

The experimental program consists of studying the characteristics of the hydrogenation reactions such as orders with respect to hydrogen and substrate. Concentration ranges are then established experimentally where reaction rate is first order with respect to substrate concentration. Reaction rates are measured in this region at different hydrogen pressures and data obtained are plotted in accordance with equation (3.30),

to obtain the experimental values of $k_{p,A}\, a_p$. Hydrogenation rates are also measured as a function of substrate concentration over a wide range of concentrations, covering the region from zero order to first order with respect to the substrate. These results are used to study the internal and external mass transfer effects. Activation energy is obtained both in the first order region and zero order region for allyl alcohol in ethanol. Hydrogen concentration data are obtained from the hydrogen solubilities in the various solvents.

3.2 Solvent Effects in Heterogeneous Hydrogenation Reactions

3.2.1 Rate Equation for Acetone Hydrogenation

The hydrogenation of acetone on Raney nickel in various solvents is taken as a model reaction to study the solvent effects.

$$O = C\begin{matrix}\diagup CH_3 \\ \diagdown CH_3\end{matrix} + H_2 \xrightarrow[\text{cat.}]{} HO - HC\begin{matrix}\diagup CH_3 \\ \diagdown CH_3\end{matrix}$$

acetone isopropanol

The characteristics of this reaction are the same as those listed earlier in section 3.1.3. The additional reasons for choosing this reaction were its widespread use in the solvent effects studies and ease of handling.

For a catalyst with homogeneous active sites, mechanism for acetone hydrogenation assumed here is identical to the one used by Iwamato et al. [16] Assumed features of the reaction are:

(i) acetone and solvent are adsorbed on the catalyst active sites,

(ii) hydrogen undergoes dissociate adsorption,

(iii) adsorbed acetone and adsorbed hydrogen form a complex via steps (i) and (ii),

(iv) the complex is transformed to 2-propyl alcohol

The chemical equations corresponding to each of the above steps can be written as

$$\text{(i)}\quad A + * \underset{\underline{k}_A}{\overset{k_A}{\rightleftharpoons}} A - * \quad , \qquad K_A = \frac{k_A}{\underline{k}_A}$$

$$S + * \underset{\underline{k}_S}{\overset{k_S}{\rightleftharpoons}} S - * \quad , \qquad K_S = \frac{k_S}{\underline{k}_S}$$

$$\text{(ii)}\quad H_2 + 2 * \underset{\underline{k}_H}{\overset{k_H}{\rightleftharpoons}} 2\,H - * \quad , \qquad K_H = \frac{k_H}{\underline{k}_H}$$

$$\text{(iii)}\quad A - * + H - * \underset{\underline{k}_1}{\overset{k_1}{\rightleftharpoons}} A - H - * + * \quad , \qquad K_1 = \frac{k_1}{\underline{k}_1}$$

$$A - H - * + H - * \underset{\underline{k}_2}{\overset{k_2}{\rightleftharpoons}} A - 2H - * + * \quad , \qquad K_2 = \frac{k_2}{\underline{k}_2}$$

$$\text{(iv)}\quad A - 2H - * \underset{\underline{k}_3}{\overset{k_3}{\rightleftharpoons}} A - 2H + * \quad , \qquad K_3 = \frac{k_3}{\underline{k}_3}$$

Here A represents an acetone molecule and * is a vacant active site. K_A , K_S , and K_H are the adsorption equilibrium constants of acetone, solvent, and hydrogen, respectively. K_1 and K_2 are equilibrium constants for reactions in step (iii).

In the above mechanism it is assumed that the adsorption steps (i) and (ii) are much faster than the reaction steps and hence are not rate controlling. This assumption is justified in light of the previous work available in the literature [16, 40]. Also the adsorption of hydrogen and unsaturated compounds on Raney nickel catalyst has been shown to be instantaneous [17].

The rate equations corresponding to the above mechanism steps can be written as

$$r_A = k_A C_{A,b} C_* - \underline{k}_A C_{A-*}$$

$$= k_A \left(C_{A,b} C_* - \frac{1}{K_A} C_{A-*}\right) \quad (3.35)$$

$$r_H = k_H C_{H,b} C_*^2 - \underline{k}_H C_{H-*}^2$$

$$= k_H \left(C_{H,b} C_*^2 - \frac{1}{K_H} C_{H-*}^2\right) \quad (3.36)$$

$$r_S = k_S C_S C_* - \underline{k}_S C_{S-*}$$

$$= k_S \left(C_S C_* - \frac{1}{K_S} C_{S-*}\right) \quad (3.37)$$

$$r_1 = k_1 C_{A-*} C_{H-*} - \underline{k}_1 C_{A-H-*} C_*$$

$$= k_1 \left(C_{A-*} C_{H-*} - \frac{1}{K_1} C_{A-H-*} C_*\right) \quad (3.38)$$

$$r_2 = k_2 C_{A-H-*} C_{H-*} - \underline{k}_2 C_{A-2H-*} C_*$$

$$= k_2 \left(C_{A-H-*} C_{H-*} - \frac{1}{K_2} C_{A-2H-*} C_*\right) \quad (3.39)$$

$$r_3 = k_3 C_{A-2H-*} - k_{-3} C_{A-2H} C_* \qquad (3.40)$$

Assuming the first reaction in step (iii) to be rate controlling, the rate is given by

$$r = k_1 C_{A-*} C_{H-*} \qquad (3.41)$$

For steps (i) and (ii) at equilibrium, equation (3-41) becomes

$$r = k_1 K_A C_{A,b} \sqrt{K_H C_{H,b}}\, C_*^2 \qquad (3.42)$$

The value of C_* is obtained from the total number of active sites on the catalyst. At any time, in this case

$$C_t = C_* + C_{A-*} + C_{H-*} + C_{S-*} + C_{A-2H-*} \qquad (3.43)$$

Substituting from equations (3.35), (3.36), (3.37) and (3.39) into equation (3.43) and simplifying,

$$C_* = \frac{C_t}{1 + K_A C_{A,b} (1 + K_1 K_2 K_H C_{H,b}) + (K_H C_{H,b})^{\frac{1}{2}} + K_S C_S} \qquad (3.44)$$

where C_t is a characteristic property of the catalyst, independent of process variables and primarily depends upon the catalyst material and its method of preparation.

Substituting from (3.44) into (3.42) one gets

$$r = \frac{k_1 K_A C_{A,b} (K_H C_{H,b})^{\frac{1}{2}} C_t^2}{[1 + K_A C_{A,b} (1 + K_1 K_2 K_H C_{H,b}) + (K_H C_{H,b})^{\frac{1}{2}} + K_S C_S]^2} \qquad (3.45)$$

If in equation (3.45), the term $K_A C_{A,b}$ in the denominator is much larger compared to the other terms, then equation (3.45) shows that the reaction rate is zero order in acetone and one half order in hydrogen.

If the second reaction is step (iii) is the rate determining step then the reaction rate is given by

$$r = k_2 C_{A-H-*} C_{H-*} \qquad (3.46)$$

Assuming again that all other steps are in equilibrium and proceeding in an identical manner as above, one gets from equation (3.46)

$$r = \frac{k_2 C_t^2 K_1 K_A K_H C_{A,b} C_{H,b}}{[1 + K_A C_{A,b} (1 + K_1 \sqrt{K_H C_{H,b}}) + \sqrt{K_H C_{H,b}} + K_S C_S]^2} \qquad (3.47)$$

Equation (3.47) is identical to equation (1) of Iwamoto et al. [16]. If the quantity $K_A C_{A,b}$ is much larger than the other terms in the denominator, then equation (3.47) shows that the hydrogen dependence of rate is of first order.

Since hydrogen concentration in a solution is directly proportional to the hydrogen partial pressure over that solution, in the above equation, the concentration term $C_{H,b}$ can be replaced by P_H, introducing an

additional constant for each system. Also assuming that the variations in the partial pressure of hydrogen are not much for the different runs, the quantity $K_H P_H$ is taken as a constant. Thus upon rearranging equation (3.45) one gets

$$\left(\frac{C_{A,b} P_H^{\frac{1}{2}}}{r} \right)^{\frac{1}{2}} = \frac{1 + \sqrt{K_H P_H}}{K'_1} + \left(\frac{K_A + K_1 K_2 K_A K_H P_H}{K'_1} \right) C_{A,b} + \frac{K_S}{K'_1} C_S \qquad (3.48)$$

where

$$K'_1 = k_1 K_A \sqrt{K_H} C_t^2 \qquad (3.49)$$

The relation between $C_{A,b}$ and C_S is now introduced assuming that there is no volume change on mixing

$$\frac{M_A C_{A,b}}{\rho_A} + \frac{M_S C_S}{\rho_S} = 1.0 \qquad (3.50)$$

Here M_A and ρ_A are, respectively, the molecular weight and the specific weight (g/liter) of acetone, M_S and ρ_S refer to those of the solvent. Equation (3.48) then can be written as a function of acetone concentration as

$$\left(\frac{C_{A,b} P_H^{\frac{1}{2}}}{r} \right)^{\frac{1}{2}} = K'_3 C_{A,b} + K'_2 \qquad (3.51)$$

where K'_2 and K'_3 are a new set of constants obtained by combining various constants together.

A similar treatment to equation (3.47) will lead to the equation

$$\left(\frac{C_{A,b}\, P_H}{r} \right)^{\frac{1}{2}} = K''_3\, C_{A,b} + K''_2 \qquad (3.52)$$

where K''_2 and K''_3 are a different set of constants. Equation (3.52) is identical to equation (9) of Kishida and Teranishi [9], who used this equation to represent their data of acetone hydrogenation in liquid phase in different solvents.

Experimental data can be plotted in a manner suggested by equations (3.51) and (3.52) to determine which of the two models better represents the data.

3.2.2 Rate Equation in the First Order Region

At very low concentrations of acetone in solution where first order behavior is observed, equation (3.45) can be simplified in the limit $C_{A,b} \to 0$ as

$$r = \frac{k_1 C_t^2 K_A C_{A,b} \sqrt{K_H C_{H,b}}}{\left(1 + \sqrt{K_H C_{H,b}} + K_S \frac{\rho_S}{M_s}\right)^2} \qquad (3.53)$$

If the solvents used for the hydrogenation reaction are relatively non-adsorbing and if it is assumed that the properties of adsorbed hydrogen are independent of the solvents [16], then equation (3.53) for a constant hydrogen partial pressure can be written

$$r = K k_1 K_A C_{A,b} \qquad (3.54)$$

where
$$K = \frac{C_t^2 \sqrt{K_H C_{H,b}}}{\left(1+\sqrt{K_H C_{H,b}} + K_S \frac{\rho_S}{M_s}\right)^2} \qquad (3.55)$$

An identical treatment to equation (3.47) also results in an equation similar to equation (3.54).

Equation (3.54) represents the kinetic behavior in the first order region for constant hydrogen partial pressure. It consists of two terms, the kinetic constant, k_1, and the adsorption equilibrium constant, K_A, which are affected by the solvent. Also if in equation (3.54), the concentration term, $C_{A,b}$, is replaced by the activity of A in the bulk, a_A, then the new equation would show the effect of bulk activity on the reaction rate.

For different solvents, surface coverage of acetone can be obtained experimentally in the first order region where kinetic equation (3.54) is applicable. The reaction rates obtained can be correlated with surface coverage and liquid phase interactions to reveal the solvent effects.

3.2.3 Experimental Program

An experimental program can be drawn in view of the above discussions. The solvents to be used in this part of the study are benzene, cyclohexane, and isopropanol. These solvents are selected with the consideration that they should be non-adsorbing and their chemical nature be different so that their interactions with acetone fall on a wide range of values. Preliminary considerations show that acetone-isopropanol binary behaves like a regular solution [41], acetone -

cyclohexane forms a highly non-ideal solution [42], and acetone-benzene is a moderately non-ideal binary [43]. Other considerations of solvent selection were same as discussed in section 2.2.1.

The experimental program consists in studying the order of acetone hydrogenation reaction with respect to hydrogen partial pressure and acetone concentrations in different solvents. Pseudo-steady state rates of hydrogenation reactions are obtained for acetone concentration from 0-100 percent in the three solvents. The regions of concentration are established experimentally where the reaction is first order in acetone, and rate is tested for its being only kinetically controlled in this region. For these low acetone concentrations in the solution the quantity of acetone adsorbed on the catalyst surface is appreciable compared to the total quantity of acetone in the system. Thus the amount of acetone on the catalyst surface can be obtained by knowing the total quantity of acetone present in the system and at any instant measuring the concentration of acetone in solution by analyzing the liquid samples by gas chromatography.

Hydrogen solubility data for the pure components and the solvent-acetone binary systems are obtained experimentally. These data are needed to calculate both gas absorption resistance and the liquid phase concentration of hydrogen.

The vapor pressure-liquid composition data for acetone-benzene binary are taken from the literature, and those for acetone-cyclohexane and acetone-isopropanol binaries are obtained experimentally since these data are not available in the literature. Thermodynamic data are needed to establish acetone activity as a function of concentration for

purposes of investigating adsorption isotherms and reaction rates in different solvents as a function of acetone activity. Also, the hydrogen partial pressure in the gas phase is obtained by using vapor pressure-composition data for binary systems.

4. EXPERIMENTAL

4.1 Introduction

The experimental portion of this work was suggested by the need for a comprehensive set of reaction rates and gas solubility data for different systems at different pressures, temperatures, and substrate concentrations. For this purpose, the apparatus adopted was a modification of the gas solubility measurements apparatus used by Ben-Naim and Baer [44]. Changes were made in the design of the solubility cell, burets, and the manometer. The apparatus could successfully fulfil the requirements desired in a laboratory slurry reactor for precise work. These requirements were; precise temperature control, precise measurements of the system pressure, gas absorption rates, versatility of the apparatus to work at different system pressures and temperatures, and thorough suspension of the solid catalyst in the liquid phase.

A wide variety of experiments were performed in this study. They included measuring hydrogen solubility in liquids and liquid mixtures, obtaining data to calculate hydrogen-liquid mass transfer coefficients, measurements of reaction rates, studying the effect of the hydrogen pressure and substrate concentration on the reaction rates, effect of temperature to obtain the apparent activation energy of reactions, and simultaneous measurements of reaction rates and the catalyst surface concentrations. The experimental procedure for most of these measurements was similar. It mainly consisted of three steps. The first was to degas the liquid which was to act as the medium for the reaction, then to transfer the liquid from the degassing apparatus to the reaction cell, and finally to measure the hydrogen absorption rates. Details of the apparatus used, experimental procedures, and analytical techniques are given in the following pages.

4.2 Equipment

4.2.1 Unit for Liquid Degassing

The apparatus used for the liquid degassing was similar to the one reported by Clever et al. [45]. It consisted of a 500 ml bottle which was externally heated with an electric heating tape, the voltage of the power supply to which was controlled with a variable autotransformer. The top of the bottle was connected to the vacuum pump through cold traps. A 1 meter long, 2.5 cm diameter glass column was connected at the bottom of the bottle with a 8 mm glass tubing. A 2 mm high vacuum stopcock was provided between the bottle and the column. At the opening of the 8 mm glass tube in the column, a fine glass nozzle was connected to spray the liquid passing through it into fine droplets. The top of the column was also connected to the vacuum system. The bottom of the column was connected to a tygon tubing, through a 2 mm stopcock. The other end of the tygon tubing was connected to a 10/30 glass joint which could be connected to the solution flask.

4.2.2 Solution Flask

The solution flask was used to carry the degassed liquid under vacuum from the degassing apparatus to the slurry reactor. It consisted of a 1 liter round bottomed pyrex flask. At the opening of the flask a ₹ 45/50 male joint was connected. The female part of the joint was provided on the top of the male joint as a cap on the flask. Through this were made two connections, one with a ₹ 10/30 female joint connecting a 8 mm glass tubing through a 2 mm high vacuum stopcock. This served to connect the solution flask with the liquid degassing unit. The other end of this connection was about 3 cm

inside the cap. The second connection to the flask was a liquid delivery tube, consisting of a 8 mm glass tubing extending to the bottom of the flask. The other end of this tubing was connected to a male part of a ₹ 10/5 ball and socket ground joint through a 2 mm high vacuum stopcock. The flask was provided with a thermometer well to measure the temperature of the liquid in it. A side tube was provided with a 2 mm high vacuum stopcock to bring the apparatus to atmospheric pressure. The flask was externally heated with an electric heater; temperature was controlled by controlling the voltage of the input supply.

4.2.3 Reactor Set-up

The apparatus used for the measurements of the reaction rates and the gas solubilities in the liquids is schematically shown in figure 4-1. The apparatus can be divided for discussion purposes into three main segments. They were the bubbler or the saturator, the buret-manometer system, and the reaction cell.

The Bubbler

The bubbler A contained a solution of the same composition as in the reaction cell and served to saturate hydrogen gas taken in the burets with the liquid vapors.

It consisted of a glass container 4 cm diameter and about 30 cm long, the bottom being closed and the upper end having three different connections. The one in the center was a 10 mm glass tube extending to the bottom of the container. At the bottom end was connected a fritted glass tube of a size 2 cm long and 1 cm diameter for dispersing the gas in the liquid. The other two connections served as inlet for the liquid to the bubbler and the outlet for the gases, respectively.

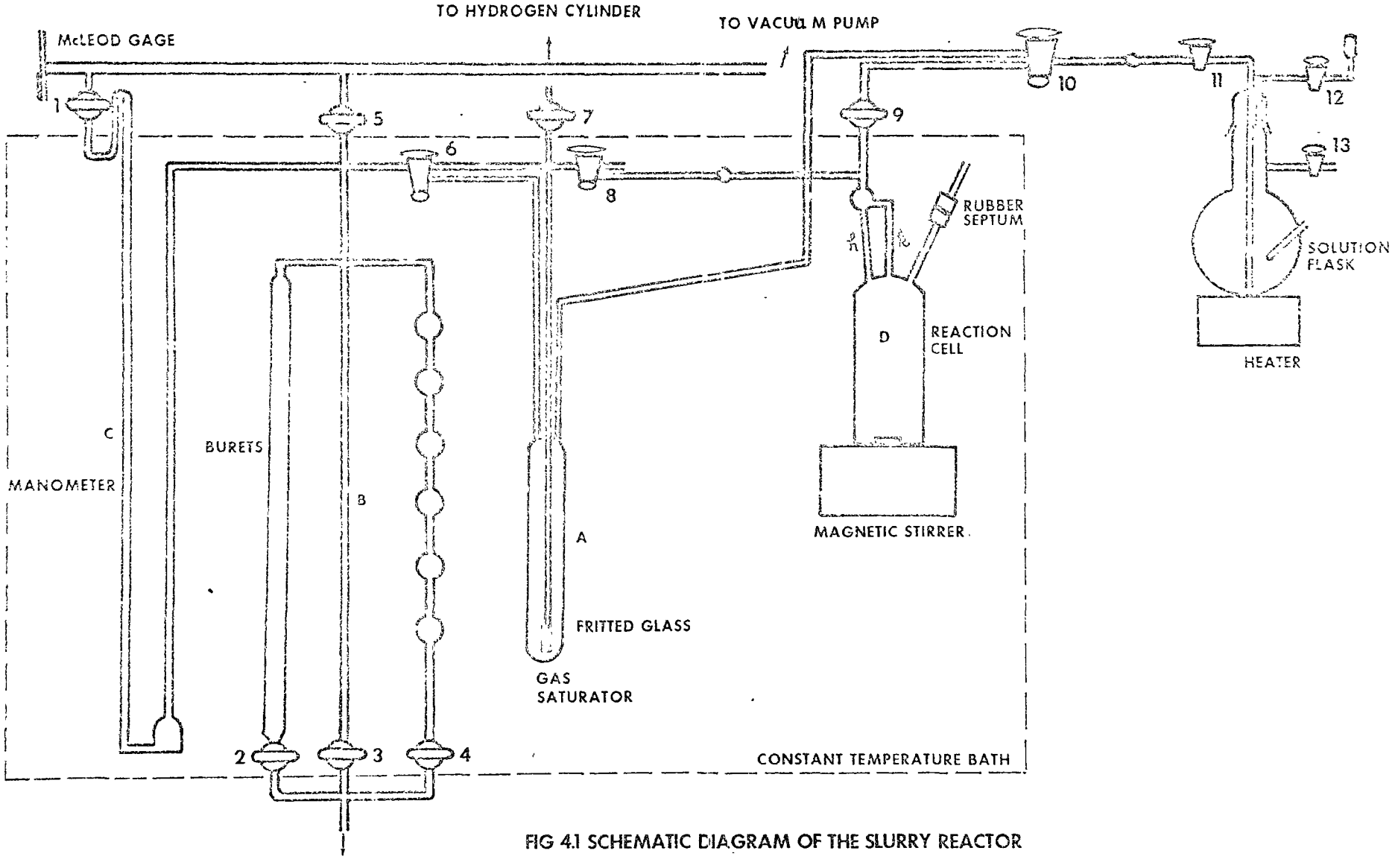

FIG 4.1 SCHEMATIC DIAGRAM OF THE SLURRY REACTOR

NOT TO SCALE

The gas outlet was connected to the burets. A 6 mm glass tube was provided near the top of the bubbler, which had a ground joint cap of ₹ 10/30 size. This was used to syphon the liquid from the inside of the bubbler when replacement of the liquid was desired.

The Buret-Manometer System

The buret-manometer system consisted of two distinct parts, the gas buret and the manometer. The gas buret B consisted of three arms, one made up of seven bulbs of known volumes connected with each other with a fine capillary tubing, the other a 10 ml fine bore buret with the smallest calibration of 0.02 ml. The third arm consisted of a straight column of uniform internal diameter, divided into three parts. The upper ends of the burets were joined at a common junction which was split into three branches, connected to the mercury reservoir of the manometer, vacuum system, and to the reaction cell, respectively. The reaction cell connection had a three way high vacuum stopcock; the two exits of the stopcock were connected to the bubbler and to the reaction cell, respectively. The bottoms of the burets were also connected to a single junction through separate stopcocks of 2 mm bore. The mercury reservoir was connected here with a tygon tubing.

The manometer C was absolute differential type with a mercury bulb at its lower end and its upper end sealed under vacuum. It was made of a 2 mm uniform bore capillary of a height of 80 cm, with mercury bulb of about 100 ml volume.

The Reaction Cell

The reaction cell D is shown in Figure 4-2. Its main body had a volume of about 250 ml with dimensions approximately 14 cm long and

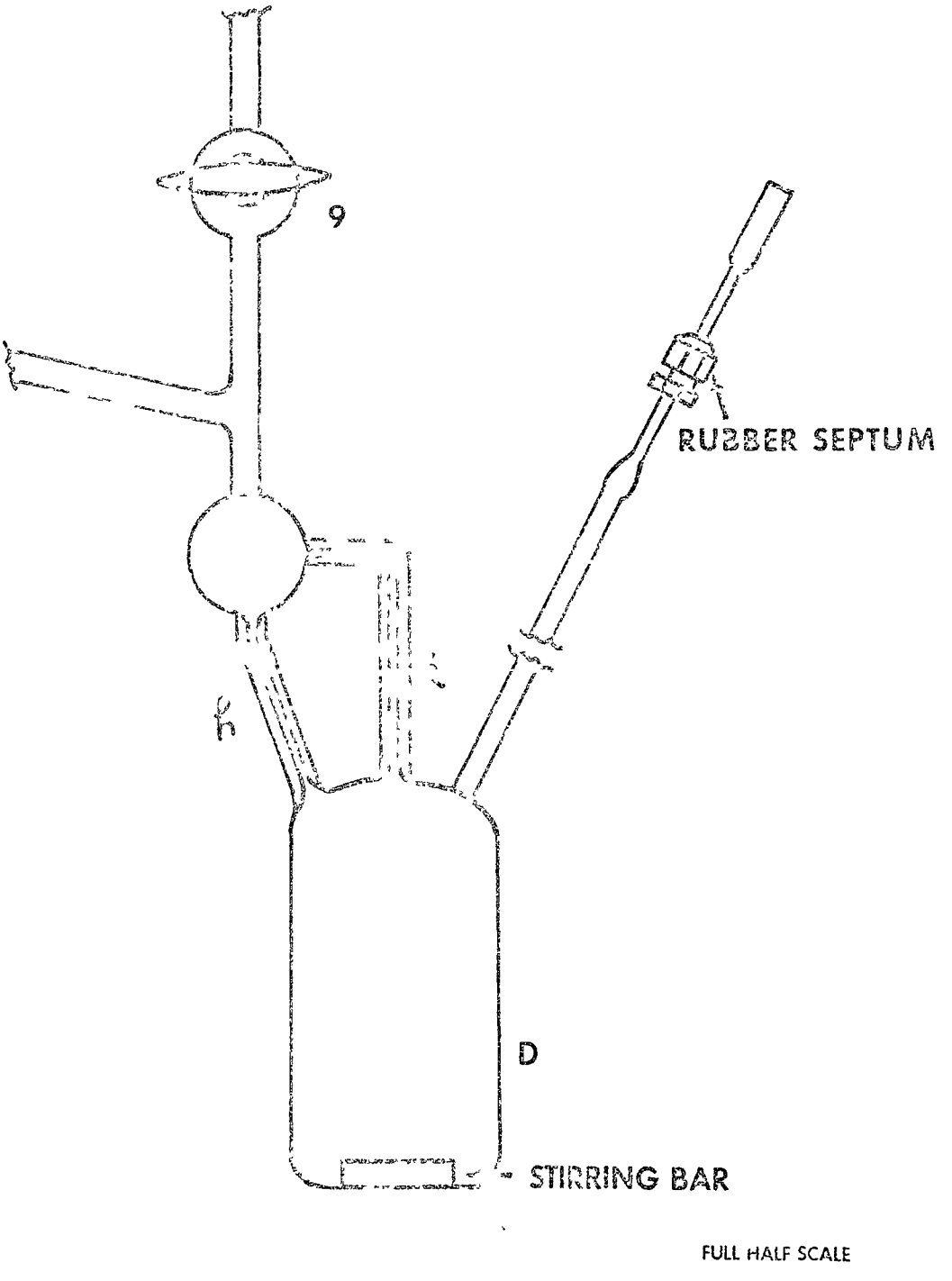

FIG 4.2 REACTION CELL

5 cm diameter. Two capillaries h and k of internal diameter 2 mm were connected to the vessel, one on the top center and the other on one of the sides near the top. The capillaries acted as the entrance and the exit of the liquid and the vapors, respectively. The upper ends of these capillaries were connected to a bulb of about 10 ml capacity. Two outlets connected to this bulb served to connect the reaction vessel to the buret-manometer system and to the solution flask, respectively. These connections were made with ₹ 10/5 grounded ball and socket joints. A side arm was provided to the vessel with a sealed rubber septum, where the desired quantity of the substrate could be injected into the reaction vessel or a sample of the liquid could be withdrawn with a syringe. A teflon coated magnetic bar, roughly 2.5 cm long and 0.62 cm in diameter was placed inside the vessel D, which served as a stirrer.

The whole apparatus was constructed inside a large plexiglass tank provided with a sealed box in it to place a motor for rotating the magnetic stirrer bar. A Colora ultra thermostat, model N, was used to circulate water in the tank and to maintain it at a constant temperature. A high speed stirrer was provided inside the tank to keep the water in it at a uniform temperature . The temperature inside the tank was measured with a calibrated thermopile by measuring the voltages with a Leeds-Northrup, type K-3, Universal potentiometer. The thermopile was calibrated against a Platinum resistance thermometer calibrated by the National Research Council of Canada. The expression correlating EMF with temperature is given in appendix II-9. The height of the mercury in the manometer was read using a kathetometer. Pressure in the apparatus was kept constant during the absorption of hydrogen with the help of a variable speed motorized elevator that raised the mercury

level in the burets. The quantity of the liquid contents in the reaction vessel were determined by weighing.

4.3 Precision of the Measurements

The temperature inside the tank was maintained within $\pm$ 0.05°C of the set temperature. The uniformity of the temperature in the tank was confirmed by measuring temperature at several different locations. The precision of the pressure measurements was of the order of $\pm$ 0.01 Torr. The measurements of gas volumes was of a precision better than $\pm$ 0.01 ml. The quantities of the liquid were weighed within $\pm$ 0.05 g.

4.4 Calibration of the Burets

The volumes of the three burets were determined at 25°C by filling them with mercury and then weighing the amount of mercury contained up to the specific marked heights of the burets or the bulbs. The mercury employed in these determinations was cleaned with weak sodium hydroxide and nitric acid solutions before being distilled under vacuum. The results of these determinations are presented in table 4-1. Since most of the experimental work was done in the vicinity of 25°C, volume variations with temperature were neglected.

4.5 Testing of the Vacuum for the System

A Precision Scientific Company vacuum pump was employed for evacuating the apparatus before a run was to begin. The pump was protected from the carryover of harmful vapors by inserting a liquid nitrogen cold trap between the apparatus and the pump. A McLeod gauge was connected to the mainline of the apparatus for determining the

TABLE 4-1

Calibration of Burets

BULBS

No. of Bulb	Average volume* ml
1	9.48
2	9.29
3	9.64
4	10.48
5	10.03
6	10.64
7	10.47

COLUMN

Section of Column	Average volume* ml
I	7.54
II	11.73
III	15.09

BURET

Average error of the buret calibration over the readings marked is 0.67%

* Average of three measurements

pressure inside the apparatus. In practice, the system including the burets and reaction cell could be evacuated to 2 or 3 microns very quickly. A 75 hour leak test of the reaction vessel and the burets under vacuum indicated a leak rate of 0.05 microns/hr. This was considered quite acceptable since in operation the system was mostly in the vicinity of atmospheric pressure and most of the runs took only 3 - 4 hours.

4.6 Materials

The various materials used during the course of this study included hydrogen gas, Raney nickel catalyst, and several unsaturated compounds and solvents. The quality and the sources of these materials are given below.

4.6.1 Gases

Except for the runs which were made to test the performance of the apparatus in which oxygen gas was used, all other experiments were performed using hydrogen gas. The oxygen used was of ultra pure quality obtained from Matheson of Canada Ltd. The hydrogen gas was obtained from the liquid carbonic Canada Corporation Ltd., and was of a guaranteed minimum purity of 99.97 percent. Before introducing hydrogen gas into the apparatus, it was passed through a Deoxo catalytic purifier to remove any traces of oxygen present and then through a bed of "Drierite", obtained from W.A. Hammond Drierite Company, Ohio, to absorb any moisture present in it.

4.6.2 Substrates

Certified grade allyl alcohol was obtained from Fisher Scientific Company. Fumaric acid was 99 percent pure from Matheson, Coleman and Bell. Acetone used was "Reagent grade" (99.9 percent assay) from J.T. Baker Chemical Company. All these substrates were used

without any further purification. In the solvent effect studies, where the liquid phase was analyzed by Gas Chromatographic method, GC - Spectrophotometric quality of acetone was used.

4.6.3 Solvents

The solvents used in the mass transfer studies were distilled water and 99.9 percent ethyl alcohol obtained from Canadian Industrial Alcohols and Chemicals Ltd. Those used in the studies of solvent effects were benzene, cyclohexane and iso-propanol. All these were "Reagent Grade" obtained from J.T. Baker Chemical Company. Solvents used in the chromatographic studies were GC - Spectrophotometric quality, obtained from J.T. Baker Chemical Company. All solvents were used without any further purification.

The purity of the chemicals used was confirmed by measuring their densities and refractive indices and comparing them with the literature data. These data are presented in table 4-2.

4.6.4 Catalyst

The Raney nickel catalyst used in this study is designated No. 28 Standard Active Nickel by the manufacturer, W.R. Grace and Co., and corresponds to a W-1 catalyst. The catalyst was stored at 10°C. All experiments were conducted over a period of 2 years during which time no systematic change in catalyst activity occurred. A histogram supplied by the manufacturer based on the Sieve analysis yielded a Sauter mean diameter of 16 microns. In calculations the internal void was taken as 0.50. This value is reported by Freel et al. [67] for a similar Raney nickel catalyst. The BET surface area of the catalyst was determined at the Energy Mines and Resources Branch in Ottawa. The average value of the duplicate runs was 58.1 m^2/g.

TABLE 4-2

Physical Properties of Pure Solvents at 25°C

	Acetone	Benzene	Cyclohexane	Isopropanol
Density g/cm^3				
Experimental	.78554	.8735	.77291	.78092
Literature	.78508 [48]	.87368 [48]	.77375 [48]	.7809 [48]
Refractive Index				
Experimental	1.3566	1.4979	1.4233	1.3744
Literature	1.35662 [48]	1.4979 [48]	1.4233 [48]	1.3743 [49]

4.7 Procedure

General Procedure

The procedure described under this head covers the general steps which were common in all the measurements made with the setup described above. For specific experiments, the procedures have been outlined separately.

4.7.1 Preparation of a Run

Before proceeding with a run it was necessary to evacuate the apparatus. In order to protect the vacuum pump from the vapors of the solvents, the cold trap was cooled with liquid nitrogen. Before starting the vacuum pump the mercury levelling reservoir was set in a proper position and all the three stopcocks, Nos 2, 3 and 4, were closed. The vacuum pump was then started and the entire system including the saturator, burets, and the reaction cell were evacuated. The water bath was set at the desired temperature of the measurements.

4.7.2 Degassing of the Solvents

About 400 ml of the solvent was charged into the bottle of the degassing unit and the electric heating tape was turned on. Depending on the nature of the solvent, the heat load was adjusted by varying the voltage of the electric supply. After a little initial heating the pressure in the vessel was reduced by connecting it to a vacuum pump through two cold traps, the first containing crushed ice (in certain cases liquid nitrogen) and the second liquid nitrogen, to recover the vapors of the solvents. The vacuum pump at the same time was evacuating the column. After boiling liquid under vacuum for about 20-30 minutes, during which time about 20 percent of the solvent evaporated, the liquid was sprayed through the nozzle into the column. Liquid, partly in small droplets and

partly in the form of mist, flowed down to the bottom of the column where it was collected into a previously evacuated flask. Time taken to collect a volume of 250 - 300 ml of degassed solvent was roughly 30 - 40 minutes.

The total quantity of the absorbed gases removed from the liquids is expected to be more than 97-98 percent [50].

4.7.3 Introduction of Solvent into Reaction Vessel and Saturator

The solution flask after disconnecting from the degassing apparatus was connected through a ball and socket joint to the main apparatus, which was already under vacuum. The connecting lines were then evacuated by opening stopcock number 10. The liquid contained in the flask was heated with an electric heater so as to establish pressure inside the flask. Stopcock numbers 9, 10 and 11 were then opened to connect the flask with the reaction cell. The liquid flowed from the flask to the cell without coming in contact with air and was filled in the cell to a level about 2 cm from the top. During all this operation the vacuum pump was cut off from the apparatus. Solvent was also introduced into the saturator in an identical manner. The level of solvent in the saturator was mostly about 4-5 cm above the upper end of the fritted glass tube.

Liquid was allowed to stand in the reaction vessel and in the saturator for 15-20 minutes to bring it to the temperature of the system.

4.7.4 Introduction of the Gas

Hydrogen gas from the gas cylinder was taken with a two step pressure regulator with the output pressure of 50 psi. To this was

connected, in series, a low pressure regulator the output of which was adjusted to 1-2 psi. The gas after passing through a "Deoxo-catalytic purifier" and a bed of "Drierite" was introduced into the saturator through a needle valve. Gas was bubbled in the liquid at a very slow rate so as to give it a maximum residence time in the liquid for a better saturation. This gas was then taken into the buret and the reaction cell. Since in the design of the present setup, gas stays in contact with the liquid during the whole period of measurements, it was assumed that eventually the gas was fully saturated with the solvent vapors. Sufficient amount of the gas was introduced into the system till the pressure inside was reached to the desired value which was indicated by the mercury level in the manometer. The telescope of the kathatometer was then set at that position.

4.8 Specific Procedures

4.8.1 Determination of the Gas-Liquid Mass Transfer Coefficients

Steps 4.7.1 to 4.7.4 were performed as explained above. The telescope on the cathetometer was set at a height which corresponded to approximately one atmosphere pressure in the system. The initial reading on the burets were read and the magnetic stirrer was turned on. The mercury level in the burets was continuously adjusted to maintain constant pressure in the apparatus. The volume of gas absorbed was recorded as a function of time. Initial absorption rate data were plotted in a manner as given in Appendix II for the determination of the gas - liquid mass transfer coefficients. The quantity of the liquid was obtained by weighing the contents of the cell.

4.8.2 Determination of the Gas Solubilities

Experimental procedure was identical to the one outlined above with the exception that the amount of the gas absorbed did not need to be recorded as a function of time. Gas was absorbed in the liquid until the mercury level in the manometer was constant for about one hour. The final readings on the burets were noted. The difference between the initial and the final readings represented the quantity of the gas absorbed. The quantity of the liquid was obtained by weighing the contents of the cell.

4.8.3 Determination of the Reaction Rates (Low Substrate Concentration)

Steps 4.7.1 to 4.7.4 were performed as explained above, with the exception that in this case an approximately known quantity of the catalyst was introduced in the reaction vessel before connecting it to the apparatus. The catalyst was introduced with a 2 ml syringe having a 22 cm long needle of approximately 0.15 cm inner diameter, through the side arm of the reaction cell. The solvent and the catalyst were then saturated with hydrogen by turning the magnetic stirrer on. A known quantity of substrate was injected into the system through the rubber septum provided on the side arm of the reaction vessel. Vigorous stirring was continued. The hydrogen absorption rate was measured as a function of time. These data were then used to determine the reaction rates. The quantity of catalyst in the reaction system was estimated using a spectrophotometer, as described in section 4.9.1.

4.8.4 Determination of Reaction Rates (High Substrate Concentration)

In this, steps 4.7.1 to 4.7.4 were performed as above with the exception that the catalyst was introduced into the cell before the liquid, and the liquid introduced consisted of a solution of the substrate and the

solvent. The solutions were made by degassing the substrate and the solvent separately and then mixing the known quantities in the solution flask. The liquid mixture and the catalyst were first allowed to saturate with hydrogen for 20-30 minutes and then the reaction rates were measured. The two processes, gas absorption and the chemical reaction, started simultaneously in this case. It was thus essential to use small quantities of the catalyst so that the reaction rates were slower than the gas absorption rates. In that case it could be assumed that after some time the solution was saturated with hydrogen and the hydrogen being absorbed was only used for the chemical reaction. Data treatment to obtain reaction rates is outlined in Appendix II.

4.8.5 Simultaneous Measurements of Reaction Rates and Surface Concentrations

Steps 4.7.1 to 4.7.4 were performed, except the catalyst taken in the reaction vessel was dried under vacuum before the solvent was introduced. Drying of catalyst removed any traces of different solvents which could have been introduced into the system by the liquid carried with it. These small quantities, however, had no effect on the reaction rates but could hinder the analysis of the liquid phase by chromatography when analyzing very dilute solutions of acetone.

Catalyst and solvent were saturated with hydrogen by stirring the contents of the cell for about one hour. A known quantity of acetone was then injected into the cell through the rubber septum. The volume of hydrogen absorbed was recorded as a function of time. At known intervals of time, liquid samples were taken from the cell with the help of a hypodermic syringe with a long fine needle. These samples were analyzed by gas chromatography, details of which are given under a

separate heading. The changes in the volume of the system caused by the removal of these samples were immediately measured by mercury displacement in the buret and was accounted in the volume of the gas reacted. The quantity of acetone on the catalyst surface was then obtained by simple mass balance in the reacting system.

4.9 Analytical Techniques

4.9.1 Analysis of Nickel

The quantity of Raney nickel catalyst used was determined as grams of nickel with a Unicam Atomic Absorption Spectrometer, Model SP 90A. Catalyst contained in the reaction vessel was dissolved in hydrochloric acid and the solution was diluted to a known volume. A standard solution of Nickel prepared from the metal obtained from J. T. Baker Chemicals Company was diluted to make thirteen standard solutions of nickel concentration varying from 1 ppm to 15 ppm. These solutions were used to make a calibration curve for the spectrometer. A typical calibration curve is shown in Figure VI - 4. The operating conditions for the spectrometer used in this analysis were as follows:

slit width	0.15mm
lamp current	10 μA
wave length	232 mμ
air flow rate	5 l/min
acetylene flow rate	800 ml/min

Under these conditions, the sensitivity of the spectrometer was 0.8 ppm Ni.

The spectrometer was calibrated every time before analyzing the samples. The range of duplicate measurements was within 4 percent of the mean.

4.9.2 Analysis of Acetone

The quantity of acetone was determined in the liquid phase while the reaction was in progress. The analysis was done with a Fisher Gas Chromatograph, Series 2400, using a flame ionization detector. Nitrogen was used as a carrier gas.

Acetone in Benzene and Isopropanol

Acetone was analyzed in solutions of acetone-benzene and acetone-isopropanol binaries using a 10' x 0.125 ", stainless steel column with 10 percent Carbowax 600 on chromosorb W, acid wash, of mesh size 60/80. The operating conditions for the chromatograph were:

column temperature	45°C
injector temperature	150°C
detector temperature	150°C
nitrogen flow rate	25 ml/min
hydrogen flow rate	25 ml/min
air flow rate	250 ml/min
range	10^{-12} amps/mv

Five standard solutions of each acetone in benzene and acetone in isopropanol, were made in the concentration range of acetone from 0.001 to 0.01 g mol/l. These samples were run in duplicate into the chromatograph using samples of 2 µl. A Repro-jector, automatic

sample injector obtained from Shandon Scientific Company Limited, was used for injection purposes. Reproducibility of the chromatograph was within 1 percent of the mean. Reproducibility of analyses from duplicate hydrogenations was within 2.5 percent of the mean.

Chromatograms were recorded on a Series A-25, Varian Aerograph Strip Chart Recorder using a Series 200 Disc integrator. Calibration curves were made using both the areas of the peaks and the peak heights. More reliable analysis was obtained by using the peak heights than peak areas, because peak heights could be determined with greater accuracy than peak areas in the case of smaller peaks.

Typical chromatograms are shown in Figures VI-5 and VI-9 and the calibration curves in Figures VI-6 and VI-10.

Acetone in Cyclohexane

On a Carbowax 600 column, for an acetone-cyclohexane mixture, cyclohexane peak appeared first and hence separation was not possible for very dilute solution of acetone. Several other columns were tried and Squalane column was accepted for this analysis. The column used was 25' x 0.125" copper column with 4 percent Squalane on Chromosorb G, acid washed, of a size 80/100 mesh. The operating conditions for the chromatograph were:

column temperature	82°C
detector temperature	150°C
injector temperature	150°C
nitrogen flow rate	18 ml/min
hydrogen flow rate	25 ml/min
air flow rate	250 ml/min
range	10^{-12} amps/mv

Isopropanol, which was the product of the reaction, and acetone peaks overlapped on the chromatograms obtained. The area of the individual peak was obtained by using the relation [46]:

$$\text{First peak area} = \frac{h_1}{h_1 + h_2} \times \text{Total area}$$

where h_1 and h_2 are the heights of acetone peak and isopropanol peak, respectively.

The calibration curve obtained from the standard solutions is presented in Figure VI-7. A typical chromatogram obtained is shown in Figure VI-8.

4.10 Performance Test

Solubility of Oxygen in Distilled Water at 25°C

To test the performance of the equipment, the accuracy and the reproducibility of the measurements, oxygen solubility data in distilled water was measured. These data were obtained in accordance with the procedure outlined in section 4.8.2. The average value of the Bunsen coefficient obtained was 0.0283; the value recommended by Battino and Clever [47] to be used as a comparison standard is 0.02847. The standard deviation based on seven replicate runs was, in the units of Bunsen coefficients, 2×10^{-4}. The scatter in the data are thought due principally to imperfect degassing of water.

5. RESULTS AND DISCUSSIONS

In accordance with the objectives in section 1. 4, this chapter is discussed in two parts. First, the results obtained from the mass transfer studies are discussed, and then solvent effects on hydrogenation of acetone are presented. The general method of calculations and some of the sample calculations are presented in Appendix II. Hydrogen solubility data are discussed in details in Appendix IV. In Appendix V and VI are given the experimental data used in this chapter. In Appendix VII calculations are given to show that the temperature difference between the catalyst particles and the solution was negligible. Complete experimental and calculated data covering all phases of the work done in this study are with the Department of Chemical Engineering, University of Ottawa, Ottawa.

5.1 Mass Transfer Effects

The model reactions used in the mass transfer studies were the liquid phase hydrogenation of allyl alcohol in the solvents water and ethanol and of fumaric acid in the solvent ethanol on Raney nickel catalyst. Reactions were conducted in the temperature range 24. 5-35. 3°C, most runs being at 25°C. Hydrogen partial pressure ranged from 100-730 mm Hg.

5.1.1. Characteristics of Hydrogenation Reactions

For all three systems, the rate was approximately zero-order in substrate at substrate concentration greater than about 0. 01 mol/l. The reaction order for hydrogen in the regions zero-order with respect to substrate was measured and are shown in figure 5. 1. The abscissa in figure 5. 1 is the partial pressure of hydrogen that would be in equilibrium with the measured $C_{H,b}$. The reaction orders calculated from the slopes of figure 5. 1 are 0. 96 for allyl alcohol in water, 0. 42

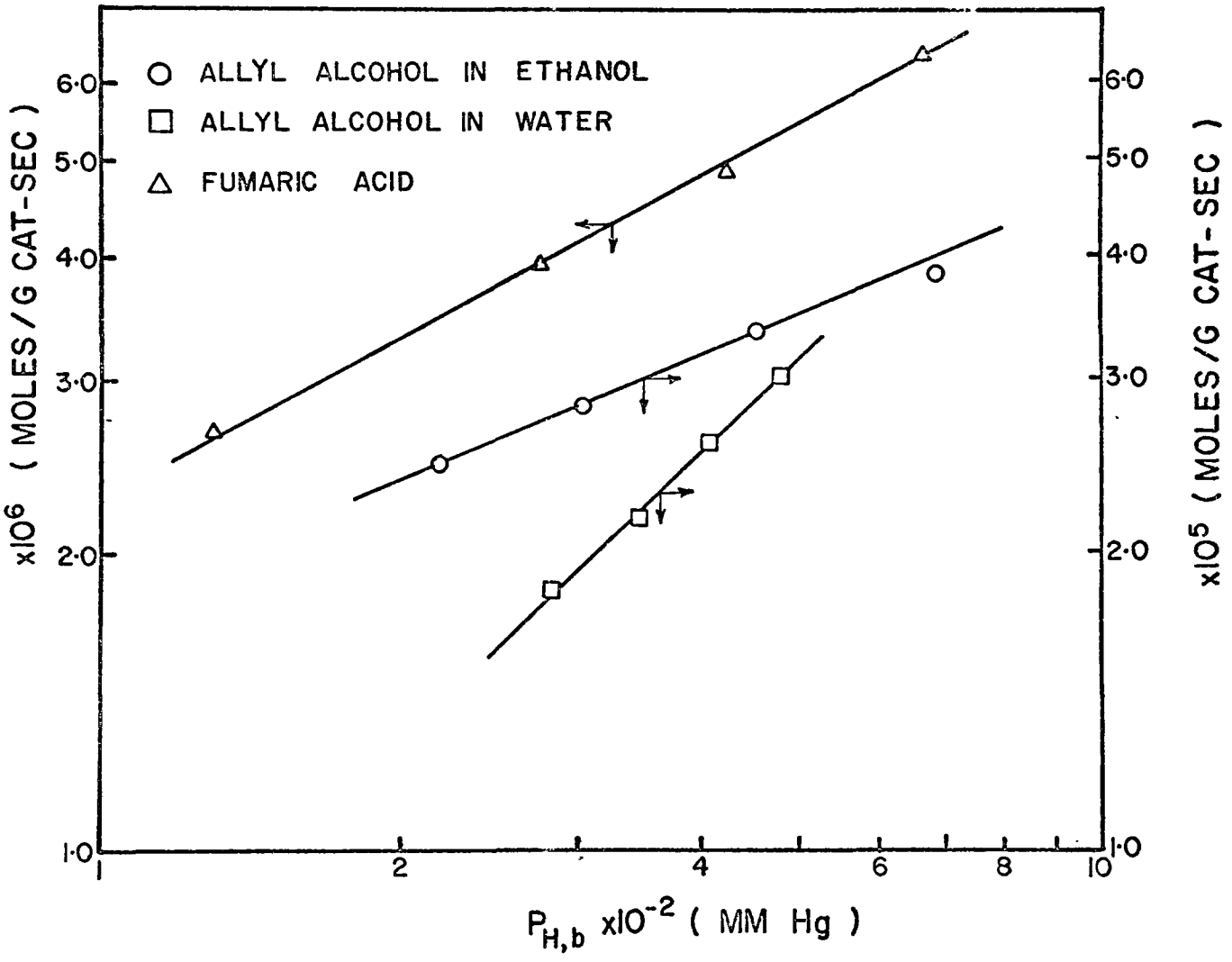

Figure 5.1 Dependence of reaction rate on hydrogen partial pressure at 25°C

for allyl alcohol in ethanol, and 0.53 for fumaric acid in ethanol. By use of $C_{H,b}$ or equivalently $P_{H,b}$ to investigate the effect of hydrogen partial pressure on rate, the effect of gas absorption resistance has been eliminated. The plots yield no information, however, about possible mass transfer resistance involving the catalyst particles.

The effect of substrate concentration on reaction rate is shown in figure 5.2, where the portion of the figure at the right is an enlargement of the region where the abscissa approaches unity. The quantity $C_{A,o}$ is the initial substrate concentration for a reaction. The figure is meant to show that for all three systems the rate is nearly zero-order in substrate over a sizable range in substrate concentration, and that at sufficiently low substrate concentration the rate is first-order in substrate. The high concentration portions of the plots for the system containing allyl alcohol do not look to be zero-order, but it should be noted that passing from an abscissa value of zero to 0.95 represents a 20-fold concentration change. When these data are plotted on a log-log graph the measured order is -0.08 for allyl alcohol in water and 0.15 for allyl alcohol in ethanol. Fumaric acid in ethanol shows zero order. These data are shown in figure 5.3

5.1.2 Determination of Mass Transfer Coefficients

To obtain the particle-liquid mass transfer coefficients, reaction rates were measured for the three systems at a number of hydrogen partial pressures in the region of sufficiently low $C_{A,b}$ that the rates were first-order in substrate; only for the fumaric acid system was the quantity $C_{A,b}/r$ a function of $C_{H,b}$. Since the rate in the fumaric acid system was found to be one half order with respect to hydrogen,

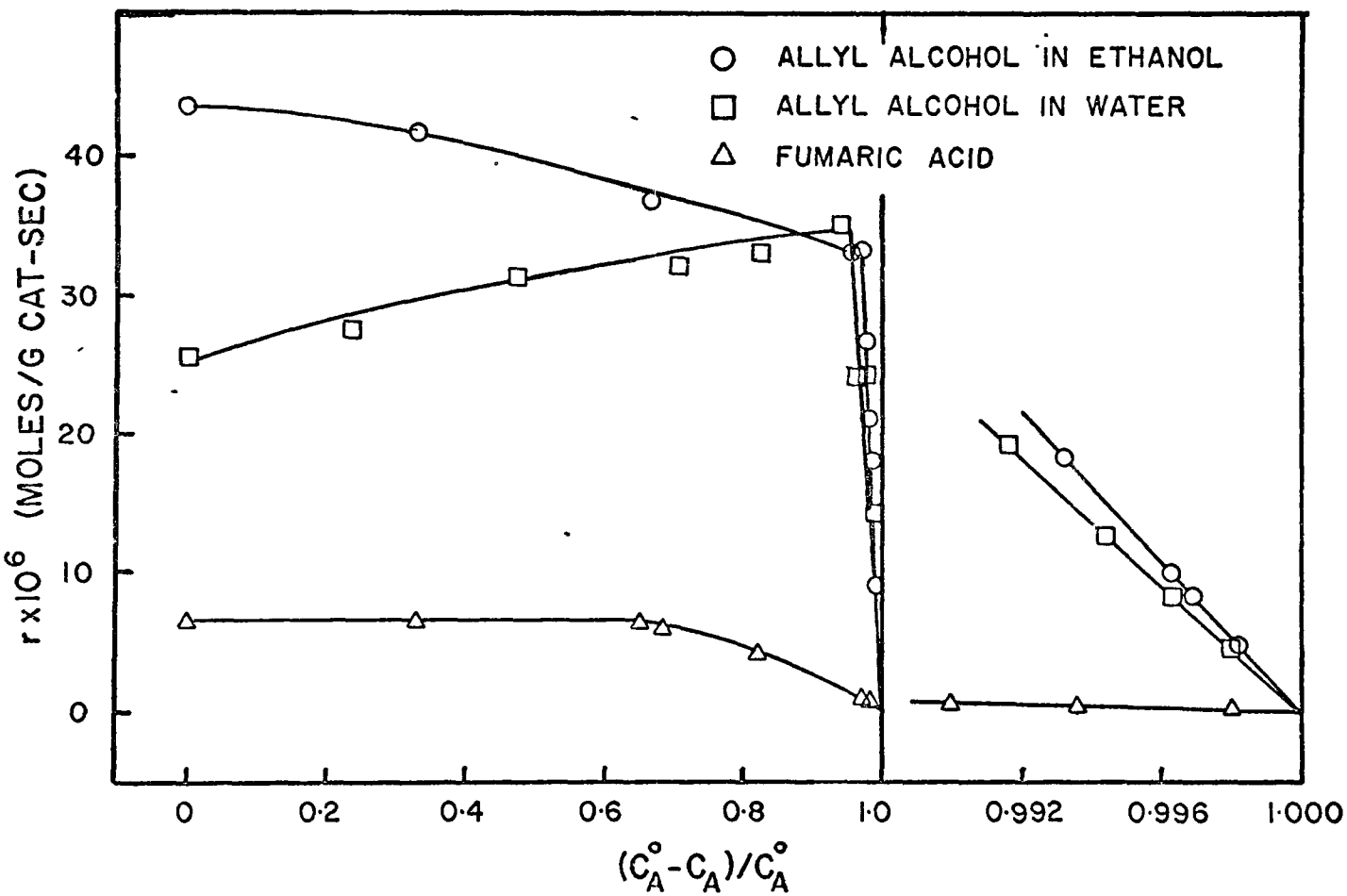

Figure 5.2 Reaction rate as a function of substrate concentration at 25°C. Allyl Alcohol in water: $C_{A,O}$ = 0.1144 mol/l. Allyl alcohol in ethanol: $C_{A,O}$ = 0.201 mol/l. Fumaric acid in ethanol: $C_{A,O}$ = 0.1148 mol/l.

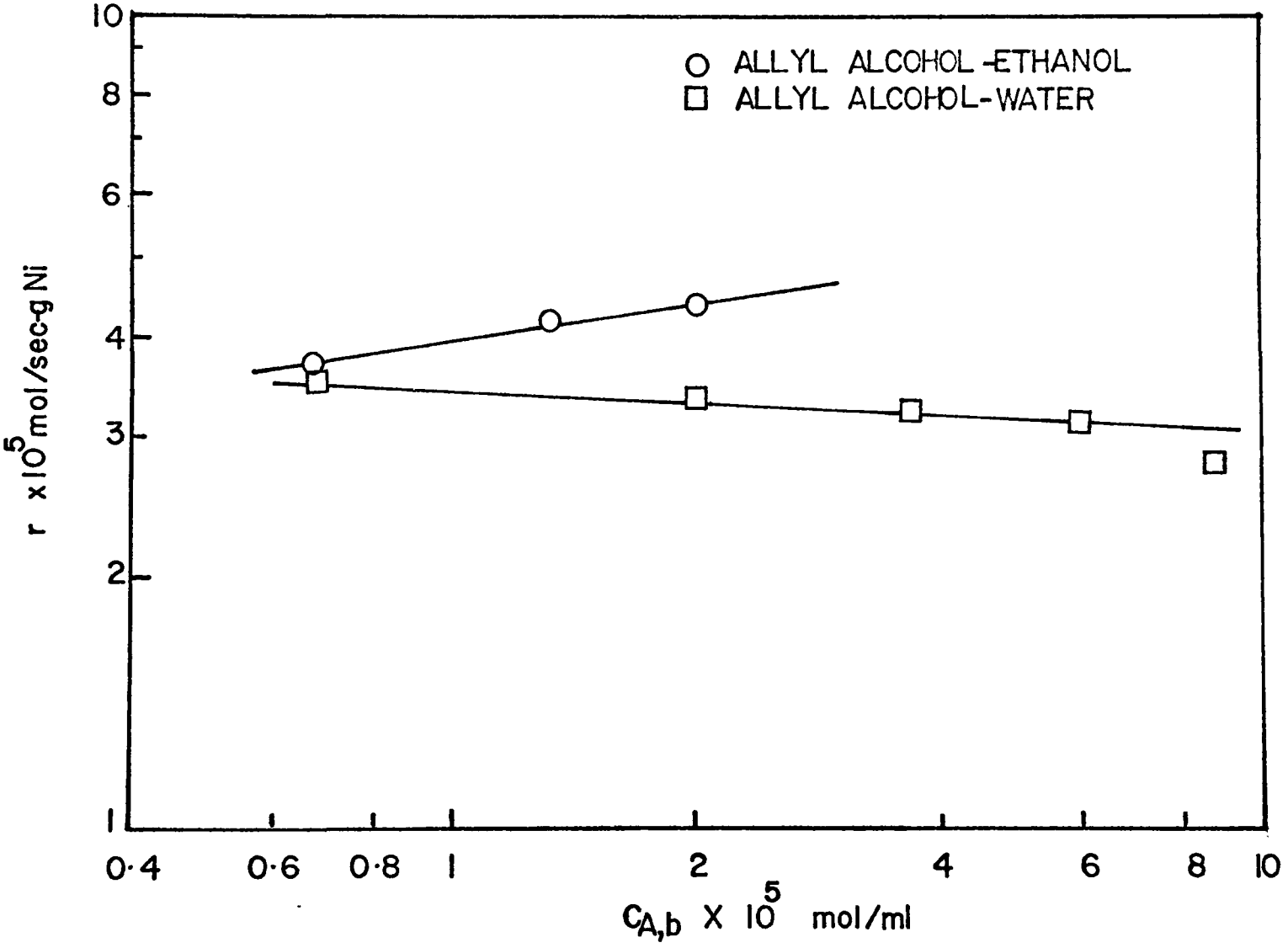

Figure 5.3 Dependence of reaction rate on substrate concentration at 25°C

the data are plotted in the manner suggested by equation (3-30) with the abscissa being $1/P_{H,b}^{0.5}$. The data are shown in figure 5.4. Since the ordinate used in the plot employs rate per unit mass of catalyst, r, the intercept predicted by equation (3-30) is the quantity $(k_{p,A}a_p)^{-1}$.

The reciprocal intercepts of the plots for the system allyl alcohol in water and allyl alcohol in ethanol are 20.0 and 13.3 cm^3/sec-g, respectively. These values were obtained by assuming that the graphs for the data of both systems had zero slope. A least squares fit of the data for the two systems yields a slightly negative slope in each case. A negative slope implies an inverse correlation of rate with hydrogen pressure, which was not observed in any other experiments. It was therefore decided that the slightly negative slopes were due to experimental error, and the y-intercept for each system was calculated as the mean of all the measured $C_{A,b}/r$ values. Again, a least squares slope of the data for fumaric acid in ethanol yields a value for $k_p a_p$ of 16.2 cm^3/sec-g. The concentration of reactants for all experiments whose results are shown in Figure 5.4 were extremely dilute. It is therefore expected that only the solvent should affect the value of $k_p a_p$. For this reason the intercept of the data for fumaric acid is shown as equal to that for allyl alcohol in ethanol.

For several reasons it is believed that the values of $k_p a_p$ in the water and ethanol solvents were 20 and 13 cm^3/sec-g, respectively. First, they are reasonable based on published correlations on k_p for particles in agitated liquids. Using a mean particle diameter of 16 microns, and assuming liquid agitation was "mild", calculated values of $k_p a_p$ using the correlation of Levins and Glastonbury[5] were 20 and 17 cm^3/sec-g for the solvents water and ethanol, respectively. Detailed calculations of these are presented in Appendix II-6. It should be admitted that the intensity of agitation used in these calculations was chosen to give the best agreement. Levins and Glastonbury define three levels of agitation intensity based on experiments in baffled tanks. There is no obvious way to determine agitation intensity in the experiments performed in this work, where agitation was by a magnetic stirring bar in an unbaffled cell.

The reciprocal intercepts for the allyl alcohol systems in figure 5.4 are apparently $k_{p,A}a_p$ also because the theory leading to equations (3-29) and

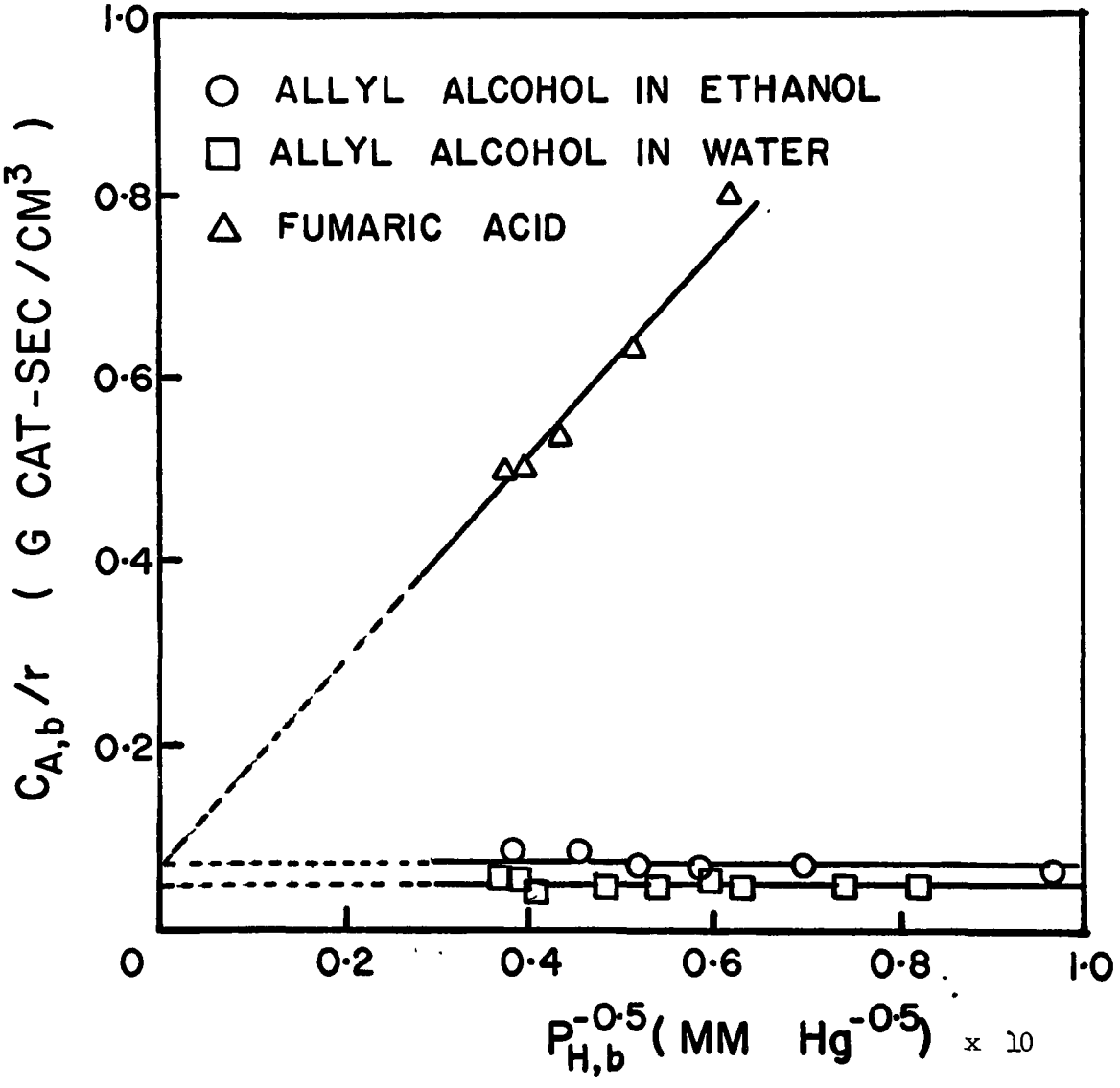

Figure 5.4 Reaction rates with linear dependence on bulk substrate concentration at 25°C.

(3-30) describes the two systems. If the reactions were either kinetically controlled or in the asymptotic region of internal particle resistance, the rates would have shown a dependence on $P_{H,b}$. In the allyl alcohol ethanol system the range of $P_{H,b}$ was 108-677 mm Hg, a 6.3 fold change. Assuming the intrinsic rate expression depends on $P_H^{\frac{1}{2}}$, the expected range of $C_{A,b}/r$ would have been $6.3^{\frac{1}{2}} = 2.5$ if the reaction were kinetically controlled. If the reaction were in the asymptotic region of internal partical resistance, the expected range of $C_{A,b}/r$ would have been $6.3^{\frac{1}{4}} = 1.6$. No such dependence on $P_{H,b}$ was observed. If the intrinsic rate expression for allyl alcohol in water depends on $P_H^{1.0}$, an even greater dependence on $P_{H,b}$ would be predicted, which again was not observed. Further evidence that $k_{p,A}a_p$ has been measured, based on activation energies, is presented here.

5.1.3 Use of $\mathcal{J}$ to Detect Significant Diffusion Resistance

The experimentally measured values of $k_{p,A}a_p$ were used to verify that the external particle diffusion resistance for hydrogen was negligible for reactions in which $C_{A,b}/r$ was measured, as is required for equation (3-30) to apply. It was assumed that $k_{p,A}a_p$ and $k_{p,H}a_p$ are related as the ratio of the diffusivities of allyl alcohol and hydrogen in the solvent, to the first power. A transport factor for hydrogen $\mathcal{J}_H$ is defined analogously to $\mathcal{J}_A$ in equation(3-17). For the solvent ethanol $\mathcal{J}_H$ was greater than 0.9 for all allyl alcohol and fumaric acid concentrations, indicating negligible external particle diffusion resistance. For the solvent water, $\mathcal{J}_H$ was greater than 0.9 only for allyl alcohol concentrations less than 2×10^{-4} mol/l. Though the concentration is small, the rate could still be measured in this region. The possibility of significant internal particle diffusion resistance to hydrogen was checked by application of the Weisz-Prater criterion[50]. The criterion is given in Appendix II-7 and the numerical values calculated for the application of this criteria are presented in Appendix V. These values indicate that the internal diffusion resistance was negligible when $\mathcal{J}_H > 0.9$. Thus data for which $\mathcal{J}_H > 0.9$ could be used to prepare a plot of equation (3-30).

The transport factors $\mathcal{J}_A$ and $\mathcal{J}_H$ for a reaction can be used to determine whether the measured rate is given by the intrinsic rate

expression, or if not, what is the magnitude of mass transfer resistance of each reactant. In figure (5.5) values of $\mathcal{J}$ are shown for the reactions presented in figure (5.2). Data are not shown for the systems in which $\mathcal{J} > 0.9$ over the entire concentration range. These include $\mathcal{J}_A$ and $\mathcal{J}_H$ for the fumaric acid system, and $\mathcal{J}_H$ for the allyl alcohol - ethanol system. For the system allyl alcohol-water, there is significant mass transfer resistance over the entire concentration range. For the system allyl alcohol-ethanol, mass transfer effects are negligible for $C_{A,b}$ greater than about 0.04 mol/l. In this range the measured rate is given by the intrinsic rate expression. For the fumaric acid system, the measured rate is given by the intrinsic rate expression over the entire concentration range. The kinetic constant for the rate expression first-order in fumaric acid could be calculated from the slopes of the graph in figure (5-2).

5.1.4 External and Internal Diffusion Resistances in Slurry Reactors

The possibility of encountering zero order reactions with significant external diffusion and negligible internal diffusion resistance in slurry reactors was shown theoretically in section 3.1.2. In this case the rate of reaction would be unchanged from its value when all the mass transfer resistances were negligible, even though $\mathcal{J}$ was significantly less than unity. It is seen from figure 5.2 that the rate of the allyl alcohol-ethanol system is essentially zero order in allyl alcohol down to the allyl alcohol concentration given by the abscissa equal to 0.97. From figure 5.5 for the same system $\mathcal{J}_A = 0.57$ at the abscissa equal 0.97. This finding is compatible with the theoretical values of $\mathcal{J}$ and η shown in figure 3.1. It is possible to have a value of $\mathcal{J}$ of about 0.6 with negligible internal diffusion resistance ($\eta > 0.9$).

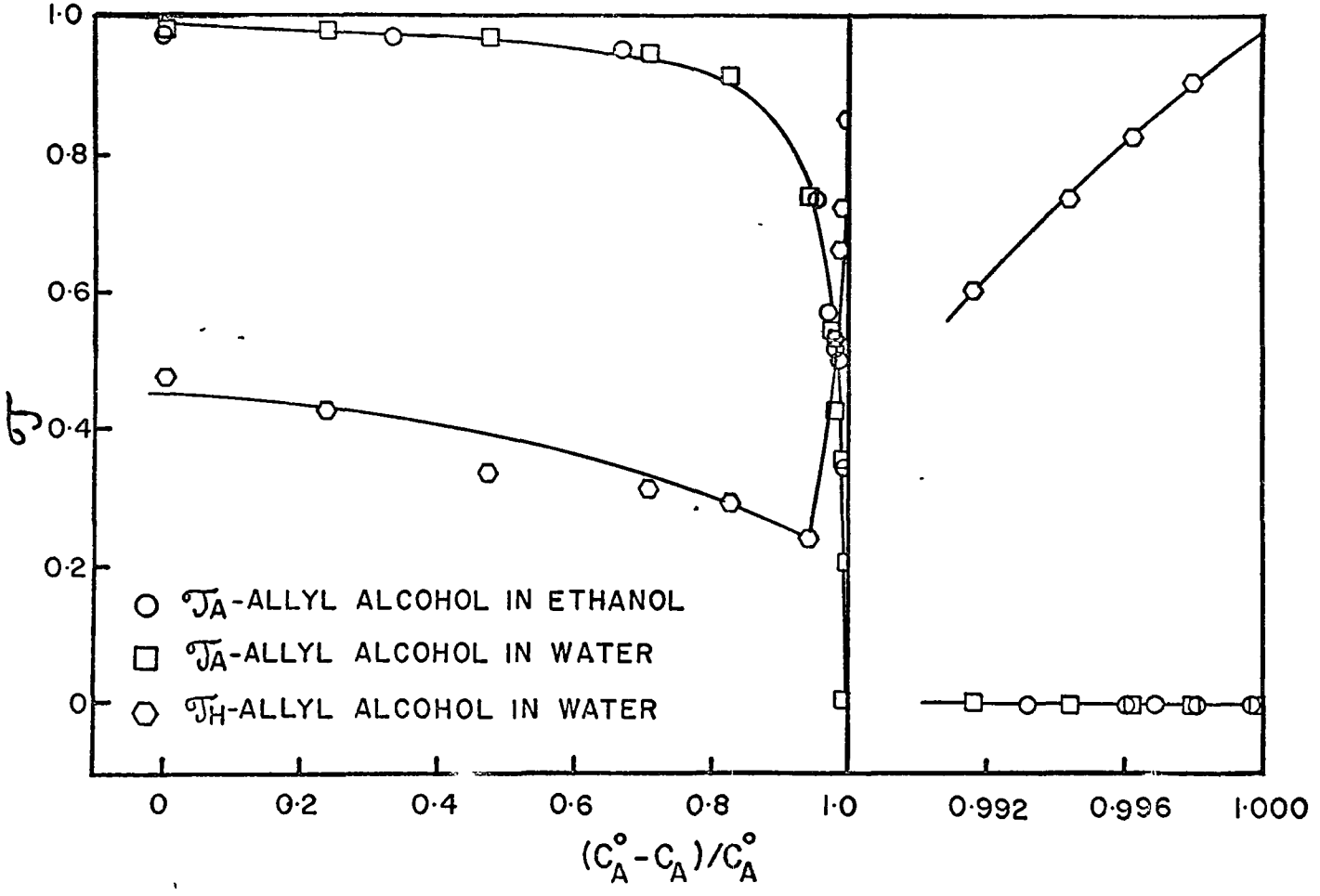

Figure 5.5 Transport factors as a function of substrate concentration at 25°C. Values of $C_{A,O}$ given in Figure 5.2.

It was pointed out in section 3.1.2 that Petersen has stated that as a rule $\eta < \mathcal{J}$ for heterogeneously catalyzed reactions. The general utility of this relation is little diminished by the finding that it does not always hold for the reactions conducted in slurry reactors. In order for $\mathcal{J} < \eta$, as was found in this work, three conditions must be fulfilled

a) Reaction order less than unity

b) Reaction in the liquid phase

c) Finely divided catalyst

Point a has been treated at length. The importance of point b is that the effective diffusivity within the porous catalyst is calculated using the molecular diffusivity, and is therefore less than the diffusivity in the bulk phase by the factor θ/τ. If Knudsen diffusion occurs within the catalyst, as is frequently the case in gas phase reactions, the internal effective diffusivity is θ/τ times the Knudsen diffusivity, which in turn is typically an order of magnitude less than the molecular diffusivity. Point c is significant because for particles of the size used in slurry reactors, the particle Sherwood number frequently approach the limiting value of 2 even though the bulk liquid is in motion due to agitation or pumping. For pelleted or otherwise prepared catalysts of at least several millimeters diameter the Sherwood number is usually much greater than 2 when the bulk liquid is in motion.

5.1.5 Integration of Rate Equation with Internal and External Diffusion Resistances

The rate equation for a constant volume batch reactor in which a zero-order reaction is taking place with external and internal diffusion resistances can be integrated analytically only when η can be expressed

by the asymptotic relation, $\eta \propto \frac{1}{h_o}$. This was done to show that an apparent change from zero-order to first-order "kinetics" may be due to a zero-order reaction passing from negligible external resistance to external diffusion controlling.

The numerical values obtained were compared with the experimental data for hydrogenation of allyl alcohol in ethanol. Initially the reaction was zero-order in allyl alcohol, and it was taken through the concentration change in which the transition from zero order to first order occurred. The pseudo-zero-order rate constant needed for the numerical solution was obtained from rate measurements in the zero-order region, and $k_p, A^a p$ from measurements in the first-order region. There remained the need to determine the value of a parameter, $R^2\tau/\theta$, containing quantities not measurable experimentally. The value of this parameter was chosen such that the best agreement possible between the data and the calculated values was obtained over the concentration range including zero-order and first-order rate dependence.

The result is shown in figure 5.6 for a reaction spanning a nearly 3-decades change in substrate concentration. Detailed calculations are presented in Appendix III. The points in figure 5.6 represent data and the curve is the analytical solution. The first data points, plotted arithmetically, show that the rate is zero order in allyl alcohol down to a concentration of 0.064 mol/l. In the analytical solution, $R^2\tau/\theta = 4.0 \times 10^{-6}$ cm^2 was used. The value of the parameter is physically reasonable: it can be generated, for instance, with particle radius value of R = 8 microns, and $\tau/\theta = 6.25$. Agreement between the experimental and calculated values is as good as can be expected, considering the approximations involved. The catalyst does not exist as spheres, but as aggregates of smaller particles. Also, when mass transfer resistances are important

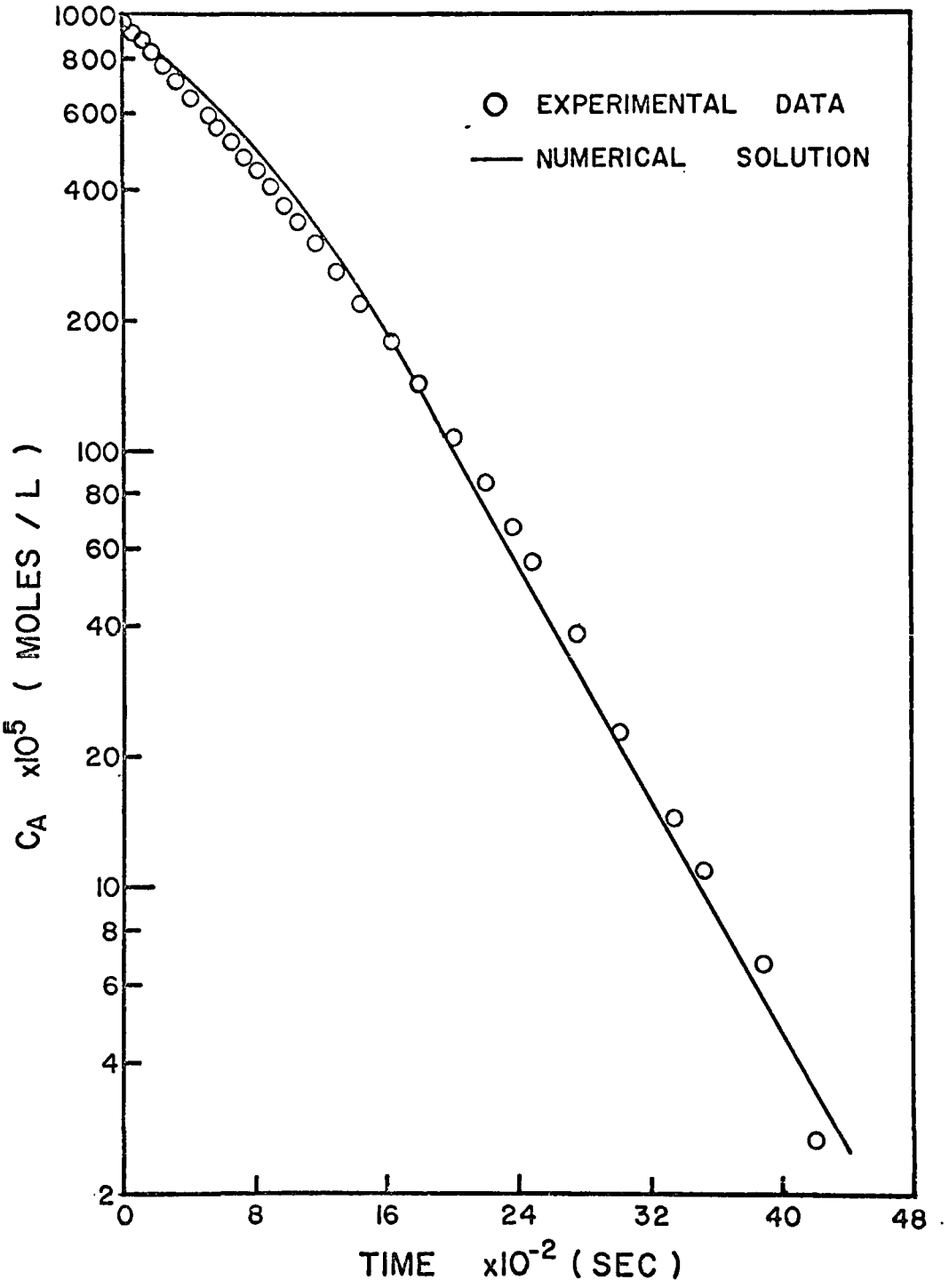

Figure 5.6 Reaction of allyl alcohol in ethanol with transition from zero-order to first order dependence on bulk substrate concentration at 25°C.

in a reaction with a distribution of particle sizes, as was true in this case, rigorous rate calculations cannot be made using a single average particle size.

5.1.6 The Apparent Activation Energy for Reaction

Reactions of allyl alcohol in ethanol in which the order with respect to allyl alcohol passed from zero to first were performed at four temperatures in the range 24.5° - 35.3°C. In the zero order region, the rate is given by the expression, $r = k_o P_{H,b}^{\frac{1}{2}}$. The values of the constants k_o and $k_{p,A} a_p$ were evaluated from rate data in the zero and first-order regions, respectively. Arrhenius plots for both constants are given in figure 5.7 and data are presented in table V-4. The apparent activation energy associated with the constant k_o is 19.0 $\pm$0.7 K cal/g mol. Its magnitude is evidence that k_o is indeed a kinetic rate constant, as was concluded after showing that γ_A and γ_H were both near unity in this concentration range. The apparent activation energy associated with the term $k_{p,A} a_p$ is -5.3 $\pm$3.5 K cal/g. mol. If temperature variations of $k_{p,A}$ were given by that of the diffusivity of allyl alcohol in ethanol to the first power, and if the group $\frac{D\mu}{T}$ is considered constant, the expected activation energy associated with $k_{p,A}$ is 3.8 K cal/g mol. Thus, if it is assumed that the measured activation energy for $k_p a_p$ has a Gaussian distribution, the measured value, -5.3 K cal/g. mol, is significantly different from 3.8 K cal/g mol at the 95 percent confidence level. The observed negative value of activation energy may be due to experimental error. Another possibility is that the tendency of the particles to agglomerate is also temperature dependent, the mean particle size being larger at higher temperatures. For the particle Sherwood number equal 2, $k_p a_p$ is proportional to the inverse square of the mean particle diameter. A reduction in the mean particle diameter of 19 percent between the temperature 24.5° - 35.3°C is

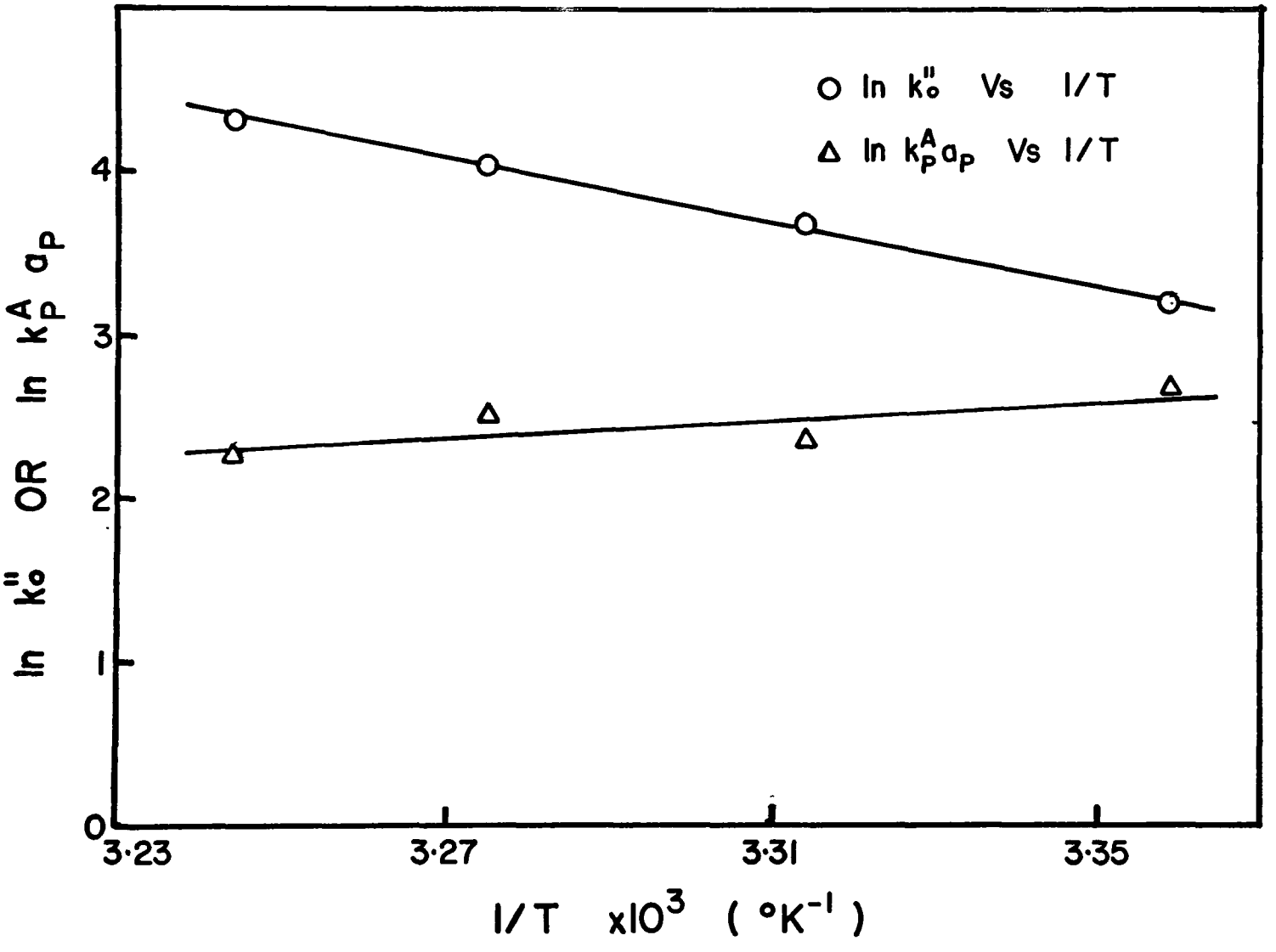

Figure 5.7 Arrhenius plots of zero-order and first-order constants for hydrogenation of allyl alcohol in ethanol.

needed to account for the observed negative activation energy. In either case, the small magnitude of the activation energy associated with $k_{p,A}a_p$ is evidence that this constant is associated with a mass transfer operation, not chemical kinetics.

5.2 Solvent Effects in Heterogeneous Hydrogenations

5.2.1 Concentration Dependence of the Rate

The liquid phase hydrogenation of acetone on Raney nickel catalyst was studied at 25°C. The solvents used in this study were benzene, cyclohexane, and isopropanol. All the measurements were made at approximately one atmosphere total pressure. The partial pressure of hydrogen in the gas phase was obtained by subtracting the vapor pressure of the liquid from the total pressure. The hydrogen absorption rate was controlled by the choice of the amount of catalyst used so that the hydrogen concentration in the bulk was not more than 5 percent different from the saturation value.

The hydrogen concentrations in the liquid phase were calculated from the hydrogen solubility data. These data were obtained experimentally at four or five different compositions of the liquid phase for each of the three binary systems - acetone - benzene, acetone - cyclohexane, and acetone - isopropanol. The solubility data expressed as Henry's law constants were correlated with the additive excess free energy models for predicting gas solubility in the mixed solvents. Thr Van Laar model represented these data best and was used for calculating gas solubilities for known solution mixtures for which the reaction rates were measured. Hydrogen solubility data in pure solvents and in acetone - solvent binary mixtures are presented in Appendix IV.

The equilibrium vapor pressures for the various liquid compositions were obtained from thermodynamic equilibrium data at 25°C for all the three binary systems. Data for acetone - cyclohexane and acetone - isopropanol systems were obtained in these laboratories, details of which can be found elsewhere [51]. Equilibrium data for the acetone-benzene system were taken from the literature [43].

For all three solvents studied the rate was approximately zero-order in acetone at acetone concentration greater than about 0.06 mol/l. The reaction orders for hydrogen at this acetone concentration were measured and are shown in figure (5-8). Here the measurements were done at such rates by choosing quantities of catalyst such that the hydrogen concentration in the bulk, $C_{H,b}$, was in equilibrium with the partial pressure of hydrogen; thus, the effect of gas absorption resistance was eliminated. The reaction orders calculated from the slopes of the lines in figure (5-8) were 0.53 for acetone in benzene, 0.57 for acetone in cyclohexane and 0.62 for acetone in isopropanol. The data used in figure (5.8) are plotted in figure (5-9) as a function of hydrogen concentration in the bulk liquid. Figure (5-9) shows that for the same concentration of acetone and hydrogen in three solvents, the reaction rates obtained are highest in isopropanol and lowest in benzene, cyclohexane being intermediate. This means that the differences in the reaction rates shown in figure (5-8) are not due to the difference in the hydrogen solubilities in the different solvents.

The initial hydrogenation reaction rates were measured, after a pseudo-steady state was achieved, at a number of acetone concentrations in each of the three solvents. The rate data as a function of bulk acetone concentration are presented in figure (5-10). These data were used to fit the reaction rate models represented by equations (3.45) and (3.47). To do this, the data were plotted in accordance with equations (3.51) and (3.52) which are based on models represented by equations (3.45) and (3.47), respectively. The plots of equations (3.51) and (3.52) are shown in figures (5.11) and (5.12). Both models (3-45) and (3-47) were found to represent the experimental data. The agreement between the simplified models and the experimental data are as good as

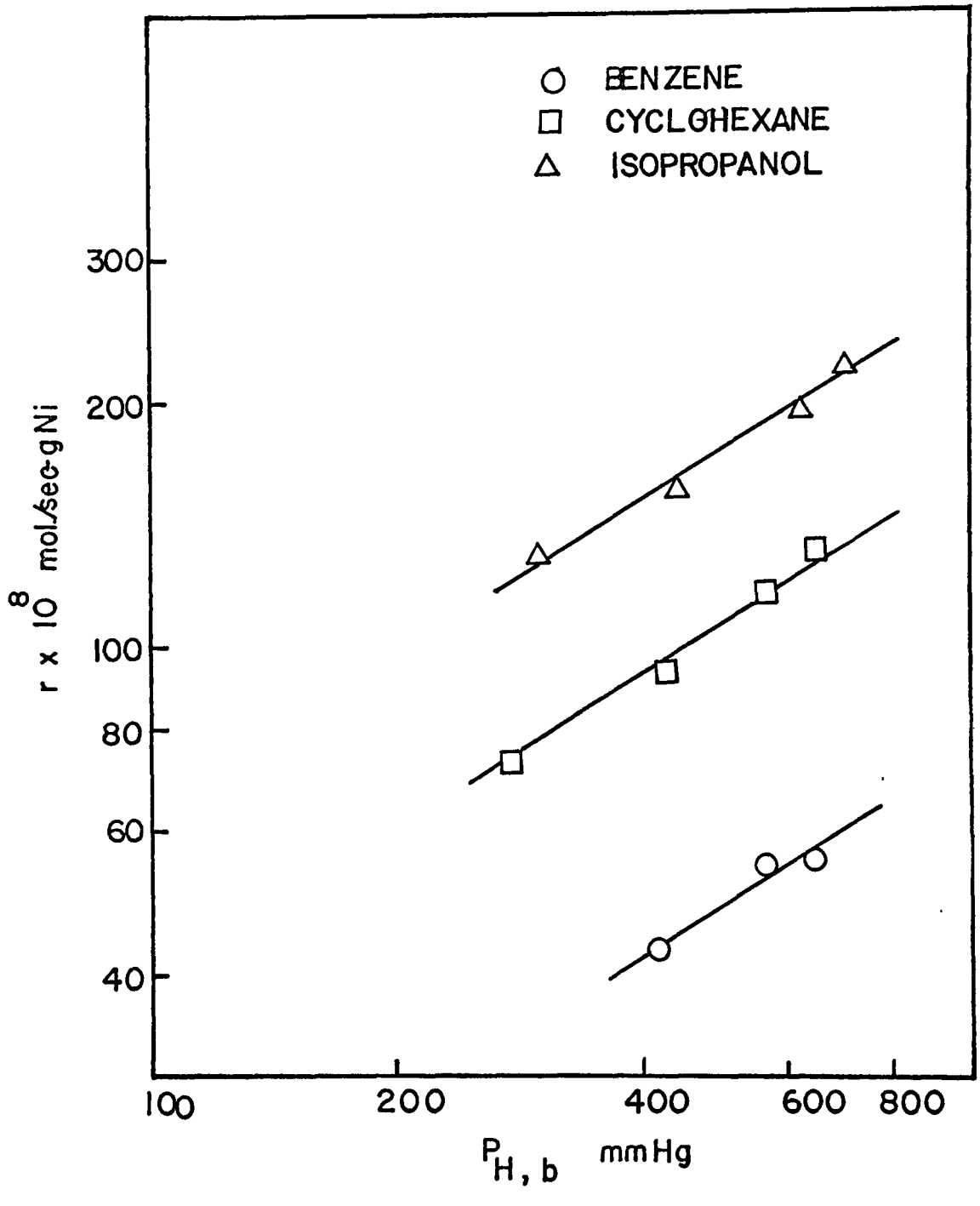

Figure 5.8 Dependence of acetone hydrogenation rate on hydrogen partial pressure at 25°C in different solvents. Acetone concentration: 0.015 mol/l.

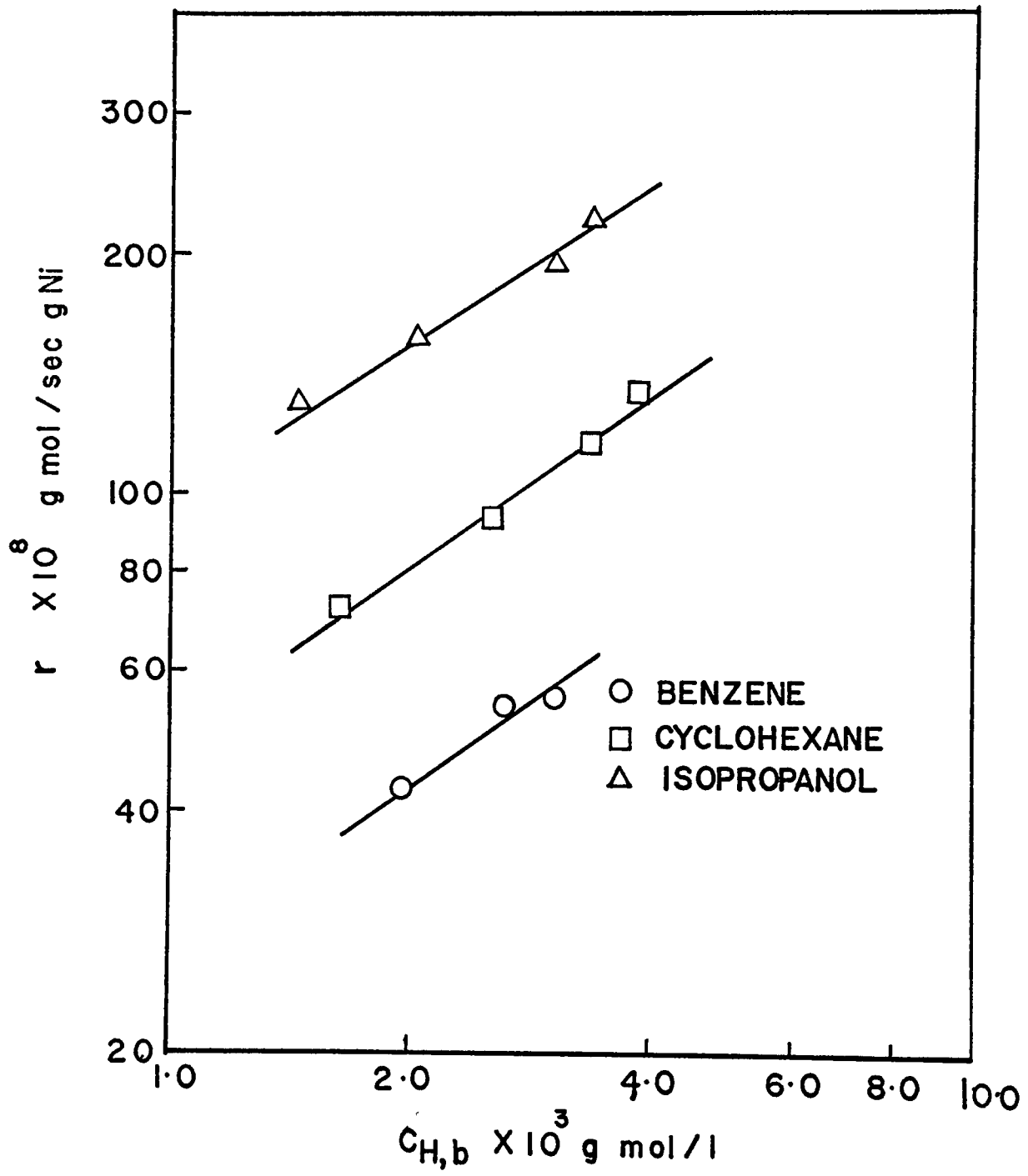

Figure 5.9 Dependence of acetone hydrogenation rate on concentration of hydrogen in the liquid phase at 25°C. Acetone concentration: 0.015 mol/l.

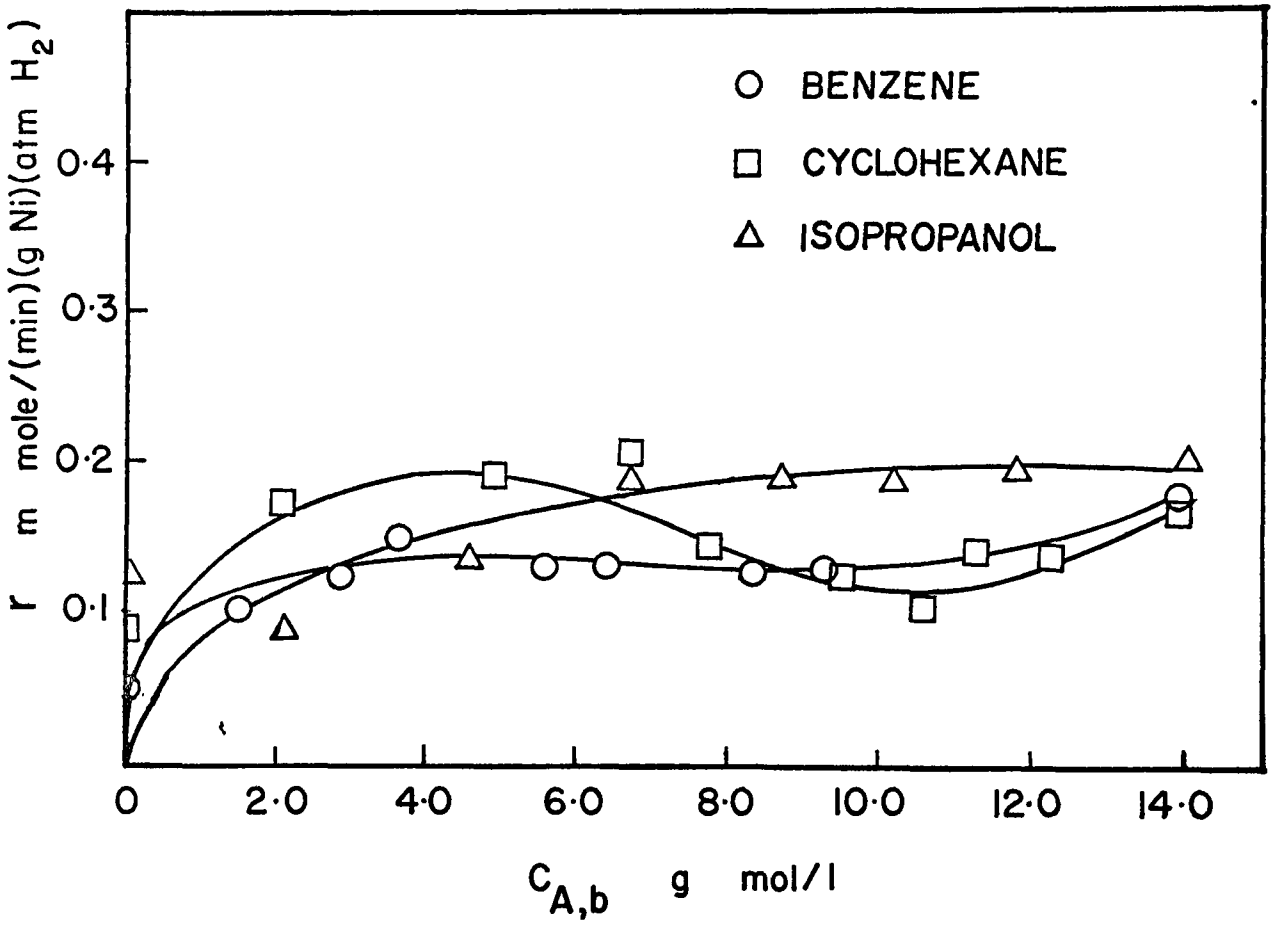

Figure 5.10 Reaction rate as a function of acetone concentration at 25°C.

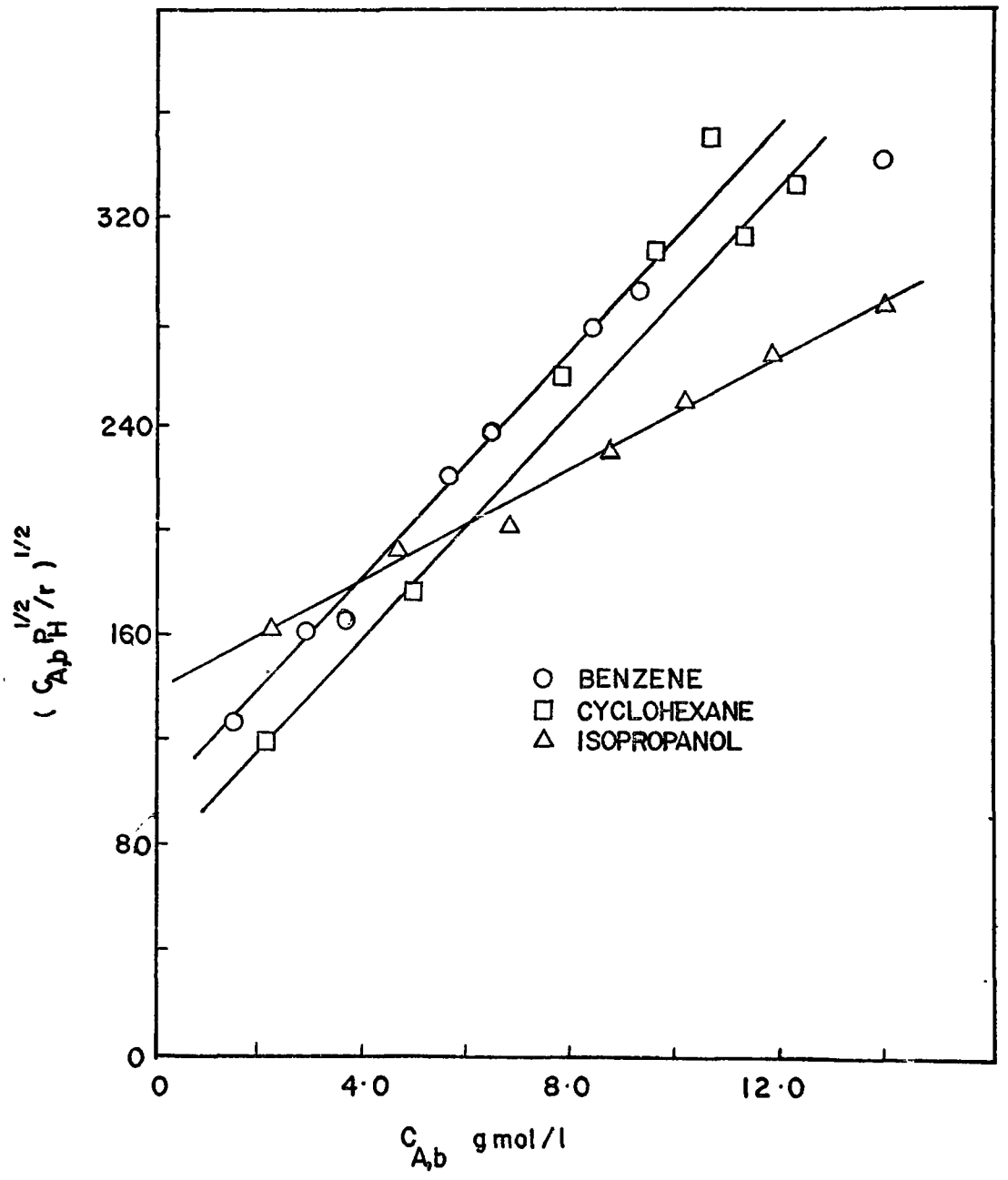

Figure 5.11 Plot of rate data in accordance with equation (3.51).

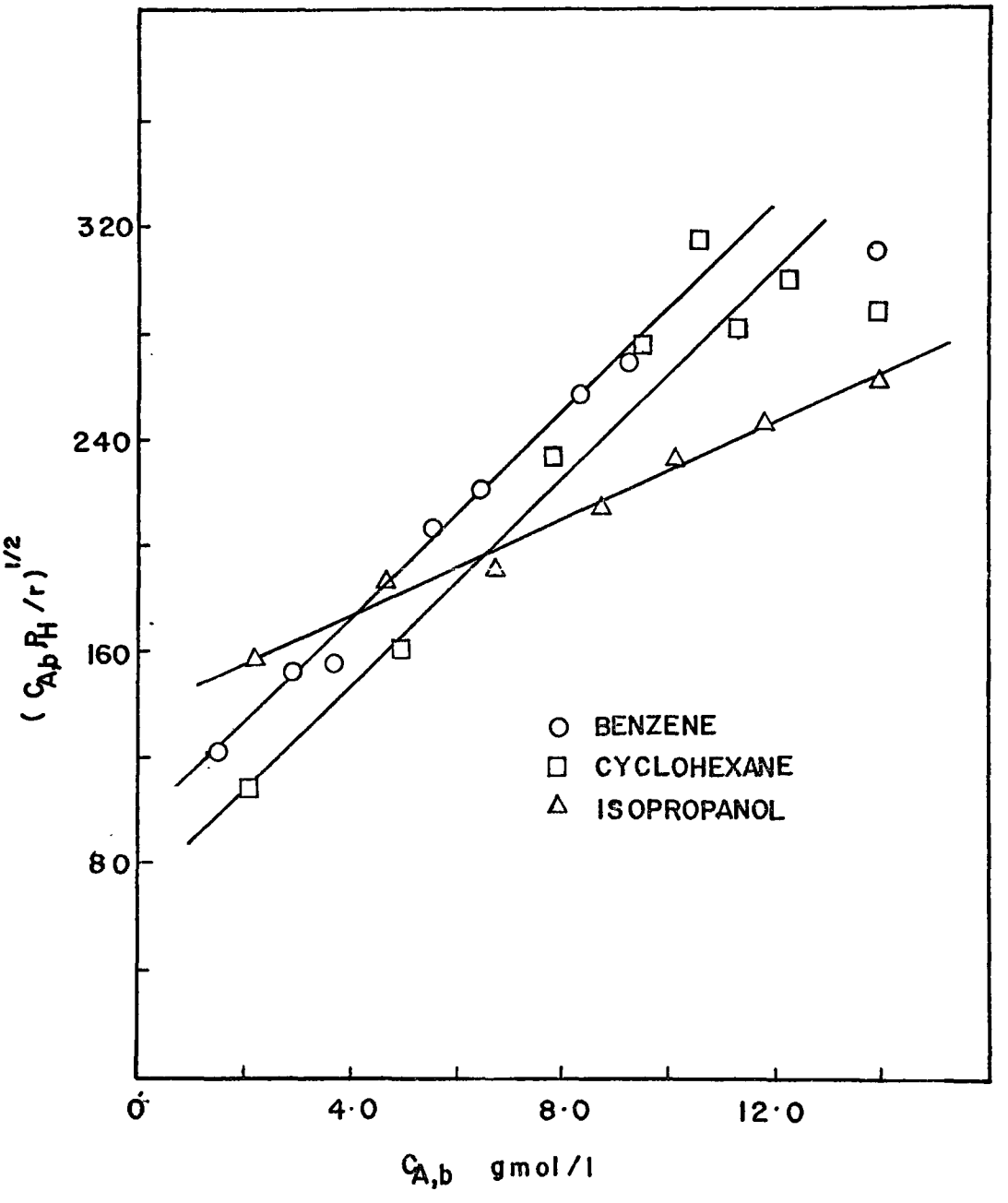

Figure 5.12 Plot of rate data in accordance with equation (3.52)

could be expected in light of the simplifications made in obtaining equations (3.51) and (3.52). In all the cases data at higher acetone concentrations show more scatter. The data for solvents benzene and cyclohexane show almost identical slopes whereas isopropanol data show a different slope. The identical behavior shown by the two models are because they differ only by a factor of $P_H^{\frac{1}{2}}$ in the ordinate, the abscissa being the same. The units of pressure chosen for these plots were atmospheres, and since the hydrogen partial pressure in all the cases was in the vicinity of one atmosphere, the effect of pressure is not revealed in the two models. It was shown earlier that the rate was approximately one-half order in hydrogen, thus the model represented by equation (3.45) which shows half order dependence on hydrogen, was believed to represent the data better.

At an acetone bulk concentration of approximately 0.06 mol/l, the apparent activation energies were obtained by measuring the reaction rates at three or four different temperatures in the range of 25° to 35°C. Here, the rate expression was assumed to be $r = k_o P_H^{\frac{1}{2}}$. The values of constant k_o obtained were plotted in the form of an Arrhenius plot and are shown in figure (5-13). The apparent activation energies obtained from the slopes of the lines in the above mentioned plot, calculated by a least squares fit along with their standard deviations are: for acetone-benzene 4.94 ± 0.47 K cal/g mol., for acetone-cyclohexane 4.91 ± 0.25 K cal/g mol., and for acetone-isopropanol 4.69 ± 1.25 K cal/g mol. These values cannot be considered to be statistically different from each other. The closeness of these values suggests that the mechanism through which hydrogenation reaction takes place in different solvents is the same.

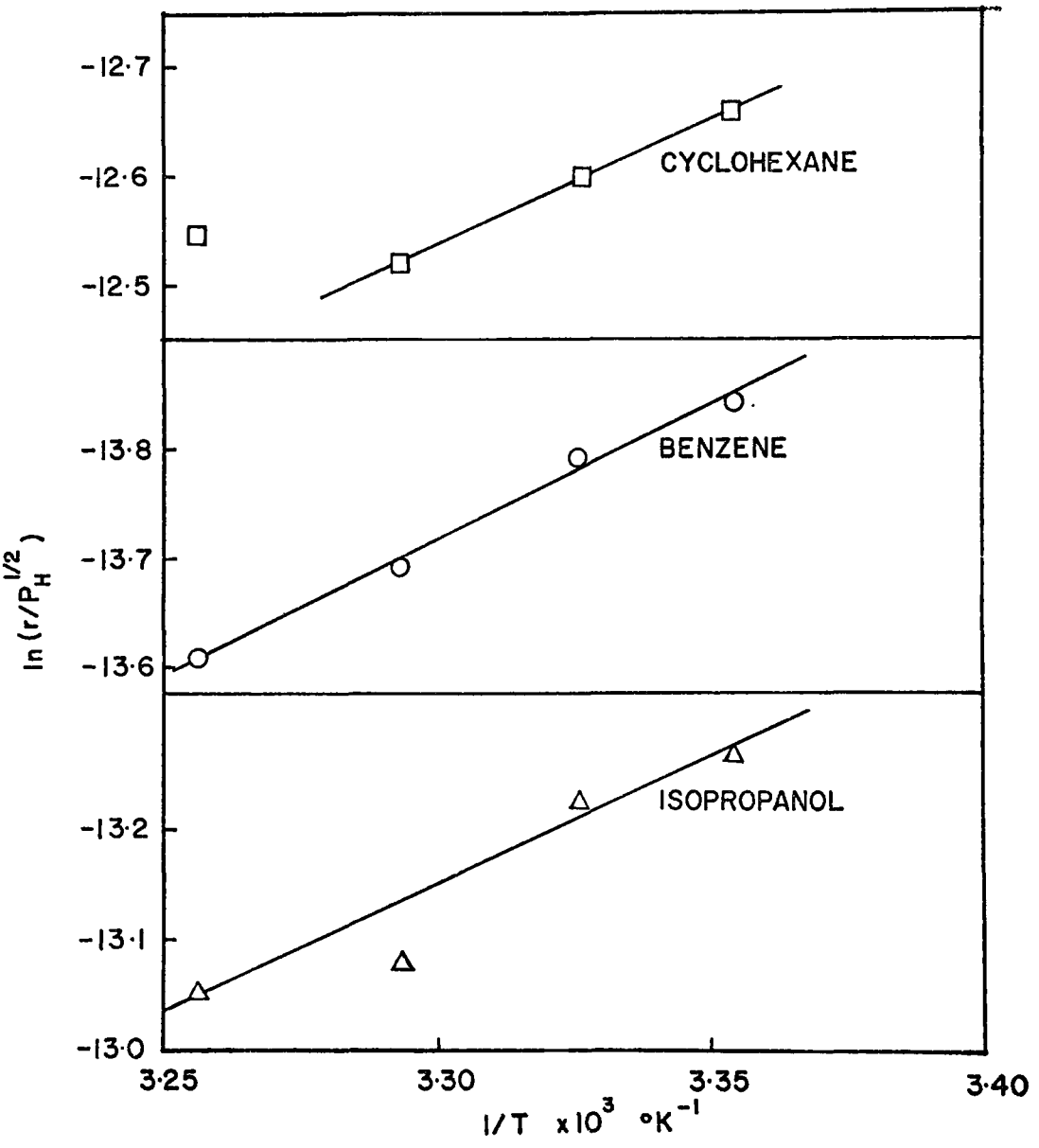

Figure 5.13 Arrhenius plot of zero-order constants for hydrogenation of acetone in different solvents. Acetone concentration: 0.06 mol/l.

5.2.2 Solvent Effects on Hydrogenation of Acetone

An attempt was made to describe the solvent effects by measuring the surface coverage of acetone and the acetone-solvent interactions in the liquid phase. The reaction rates were measured at very low acetone solution concentrations of the order of 10^{-3} and 10^{-4} mol/l where the rates were found to be first order with respect to acetone concentration. The advantage of working in this range was that a very simple kinetic equation could be used to represent the reaction rates. Also, as was discussed earlier in section 3.2.3 at these low concentrations of acetone, a gas chromatographic method of analysis could be used to determine the quantity of acetone adsorbed on the catalyst surface.

Acetone concentration in different solvents at which the reaction rates would be first order in acetone were obtained experimentally. The upper values of the acetone concentrations in the bulk where the first order behavior starts were: acetone in benzene = 7.8×10^{-3} mol/l, acetone in cyclohexane = 9.5×10^{-3} mol/l, and acetone in isopropanol = 3.8×10^{-3} mol/l. These concentrations were obtained from the linear portion of the semi-log plots of $C_{A,b}$ versus time as $C_{A,b}$ approaches zero.

In a separate set of experiments, the catalyst surface concentrations at the onset of first order region were determined to estimate the surface coverage. This was done at bulk concentrations of acetone lower than the upper range where first order region begins. The data are given in Appendix VI and are shown in figures VI-1 to VI-3. The values

obtained were: for benzene = 2.46×10^{-4} mol/g cat., for cyclohexane = 5.98×10^{-4} mol/g cat., and for isopropanol = 2.92×10^{-4} mol/g cat. These values correspond to the first order behavior observed with respect to the surface concentrations read from the plot of surface concentration versus time on a semi-log plot. The amount of acetone needed to form a monomolecular layer on the catalyst surface was calculated by assuming spherical molecules. These calculations are presented in Appendix II-8. The value obtained was 3.1×10^{-4} mol/g cat. In cases of acetone in benzene and in isopropanol, the surface coverage by acetone is about 80-90 percent of the monolayer value. The quantity obtained for cyclohexane is higher than the monolayer concentration. This is most likely because of the experimental errors which shall be discussed later.

5.2.2.1 Testing for the Absence of Mass Transfer Resistance

To establish that the reaction rates were kinetically controlled in the first order region, two different methods were used.

In the first approach, liquid-particle mass transfer coefficients obtained earlier in section 5.1.2 were used along with the diffusivity data to obtain the mass transfer coefficients in the new situations. It was assumed that the mass transfer coefficients were related to the diffusivities to the first power. The diffusivity data obtained from the literature and the calculated values of mass transfer coefficients are presented in tables II-2 and II-3 in Appendix II. These values were used to obtain the surface concentrations of hydrogen and acetone in various solutions, using the measured reaction rates. The values calculated as

$\mathcal{J}_H$ and $\mathcal{J}_A$ are found to be more than 0.99 in all the cases when rates were measured in the first order region . This indicates that the particle diffusion resistance is negligible and hence the rates measured were only being controlled by the reaction kinetics.

In the second method acetone hydrogenation rates were measured in the three solvents at two or three different hydrogenation pressures. The concentration of acetone in the bulk was so chosen that the rates were first order with respect to acetone. In all the three systems studied, the quantity $C_{A,b}/r$ was a function of P_H. Since the rate in the three systems was found to be approximately one half order with respect to hydrogen, the data were plotted in the manner suggested by equation (3.30), as $C_{A,b}/r$ versus $P_H^{\frac{1}{2}}$. These data are shown in figure (5.14). The plot shows that for all the three systems the lines joining the data points, when extrapolated, pass through the origin. Since the intercept at the ordinate of this plot is a measure of the mass transfer resistance, it is inferred that the mass transfer resistance is negligible in these measurements.

From the above discussions it is concluded that in the present case, the reaction rates in the first order region at 25°C and one atmosphere total pressure are kinetically controlled.

5.2.2.2 Activity of Acetone in the Solutions

The activity of acetone in the liquid phase was obtained from the vapor-liquid equilibrium data for the three binary systems. The binary equilibrium data were used to calculate

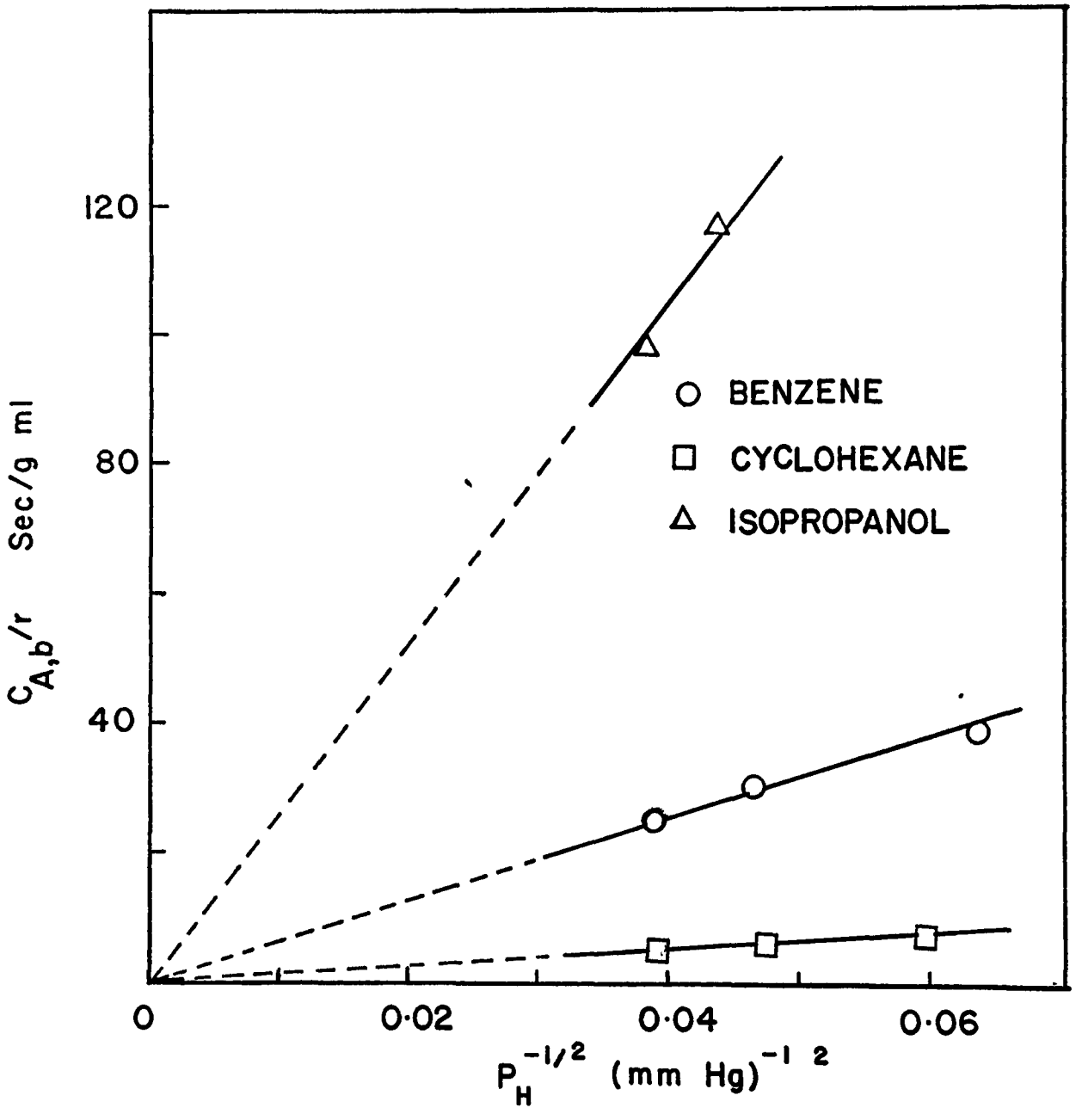

Figure 5.14 Reaction rates with linear dependence on bulk acetone concentration at 25°C.

the liquid phase activity coefficients, taking into consideration the vapor phase non-ideality. The liquid phase activity coefficients thus obtained were correlated by the Redlich-Kister three constant equation. The activity coefficients of acetone in dilute solutions were then calculated using the above correlations. Figure 5.15 shows the relative magnitude of the activity of acetone in various solvents used. It can be seen from the plot that for the same concentration of acetone in the various solvents used, the activity of acetone in cyclohexane is roughly 4-5 times that in benzene and isopropanol.

Details of the thermodynamic data used here can be found elsewhere [43, 51].

5.2.2.3 Distribution of Acetone Between Solvent and Catalyst

In the first order region the acetone distribution between solvent and catalyst was determined by knowing the acetone concentrations in reaction solution and on catalyst surface, at various stages of the hydrogenation reaction. The former was obtained by analyzing the reaction solution using a FID gas chromatograph and the corresponding concentration of acetone on the catalyst was estimated using the following acetone mass balance relation.

$$A_{surface} = A_{total} - (A_{solution} + A_{reacted})$$

where

$A_{surface}$ = amount of acetone on the catalyst surface.

A_{total} = the total amount of acetone injected initially.

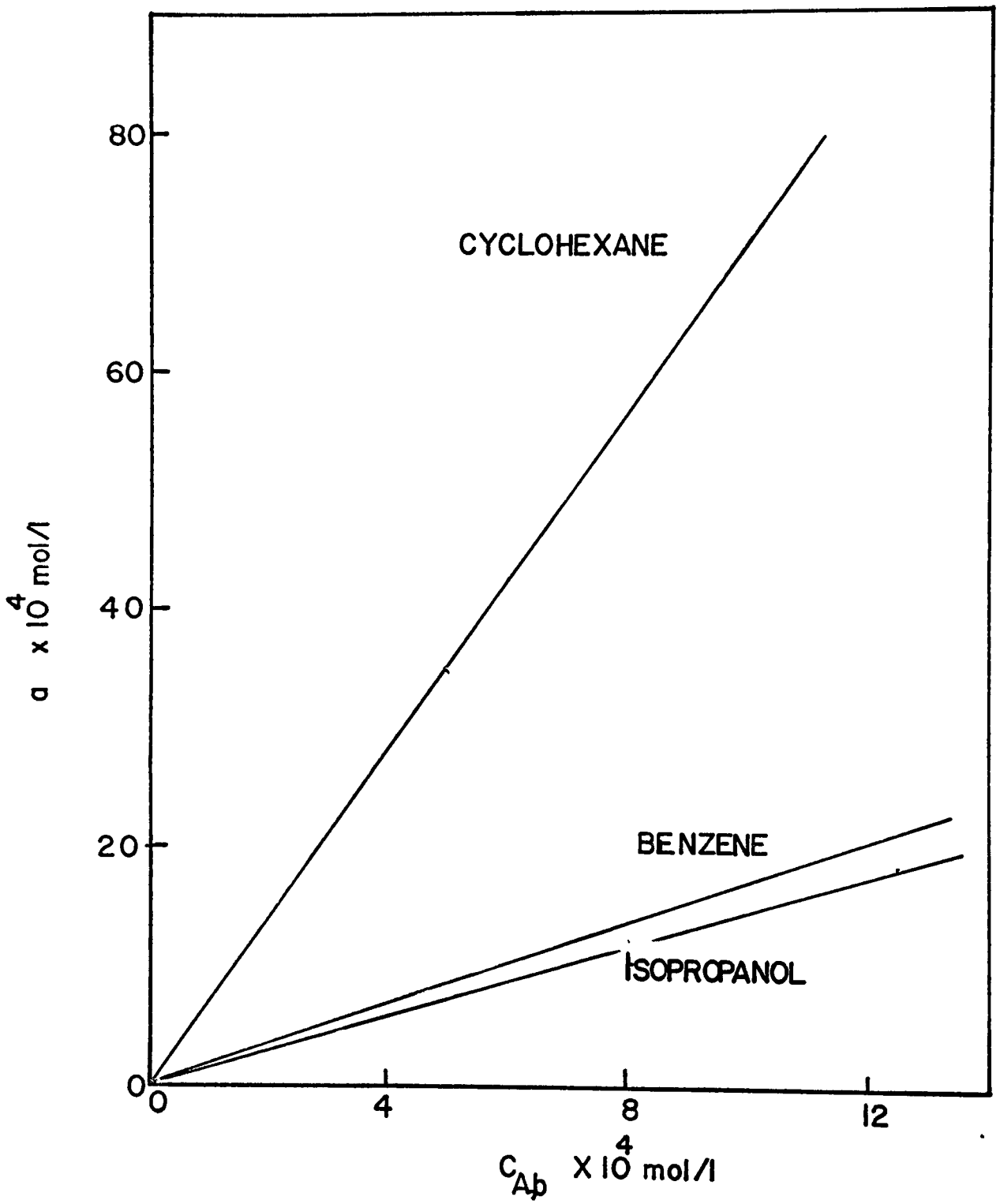

Figure 5.15 Activity versus concentration for acetone in difference solvents at 25°C.

$A_{solution}$ = the amount of acetone in solution determined using FID gas chromatograph.

$A_{reacted}$ = the amount of acetone reacted which is determined from the volume of hydrogen consumed. Before injection of acetone, and at the end of the reaction, the catalyst surface and the solvent were saturated with hydrogen.

The acetone concentrations (as hydrogen volume equivalents) in the solution and on the catalyst thus obtained were plotted against reaction time on a semi-log graph (figures VI-1 to VI-3 in Appendix VI). In each case a straight line gave the best fit for the data, indicating that the reaction rate is linear in both bulk and surface concentrations. This analysis further shows that the surface concentration, $C_{A,s}$, and the bulk concentration, $C_{A,b}$, should bear a constant ratio, and the plot of $C_{A,s}$ versus $C_{A,b}$ should pass through the origin.

A plot of surface concentration versus bulk concentration is shown in figure 5-16 for all three solvents. The solid lines represent the best linear fit, where the dotted lines represent the best curves passing through the origin. The linear plots show a zero surface concentration for a finite solution concentration. This may be because the estimated values of the surface concentrations were higher than the actual concentration. This observation is consistent with the earlier results where the surface area of catalyst computed on the basis of acetone adsorbed was found to be greater than the area measured using BET method.

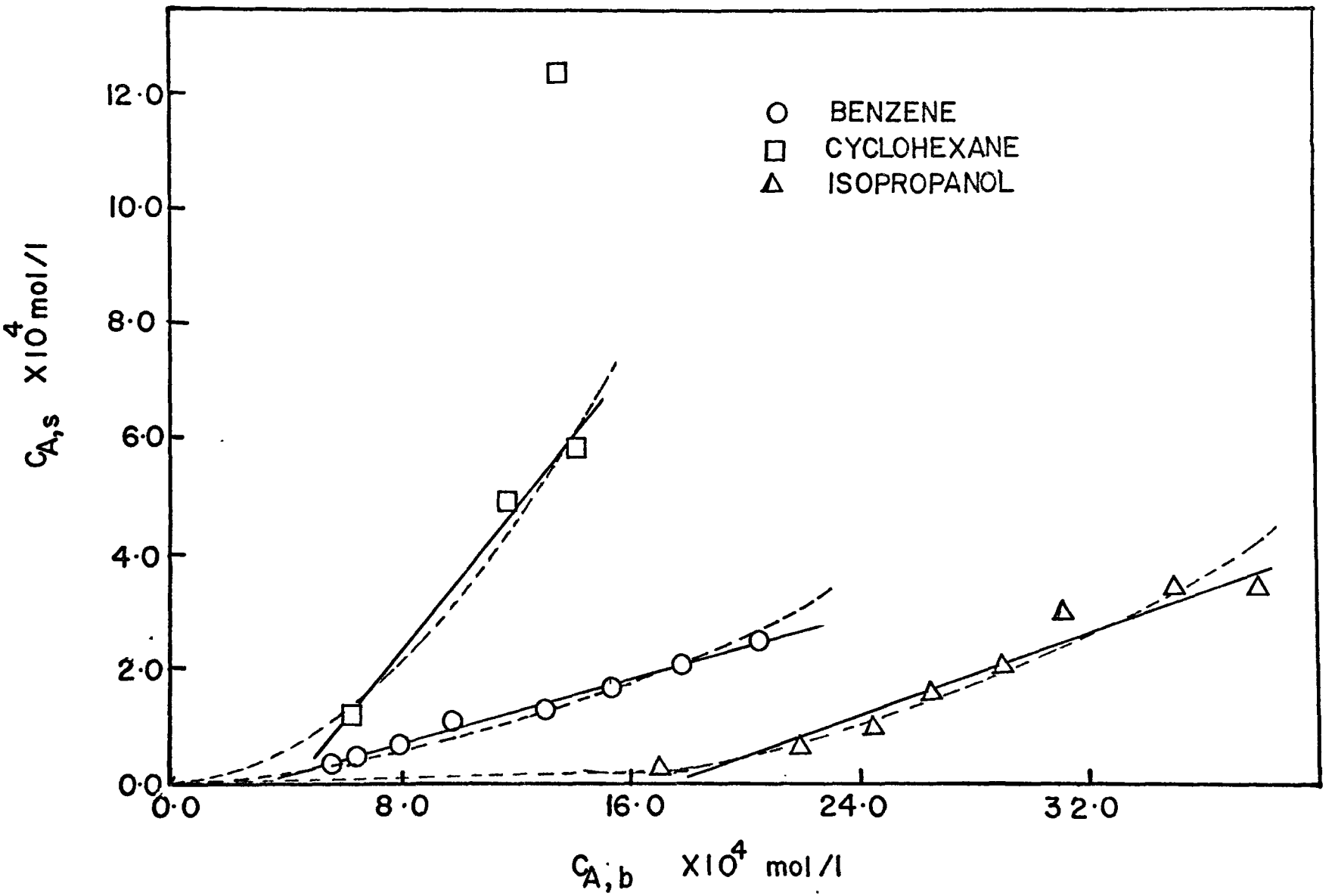

Figure 5.16 Surface concentration versus bulk concentration of acetone in different solvents at 25°C.

It seems that the error in the measurements is introduced because of the fast initial rates. Immediately upon injection of acetone, in the neighbourhood of 1-2 ml of hydrogen were consumed in a period of less than one minute, a rate of hydrogen consumption much higher than the pseudo-steady rate which subsequently established. If the rates were measured right from the point of acetone injection, the error in the volume of hydrogen absorbed was of the order of 8-10 percent. An alternate approach was to measure the reaction rates after attaining a pseudo-steady rate, and to compute stoichiometrically the volume of hydrogen required for the complete reaction from the amount of acetone injected. The error in this method could be up to 4 percent due to some possible inaccuracies in volume measurements of acetone injected. The latter method was considered more accurate and thus used. The volume of hydrogen consumed in the initial periods could be estimated by subtracting the experimentally measured volume from the total volume of hydrogen required for the acetone consumption. To test the validity of this approach, a run in solvent cyclohexane was made where the volume of hydrogen consumed in the initial period was measured very carefully. The estimated volume of hydrogen used in the initial period was about 2.40 ml compared to the experimentally observed volume of 2.04 ml. Since it was expected that the experimental volume would be lower, and the magnitude of the two volumes were not very different from each other, the approach adopted seems reasonable. Although, it seems that the values of surface concentrations obtained are higher than the actual concentrations, they represent the best estimate of the surface concentrations obtained by the experimental set up used in this work.

The different values of distribution ratios, $C_{A,s}/C_{A,b}$, obtained in the various solvents are believed to be mostly due to the differences in the liquid phase interactions between acetone and solvents. It is known that acetone and isopropanol form an almost regular solution, acetone and benzene show non-ideal behavior, and acetone and cyclohexane form a highly non-ideal solution. Because of this acetone molecules are less strongly bound in cyclohexane than in isopropanol, hence they are more freely available for the catalyst surface giving higher surface concentrations in cyclohexane.

Komarov and Ermalenko [52] have summarized the effect of deviations from Raoult's law on competitive adsorption. They stated that if the solution shows negative deviations from ideality, the component present in excess is selectively adsorbed; if the solution shows positive deviations, the component present in lower concentration is selectively adsorbed. Since in the present study, all the three solvents show positive deviations from Raoult's law, and acetone is in lower concentration, acetone will be expected to be selectively adsorbed on the catalyst. Furthermore, results show that the degree of selectivity increases with the increase in deviations from Raoult's law. The acetone molecule also has a little preference of adsorption over the solvent molecule because of its smaller size in comparison to the size of the solvent molecule [53].

5.2.2.4 Evaluation of the Solvent Effects

It is seen from the rate studies in both zero-order and first-order regions that solvents affect the reaction rates. A synopsis of a few typical runs both in zero-order and first-order are presented in table 5-1. For zero-order regions, the rate constant has the highest value for isopropanol, followed by cyclohexane, and benzene has the lowest. A look at the corresponding activities of acetone in the liquid phase shows that no trend is being followed. Thus from the zero-order results no conclusion about the solvent effects can be arrived at. In the first-order region, where both liquid phase activities and the acetone surface concentrations are known, the effect of solvents on the reaction rates can be evaluated. Here, both rate and acetone surface concentrations increased with acetone activity coefficient in comparing the three systems (table 5-1). If the liquid phase interactions between acetone and solvent are assumed to be the controlling factor then it is seen that the more non-ideal solution a solvent forms with acetone, the higher values of both surface concentrations and reaction rate constants are obtained. Neither rate nor acetone surface concentration could be correlated with the acetone activity for the three systems, however.

Also, for the rate determining reaction between adsorbed acetone and atomic hydrogen, it is necessary to know the surface concentration of hydrogen as well, which was not measured in the present work. Hence the effect of solvent on the turnover frequency could not be studied. It is, however, found experimentally that the rank of "rate" is the same as that of "acetone adsorbed". The similarities in the activation

TABLE 5-1

Hydrogenation Data for Acetone in Zero and First Order Regions at 25°C

Solvent	Zero Order Range [a]			First-order Range [b]			
	Run No.	k_o, $\frac{mol}{g\text{-}sec\text{-}atm^{\frac{1}{2}}}$	acetone activity $\frac{mol}{l}$	Run No.	k_1, $\frac{l}{g\text{-}sec\text{-}atm^{\frac{1}{2}}}$	acetone activity coefficient	$\frac{C_{A,s}}{C_{A,b}}$ [c] $\frac{l}{g}$
Cyclohexane	2-1-E	1.44×10^{-6}	0.43	2-3-E	13.3×10^{-5}	4.10	1.20
Benzene	1-2-E	0.60×10^{-6}	0.11	1-1-SE	2.0×10^{-5}	1.67	0.37
Isopropanol	3-1-E	2.28×10^{-6}	0.09	3-1-SE	1.0×10^{-5}	1.44	0.13

a $r = k_o P_H^{\frac{1}{2}}$

b $r = k_1 C_A P_H^{\frac{1}{2}}$

c obtained from figures VI-1 to VI-3 in Appendix VI.

energies obtained for the three systems were reported in section 5.2.1. This observation indicates that the turnover frequency for the reaction is independent of the solvent.

In summary, this study indicates that the effect of solvents on acetone hydrogenation rates is due to their effects on the adsorption of acetone. This thus experimentally verifies the qualitative conclusion of Wauquier and Jungers.

6. CONCLUSIONS

6.1 Mass Transfer Effects

1. For all the three systems studied the rate is approximately zero-order in substrate at concentrations greater than 0.01 mol/l and first order at very low concentrations.

2. The reaction order for hydrogen in the region of zero order with respect to substrate is approximately one for allyl alcohol in water, and one half for allyl alcohol in ethanol and fumaric acid in ethanol.

3. The utility of the method proposed for determining $k_p a_p$ has been shown in the interpretation of rate data obtained using a slurry reactor. The values of $k_{p,A} a_p$ obtained from experimental data for allyl alcohol in water and allyl alcohol in ethanol are 20 and 13.3 $cm^3/sec\text{-}g$, respectively.

4. Three systems that exhibit superficially similar rate behavior were seen to have rate controlled by different combinations of diffusion and kinetic resistances. For the system allyl alcohol - water there is significant mass transfer resistance over the entire concentration range. For the allyl alcohol-ethanol system, mass transfer effects are negligible at higher concentrations. For the fumaric acid-ethanol system, the measured rate is kinetically controlled over the entire concentration range.

5. The possibility of encountering zero-order reactions with significant external diffusion and negligible internal diffusion resistance in slurry reactors is shown theoretically and observed experimentally.

6. For allyl alcohol in ethanol, the apparent activation energy associated with k_o is 19.0 K cal/g mol. and with $k_{p,A}\, a_p$ is -5.3 K cal/g mol.

6.2 Solvent Effects

1. Reaction rate is one half order in hydrogen pressure at higher acetone concentration for all the three solvents.
2. The rate is linear in surface concentration of acetone for the region where it is linear in bulk concentration.
3. In the first order region the rate determining step is probably the reaction of adsorbed acetone with atomic hydrogen.
4. For a given concentration of acetone in the first order region the following trends are observed:

Solvent	Acetone activity	Acetone adsorbed	Reaction rate
cyclohexane	highest	highest	highest
isopropanol	lowest	lowest	lowest
benzene	middle	middle	middle

5. In the first order region, the rank of "rate" is the same as that of "acetone adsorbed".

REFERENCES

1. Ostergaard, K., Advan. Chem. Eng. 7, 71 (1968).

2. Pruden, B.B., and Weber, M.E., Canadian J. Chem. Eng., 48, 162 (1970).

3. Sherwood, T.K., and Farkas, E.J., Chem. Eng. Sci., 21, 573 (1966).

4. Satterfield, C.N., "Mass Transfer in Heterogeneous Catalysis", M.I.T. Press, Cambridge, 1970.

5. Levins, D.M., and Glastonbury, J.R., Chem. Eng. Sci., 27, 537 (1972).

6. Brian, P.L.T., Hales, H.B., and Sherwood, T.K., A.I.Ch.E.J., 15, 727 (1969).

7. Miller, D.N., Ind. Eng. Chem., Process Des. and Dev., 10, 365 (1971).

8. Wauquier, J.P., and Jungers, J.G., Bull. Soc. Chimique de France, 10, 1280 (1957).

9. Kishida, S., and Teranishi, S., J. Catalysis, 12, 90 (1968).

10. Eckert, C.A., Ind. Eng. Chem. 59 (9), 20 (1967).

11. Rylander, P.N., Engelhard Industries Technical Bull., 5 (1), 15 (1964).

12. McQuillan, F.J., Ord, W.O., and Simpson, P.L., J. Chem. Soc. 5996 (1963).

13. Woodward, R.B., Sondheimer, F., Taub, D., Hensler, K., and McLamore, W.M., J. Am. Chem. Soc. 74, 4223 (1952).

14. Yao, H.C., and Emmett, P.H., J. Am. Chem. Soc., 81, 4125 (1959).

15. Zajcew, M.J., Am. Oil Chemist Soc., 37, 11 (1960).

16. Iwamoto, I., Aonuma, T., and Keii, T., Int. Chem. Eng., 11 (3), 573 (1971).

17. Sokol'skii, D.V., "Hydrogenation in Solutions", Oldbourne Press, London, 1964.

18. Kindler, K., and Blaas,L., Ber. 77 B, 585 (1944). cf. Ref. 11.

19. Harriott, P., A.I.Ch.E.J., 8, 93 (1962).

20. Friedlander,S.K., A.I.Ch.E.J., 3, 43 (1957).

21. Frossling, N., Gerland's Bert, Zur. Geophys., 52, 170 (1938).

22. Garner, F.H., and Suckling, R.D., A.I.Ch.E.J., 4, 114 (1958).

23. Ranz, W.E., and Marshall, W.R., Chem. Engng. Prog., 48, 141 (1952); 48, 173 (1952).

24. Brian, P.L.T., and Hales, H.R., A.I.Ch.E.J., 15, 419 (1969).

25. Furusawa, T., and Smith, J.M., Ind. Eng. Chem. Fundamentals, 12 (2), 197 (1973).

26. Amis, E.S., "Solvent Effects on Reaction Rates and Mechanisms", Academic Press, New York, 1966.

27. Wells, P.R., Chem. Rev., 63, 171 (1963).

28. Wong, K.F., and Eckert, C.A., Ind. Eng. Chem. Process Des. Dev., 8, 568 (1969).

29. Shutt, E., and Winterbottom, J.M., Platinum Metals Review, 15 (3), 94 (1971).

30. Satterfield, C.N., and Way, P.F., A.I.Ch.E.J., 18 (2), 305 (1972).

31. Polinskii, L., and Huang, I., Ind. Eng. Chem. Process Des. Dev., 6 (4), 432 (1967).

32. Fasman, A.B., and Sokol'skii, D.V., Kinetika i Kataliz, 4 (5), 736 (1963).

33. De Ruiter, E., and Jungers, J.C., Bull. Soc. Chim. Belges., 58, 210 (1949).

34. Orito, Y., and Imai, S., Rept. Govt. Chem. Ind. Res. Inst., Tokyo, 11, 453 (1960).

35. Satterfield, C.N., Ma, Y.H., and Sherwood, T.K., Ins. Chem. Engrs., I. Chem. E. Symposium Series, No. 28, 22 (1968).

36. Petersen, E.E., "Chemical Reaction Analysis", Prentice-Hall, Englewood Cliffs, N.J., 1965.

37. Frank-Kamenetskii, D.A., "Diffusion and Heat Exchange in Chemical Kinetics", translated by N. Thon, p. 105, Princeton University Press, Princeton, 1955.

38. Dupont, G., Bull. Soc. Chim., 3, 1021 (1936).

39. Patrikeev, V.V., Balandin, A.A., and Khidekel, M.L., Chem. Abstracts 52: 19369 i.

40. Bond, G.C. and Wells, P.B., J. Catalysis, 4, 211 (1965).

41. Katti, P.K., and Chaudhri, M.M., J. Chem. Phys., 35, 756 (1961).

42. Horsley, L.H., "Azeotropic Data II", p. 33, No. 35, Advances in Chemistry Series, ACS, Washington, D.C., 1962.

43. Campbell, A.N., Kartzmark, E.M., and Chatterjee, R.M., Canadian J. Chem., 44, 1183 (1966).

44. Ben Naim, A., and Baer, S., Trans. Faraday Soc., 59, 2735 (1963).

45. Clever, H.L., Battino, R., Saylor, J.H., and Cross, P.M., J. Phys. Chem., 61, 1078 (1957).

46. Instruction Manual Series 200, Disc Integrator, p. 8, Disc Instruments Inc., Santa Ana, Calif.

47. Battino, R., and Clever, H.L., Chem. Rev., 66, 395 (1966).

48. Timmermans, J., "Physico-Chemical Constants of Pure Organic Compounds", Vol. 2, Elsevier, New York, 1965.

49. Riddick, Y.A., and Bunger, W.B., "Organic Solvents", in Techniques of Organic Chemistry (Weissberger, ed.) Wiley-Interscience, New York, 1970.

50. Weisz, P.B., and Prater, C.D., Advan. Catalysis, 6, 167 (1954).

51. Puri, P.S., Polak, J., and Ruether, J.A., J. Chem. Eng. Data, 19 (1), 87 (1974).

52. Komarov, V.S., and Ermolenko, N.F., Russ. J. Phys. Chem., 35, 5 (1961). c.f. Ref. 53.

53. Kipling, J.J., "Adsorption from Solutions of Non-Electrolytes", Academic Press, London, 1965.

54. Weekman, V.W. Jr., and Gorring, R.L., J. Catalysis, 4, 260 (1965).

55. Sporka, K., Hanika, J., Ruzicka, V., and Halousek, M., Coll. Czech. Chem. Commun., 36 (6), 2130 (1970).

56. Sporka, K., Hanika, H., and Ruzicka, V., Coll. Czech. Chem. Commun., 34 (10), 3145 (1969).

57. Anderson, D.K., Hall, J.R., and Baab, A.L., J. Phys. Chem. 62, 404 (1958).

58. Leffler. J., and Cullinan, H. T. Jr., Ind. Eng. Chem. Fund., 9, 88 (1970).

59. Hayduk, W., and Cheng, S. C., Chem. Eng. Sci., 26, 635 (1971).

60. Perry, J. H. (ed.), "Chem. Eng. Handbook", 4th ed., 14-25, 14-26, McGraw-Hill Publication, New York, 1967.

61. Lange, N. A., "Handbook of Chemistry", 9th ed., Sandusky, Ohio, Handbook Publ., 1956.

62. Freel, J., Pieters, W. J. M., and Anderson, R. B., J. Catalysis, 14, 247 (1969).

63. Puri, P. S., and Ruether, J. A., Canadian J. Chem. Eng., in press.

64. Krischevsky, I. R., Zh. Fiz, Khim., 9, 41 (1937).

65. O'Connell, J. P., and Prausnitz, J. M., Ind. Eng. Chem. Fundamentals, 3, 347 (1964).

66. Boublik, T., and Hala, E., Coll. Czech. Chem. Comm., 31, 1628 (1966).

67. Carlson, E. C., and Colburn, A. P., Ind. Eng. Chem., 34, 581 (1942).

68. Morrison, T. J., and Billett, F., J. Chem. Soc., 3819 (1952).

69. Seidell, A., "Solubilities of Inorganic and Metal Organic Compounds", 4th ed., ACS, Washington, D. C., 1958-1965.

70. Kruyer, S., and Nobel, A. P. P., Rec. Trav. Chim., 80, 1145 (1961).

APPENDIX I

Effectiveness Factor and Transport Factor for Zero-Order Reaction in Spherical Porous Catalyst Particle

Numerical data for the effectiveness factor and transport factors for the zero-order reaction in spherical porous particles used in figure (3-1) were obtained as follows:

Effectiveness factor

For zero-order reactions in spheres, without volume expansion, Weekman and Gorring [54] derived a relationship between effectiveness factor, η, and the Thiele parameter, h. They stated that if $h < \sqrt{6}$, then $\eta = 1.0$. For $h > \sqrt{6}$, the effectiveness factor is given by

$$\eta = 1 - r_e^3 \qquad (I\text{-}1)$$

where r_e is the normalized radius at which the concentration of reactant becomes zero. The Thiele parameter in terms of r_e is written as

$$h^2 = \frac{3}{(1 - r_e)\left[\frac{1}{2}(1 - r_e) - r_e^2\right]} \qquad (I\text{-}2)$$

In the present calculations, a modified Thiele parameter is used which is related to the Thiele parameter defined above by the relation

$$\hat{h}_o = \left(\frac{n+1}{2}\right)^{\frac{1}{2}} \frac{h}{3} \qquad (I\text{-}3)$$

Values of $\hat{h}_o$ and η are calculated for various values of r_e and are presented in table I-1.

Transport factors

The transport factors are calculated using the data obtained in table I-1 and equation (3.33). The various values of the group (θ/τ) (1/Sh) taken were 1/8, 1/16 and 1/40. Values of transport factors corresponding to each of them are given in table I-2. Numerical values presented in this table were used in preparing figure (3-I).

TABLE I-1

Effectiveness factors for zero order reaction in spherical porous catalyst particle

r_e	η	$\hat{h}_o$	$\eta \hat{h}_o^2$
0.99	0.0297	33.4	33.1
0.95	0.143	6.78	6.57
0.90	0.271	3.45	3.23
0.85	0.386	2.34	2.11
0.80	0.488	1.79	1.56
0.75	0.578	1.46	1.23
0.70	0.657	1.24	1.01
0.65	0.725	1.09	0.86
0.60	0.784	0.97	0.74
0.55	0.833	0.885	0.652
0.50	0.875	0.816	0.583
0.40	0.936	0.717	0.481
0.30	0.973	0.652	0.414
0.20	0.992	0.610	0.361
0.10	0.999	0.585	0.342
0.01	$\sim$1.0	0.577	0.333

TABLE I-2

Effectiveness and Transport factors for a zero-order reaction in spherical porous catalyst particle

$\hat{h}_o$	η	$\mathcal{J}$		
		1/8	1/16	1/40
33.4	0.0297	0.0197	0.0387	0.0915
6.78	0.143	0.0921	0.169	0.337
3.45	0.271	0.171	0.292	0.508
2.34	0.386	0.240	0.387	0.612
1.79	0.488	0.299	0.461	0.681
1.46	0.578	0.351	0.520	0.730
1.24	0.657	0.398	0.569	0.767
1.09	0.725	0.437	0.608	0.795
0.97	0.784	0.474	0.643	0.818
0.885	0.833	0.506	0.672	0.836
0.816	0.875	0.533	0.696	0.851
0.717	0.936	0.581	0.735	0.874
0.652	0.973	0.617	0.763	0.890
0.610	0.992	0.644	0.787	0.901
0.585	0.999	0.661	0.796	0.907
0.577	1.000	0.667	0.800	0.909
0.500	1.000	0.727	0.842	0.930
0.400	1.000	0.806	0.893	0.954
0.300	1.000	0.881	0.937	0.974
0.200	1.000	0.930	0.971	0.988
0.100	1.000	0.985	0.993	0.997

APPENDIX II

Methods of Calculations

II-I Calculations of Gas-Liquid Mass Transfer Coefficients

For the stirred reactor used in this study, the quantity, $k_L a$, which is product of the mass transfer coefficient at the gas liquid interface and the interfacial surface area, was determined for all the solvents by plotting data for gas absorption without reaction according to the integrated form of the rate equation for unsteady state absorption. A derivation of such an equation is presented here.

The rate of mass transfer at the gas-liquid interface is given by the equation

$$- \frac{dN}{dt} = k_L A (C_{H,*} - C_{H,b})$$

$$= k_L a V_L (C_{H,*} - C_{H,b}) \qquad \text{(II-1.1)}$$

Expressing the hydrogen concentration in the liquid phase in the form of Henry's law constant,

$$C_{H,*} = P_H H' \qquad \text{(II-1.2)}$$

Where H' is the Henry's law constant expressed in the units mol/l-atm. Assuming ideal gas behavior one can write

$$C_{H,b} = \frac{N}{V_L} = \frac{(V^o - V) P_H}{RT V_L} \qquad \text{(II-1.3)}$$

where V^o and V are the initial volume and volume at any time as read on the burets, respectively. For an infinitesimal small time, equation (II-1.3) can be written as

$$- \frac{dN}{dt} = \frac{P_H}{RT} \frac{dV}{dt} \qquad \text{(II-1.4)}$$

Substituting from equations (II-1.2), (II-1.3) and (II-1.4) in equation (II-1.1), and rearranging, one gets

$$\frac{dV}{dt} + k_L a V + k_L a \left[V_L \acute{H} RT - V^o \right] = O \qquad \text{(II-1.5)}$$

This is a first order differential equation solution of which under the boundary condition

$$V = V^o \text{ at } t = 0$$

is

$$- (V^o - V - V_L \acute{H} RT) \exp (k_L a t) = V_L \acute{H} RT \qquad \text{(II-1.6)}$$

rearranging equation (II-1.6) one gets

$$- \ln \left(1 - \frac{V^o - V}{V_L \acute{H} RT} \right) = k_L a t \qquad \text{(II-1.7)}$$

From equation (II-1.7), a plot of the left hand side versus time would give a straight line which passes through the origin and has a slope equal to $k_L a$.

Experimental values of $k_L a$ were thus obtained from the gas solubility rate data in various liquids. These results are presented in table II-1. As an example, in figure II-1, is shown the data used to obtain $k_L a$ for the case of hydrogen in water.

TABLE II-1

Experimental Values of $k_L a$ for Various Systems for a Fixed Stirring Rate* at 25°C for Approximately 220 ml liquid in the cell

System	$k_L a \times 10^3$ sec^{-1} (average value)
Hydrogen - water	7.9
Hydrogen - ethanol	22.2
Hydrogen - benzene	17.3
Hydrogen - cyclohexane	17.6
Hydrogen - isopropanol	7.2
Hydrogen - acetane	23.0

* The magnetic stirrer setting was fixed at a point just less than that causing instability of the magnetic stir bar.

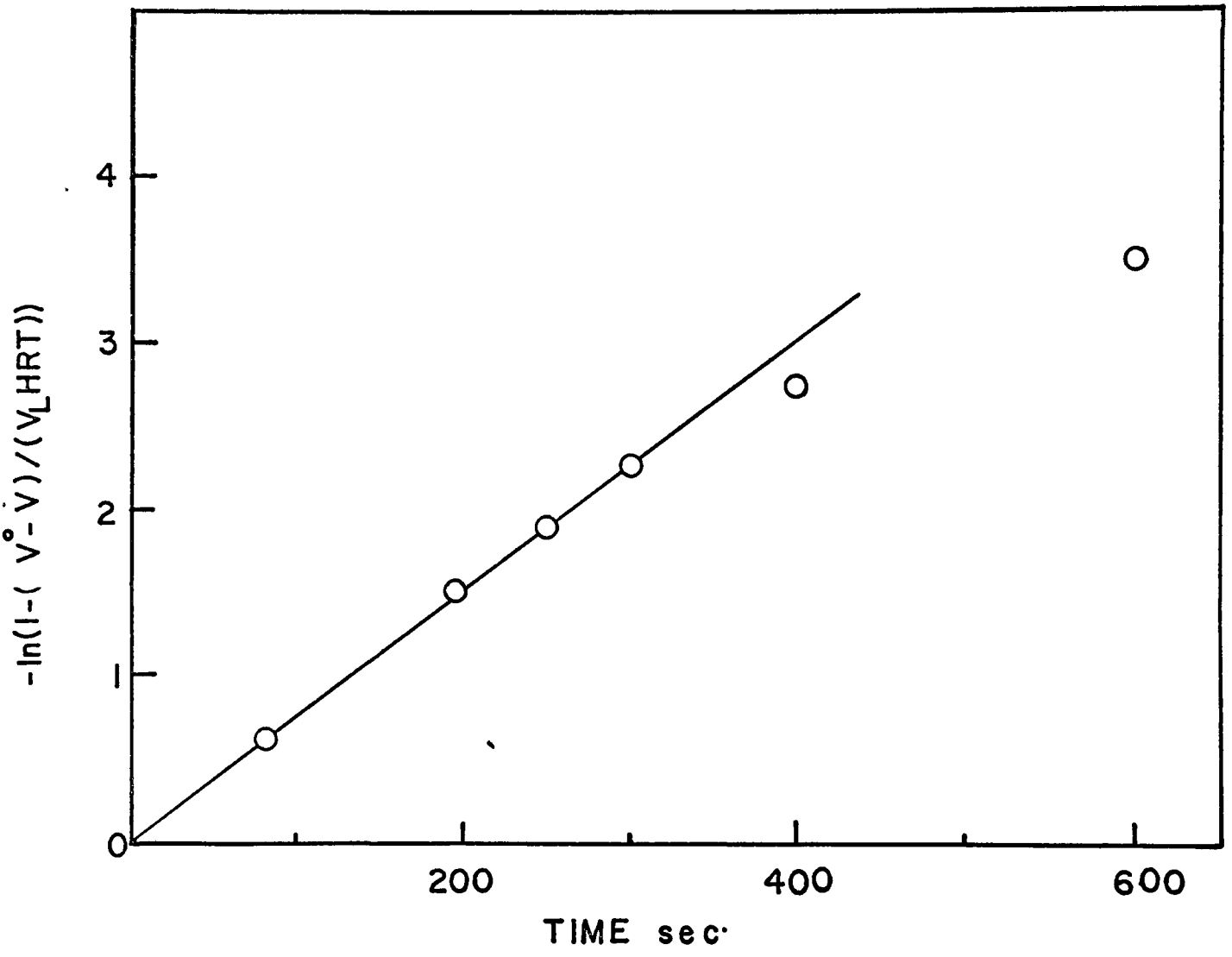

Figure II-I Plot of unsteady state absorption of hydrogen in water at 25°C for a fixed stirring speed.

II-2 Calculation of Saturated and Bulk Hydrogen Concentration

The rate of hydrogen transfer at the gas-liquid interface is given by

$$N = k_L a \, (C_{H,*} - C_{H,b}) \qquad \text{(II-2.1)}$$

Here, k_L is the mass transfer coefficient, a the interfacial area, and $C_{H,*}$ and $C_{H,b}$ are the hydrogen concentrations at the gas-liquid interface and in the bulk of solution, respectively. The equilibrium concentration of hydrogen in solution, $C_{H,*}$, is obtained from the gas solubility data of hydrogen in the solvent, when the solvent is fully saturated with the gas.

$$C_{H,*} = \frac{1000 \times 273.15}{760 \times 22400} \times \frac{V_{g,s} \times P_H}{V_L \times T} \text{ g mol/l} \qquad \text{(II-2.2)}$$

where $V_{g,s}$ is the milliliters of the gas dissolved in V_L milliliters of liquid at a hydrogen partial pressure P_H mm Hg and system temperature of T°K.

If V_g milliliters of hydrogen transfer through the gas-liquid interface in t seconds, then the rate of hydrogen transfer is given by

$$N = \frac{1000 \times 273.15}{760 \times 22400} \times \frac{V_g \times P_H}{t \times T \times V_L} \frac{\text{g mol}}{(\text{l})\,(\text{sec})} \qquad \text{(II-2.3)}$$

From Equation (II-2.1) one gets

$$C_{H,b} = C_{H,*} - \frac{N}{k_L a} \qquad \text{(II-2.4)}$$

Knowing the values of $C_{H,*}$, N, and $k_L a$, hydrogen concentration in the bulk, $C_{H,b}$, can be calculated from equation (II-2.4).

The departure of bulk concentration from the saturation concentration, $(C_{H,*} - C_{H,b}) / C_{H,*}$, can then be calculated. The magnitude of this number is a measure of the mass transfer resistance offered to hydrogen at the gas-liquid interface for a given stirring speed. For most of the experiments in this study, the concentration difference between the bulk liquid and the saturation concentration at the interface was kept not different from each other by more than 5 percent. It can thus be said that the mass transfer resistance at the gas-liquid interface was negligible in this study. In various calculations, the concentration of hydrogen used was $C_{H,b}$ or a hypothetically equivalent value of hydrogen partial pressure, $P_{H,b}$, representing that value of hydrogen partial pressure in the gas phase, which will produce a value of concentration $C_{H,b}$ when there exists no concentration difference between the gas-liquid interface and the bulk of liquids.

II-3 Calculations of the Reaction Rates

The reaction rates were obtained by measuring the rate of hydrogen consumption. From the stoichiometry of the reactions studied, one mole of hydrogen is required for one mole of substrate, the reaction rate, r, is thus given by

$$r = \frac{273.15}{760 \times 22400} \times \frac{V_g \times P_H}{t \times T \times w} \frac{\text{mol}}{(\text{sec})\ (\text{g. Ni})} \qquad \text{(II-3.1)}$$

where w is the weight of the catalyst expressed as grams of nickel.

For the experiments in the first order region, the value of $C_{A,b}/r$ was obtained from the slope of the plot of $(V^f - V)$ versus t on a semi-log plot. Here V^f and V are the total volume of hydrogen consumed and volume of hydrogen consumed at any time, respectively. The theory of this plot is as follows.

The rate of reaction of substrate in the first order region is given by

$$- \frac{d C_{A,b}}{dt} = k' C_{A,b} \qquad \text{(II-3.2)}$$

or

$$\frac{d \ln C_{A,b}}{dt} = k' \qquad \text{(II-3.3)}$$

since

$$\frac{d \ln C_{A,b}}{dt} = \frac{d \ln (V^f - V)}{dt} \qquad \text{(II-3.4)}$$

the value of k' is given by the slope of the line obtained by plotting $(V^f - V)$ versus t on a semi-log plot. The reaction rate is then

$$r = k' C_{A,b} \frac{V_L}{w} \qquad \text{(II-3.5)}$$

or

$$\frac{C_{A,b}}{r} = \frac{1}{k'} \frac{w}{V_L} \qquad \text{(II-3.6)}$$

Thus by knowing the slope of the above mentioned plot, weight of the catalyst used and the volume of the liquid, the quantity, $C_{A,b}/r$, can be calculated.

II-4 Calculations of $\mathcal{J}_A$ and $\mathcal{J}_H$

The transport parameters, defined as the ratio of the concentration on the surface to that in the bulk, were obtained from the rate data by knowing the particle-liquid mass transfer coefficients. These coefficients were measured experimentally for a few systems and for others were obtained by extrapolating the measured values. Details of the extrapolating procedures are given in section II-5.

The rate of reaction is given as

$$r = k_{p,A}\, a_p\, (C_{A,b} - C_{A,s}) \qquad \text{(II-4.1)}$$

or

$$r = k_{p,H}\, a_p\, (C_{H,b} - C_{H,s}) \qquad \text{(II-4.2)}$$

from equations (II-4.1) and (II-4.2) we have

$$\mathcal{J}_A = \frac{C_{A,s}}{C_{A,b}} = 1 - \frac{r}{k_{p,A}\, a_p\, C_{A,b}} \qquad \text{(II-4.3)}$$

and

$$\mathcal{J}_H = \frac{C_{H,s}}{C_{H,b}} = 1 - \frac{r}{k_{p,H}\, a_p\, C_{H,b}} \qquad \text{(II-4.4)}$$

Here $k_{p,A}$ and $k_{p,H}$ are particle-liquid mass transfer coefficients for substrate and for hydrogen, respectively.

II-5 Calculations of Particle-Liquid Mass Transfer Coefficients

Particle-liquid mass transfer coefficients for allyl alcohol in the solvents water and ethanol were obtained experimentally. For several other liquid phases, the mass transfer coefficients were obtained by extrapolating the experimentally measured values of $k_p a_p$. It was assumed that the mass transfer coefficient for a substrate-solvent system is related to that of the other as the ratio of their diffusivities, to the first power. Since the variations in the densities and viscosities of the various solvents used are not large and their dependence on the departure of Sherwood number from 2 is only to the 1/6th power, their effect is neglected here. Semi-emperical method of Levins and Glastonbury was also used to calculate particle-liquid mass transfer coefficients and were used for comparison with those obtained above.

Diffusivity data obtained from the literature are listed in table II-2. The calculated and experimental values of particle-liquid mass transfer coefficients for different systems are listed in table II-3. The values presented in the column at the far right were calculated entirely by the Levins and Glastonbury method assuming the same particle size of 16 microns, and "mild" agitation conditions. A sample calculation explaining the method of Levins and Glastonbury is presented in section II-6.

II-6 Sample Calculations of Levins and Glastonbury Method

The mass transfer equation proposed by Levins and Glastonbury for forced convection conditions when a significant difference exists between the densities of the particles and the fluid is

$$\frac{k_p d_p}{D} = 2 + 0.44 \left(\frac{dp\, v}{\nu}\right)^{\frac{1}{2}} \left(\frac{\nu}{D}\right)^{0.38} \qquad \text{(II-6.1)}$$

A typical example of calculations for allyl alcohol in water at 25°C is presented. Here

$$d_p = 16 \times 10^{-4} \text{ cm}$$
$$D = 1.19 \times 10^{-5} \text{ cm}^2/\text{sec}$$
$$\mu = 0.8937 \times 10^{-2} \text{ g/cm-sec}$$
$$\rho_L = 0.99708 \text{ g/cm}^3$$
$$\rho_p = 4.5 \text{ g/cm}^3$$

The slip velocity between the liquid and the particles is given by the equation

TABLE II-2

Diffusivity Data

Component 1	Component 2	T °C	$D_{12} \times 10^5$ cm^2/sec	Ref.
hydrogen	ethanol	20°C	15.1	61
hydrogen	water	25°C	4.5	60
			4.85	
hydrogen	benzene	25°C	15.1	55
hydrogen	cyclohexane	25°C	14.0	55
hydrogen	isopropanol	25°C	7.7	56
allyl alcohol	water	25°C	1.19	60
allyl alcohol	ethanol	25°C	1.06	60
acetone	benzene	25°C	2.78	57, 58
acetone	cyclohexane	25°C	2.08	58
acetone	isopropanol	25°C	1.0	59

TABLE II-3

Particle-Liquid Mass Transfer Coefficients

System	$k_{p,A} a_p$ or $k_{p,H} a_p$ from diffusivity data	$\frac{cm^3}{(g)(sec)}$ by Levins and Glastonbury method
acetone-benzene	46.2	42.4
acetone-cyclohexane	34.9	32.2
acetone-isopropanol	16.8	16.3
allyl alcohol-water*	20.0	20.0
allyl alcohol-ethanol*	13.3	17.0
hydrogen-benzene	253.7	
hydrogen-cyclohexane	190.0	
hydrogen-isopropanol	129.4	
hydrogen-water	75.6	
hydrogen-ethanol	223.8	

* Experimental results

$$v = (U_E^2 + U_t^2 + U_s^2)^{\frac{1}{2}} \qquad \text{(II-6.2)}$$

Since the contribution because of U_s arising from the difference in inertia between the particles and the fluid is usually the least, and is neglected.

From figure (15) of Levins and Glastonbury assuming "mild" stirring conditions, one gets

$$U_E = 0.18 \text{ cm/sec}$$

The particle terminal velocity, U_t, is obtained from the Stokes law

$$U_t = \frac{d_p^2 (\rho_P - \rho) g}{18 \mu} \qquad \text{(II-6.3)}$$

$$= 0.05 \text{ cm/sec}$$

thus

$$v = \left[(0.05)^2 + (0.18)^2\right]^{\frac{1}{2}} = 0.1868 \text{ cm/sec}$$

Substituting the numerical values of different variables in equation (II-6.1) one obtains

$$\frac{k_p d_p}{D} = 2.995 \qquad \text{(II-6.4)}$$

For a particle diameter of 16 microns, the ratio

$$\frac{\text{Surface}}{\text{Weight}} = \frac{6}{\rho_P d_p} = 893 \text{ cm}^2/\text{g} \qquad \text{(II-6.5)}$$

from (II-6.4) and (II-6.5) one obtains

$$k_p a_p = 19.9 \frac{cm^3}{(sec)\ (g)}$$

II-7 Calculations of Weisz and Prater Parameter

The Weisz and Prater criterion is used to assess whether intraparticle transport rates have influenced the measured overall reaction rates. The criterion for isothermal reactions on a flat slab is based upon the observation that η is of the order of unity when $\hat{h}$ is of the order of unity. The criterion is

$$f(\theta) = \frac{\left(\frac{V_p}{A_p}\right)^2 R_D}{D_e C_s} < 1 \qquad \text{(II-7.1)}$$

If the value of $f(\theta)$ is less than unity, the reaction rate is controlled by the surface reaction and the internal transport processes need not be considered in the analysis. In equation (II-7.1)

R_d = the experimentally determined rate per unit volume of catalyst

V_p = volume of pellet (solid + interior void)

A_p = external surface

D_e = effective diffusivity

$= \frac{D\theta}{\tau}$

While calculating the volume of the catalyst, the internal void was taken as 0.50, as reported by Freel et al. for a similar Raney nickel catalyst [62]. The value of τ/θ was taken to be 6.0. This value

was arrived at on the basis of the numerical solution of a set of data of allyl alcohol hydrogenation in ethanol. In that set the experimental data and the numerical values agreed for a value of $R^2 \tau/\theta = 4.0 \times 10^{-6}$ cm^2. For particles of 16 microns diameter, this gives a value of $\tau/\theta = 6.25$, which is physically reasonable.

The values of $f(\theta)_H$ and $f(\theta)_A$ calculated for the various systems are presented in table V-5.

II-8 Calculations of Acetone Concentration on Catalyst Surface for a Monomolecular layer

Molecular volume of acetone = 79.4 ml/g mole

$$\text{Volume of one molecule} = \frac{79.4}{6.0238 \times 10^{23}}$$

$$= 16.18 \times 10^{-23} \text{ cm}^3$$

$$= 131.8^\circ \text{A}^3$$

Assuming molecule to be spherical and the surface area covered on the catalyst to be the projected area of this sphere, then

$$\text{diameter of one molecule of acetone} = \left(131.8 \times \frac{6}{\pi}\right)^{1/3}$$

$$= 6.31^\circ \text{A}$$

$$\text{Projected area of one molecule} = \frac{\pi}{4} \times (6.31)^2 \, ^\circ\text{A}^2$$

$$= 31.31^\circ \text{A}^2$$

The surface area of catalyst per gram (determined experimentally at the EMR laboratories) $= 58.1 \text{ m}^2$

Amount of acetone adsorbed per unit mass of catalyst

$$= \frac{58.1\ m^2}{31.31°A^2} \text{ molecular}$$

$$= \frac{58.1 \times 10^{20}}{31.3 \times 6.02 \times 10^{23}} \text{ moles}$$

$$= 3.1 \times 10^{-4} \text{ moles}$$

Hence the quantity of acetone needed to form a monomolecular layer on the catalyst surface is equal to 3.1×10^{-4} mol/g cat.

II-9 Thermopile Calibration Expression

The expression used to calculate temperature by knowing the EMF measured is

$$E = A \times T + B \times T^2 + c \times T^3 \qquad \text{(II-9.1)}$$

Where E is EMF in volts and T is temperature in °C. The values of constants A, B and C are:

$$A = 0.0001948470$$
$$B = 0.0000002130$$
$$C = -0.0000000010$$

The tables of EMF versus temperature for temperature intervals of 0.001°C are made by using equation (II-9.1) and values of constants A, B, and C. For a particular value of EMF generated by the thermopile, the temperature is read from these tables.

APPENDIX III

Integration of Rate Equation with Internal and External Diffusion Resistances

The integration of rate expression with internal and external diffusion resistance was performed in the asymptotic region and experimental data were fitted by the expression obtained. For the non-asymptotic region which covered only a smaller portion of the data, this solution was an approximation, however, the agreement between the calculated and experimental values obtained was reasonably good. The derivation of the analytical expression is presented here. The calculated data for experimental run No. 515 are presented in tables III-1 and III-2.

The rate of hydrogenation reaction is given by the equations:

$$\begin{aligned} r &= k_{p,A}\, a_p\, (C_{A,b} - C_{A,s}) \\ &= k\, C_{H,b}^{\frac{1}{2}}\, \eta \\ &= \frac{V_L}{w} \frac{dC_{A,b}}{dt} \end{aligned} \qquad \text{(III-1)}$$

Here $k_{p,A}$ is the particle-liquid mass transfer coefficient and k is the kinetic constant. The kinetic expression has a power of one half to the hydrogen concentration because the order of reaction with respect to hydrogen was found to be approximately one half.

The effectiveness factor, η, is obtained from the Thiele parameter, h, which for a zero order reaction is given by

$$h = R \left[\frac{K'_v \, C_{H,b}^{\frac{1}{2}}}{C_{A,s} \, D_e} \right]^{\frac{1}{2}} \qquad \text{(III-2)}$$

Here K'_v is the zero-order reaction rate constant based on volume and D_e is the effective diffusivity given by

$$D_e = \frac{D \theta}{\tau}$$

where θ is the void fraction and τ is the tortuosity factor.

For asymptotic region let $\eta = d/h$, where d is a constant.

Substituting from equation (III-2) in (III-1) one gets

$$r = k \, C_{H,b}^{\frac{1}{2}} \quad \eta = k' \, C_{H,b}^{\frac{1}{2}} \quad \frac{d}{h}$$

or

$$r = \frac{k'' C_{H,b}^{\frac{1}{2}}}{R} \left[\frac{C_{A,s} \, D_e}{K'_v \, C_{H,b}^{\frac{1}{2}}} \right]^{\frac{1}{2}}$$

$$= \frac{k'' \left[C_{A,s} \, C_{H,b}^{\frac{1}{2}} \, D_e \right]^{\frac{1}{2}}}{R} = b_1 \, C_{A,s}^{\frac{1}{2}} \qquad \text{(III-3)}$$

where

$$b_1 = \frac{k'' \left[C_{H,b}^{\frac{1}{2}} \, D_e \right]^{\frac{1}{2}}}{R} \qquad \text{(III-4)}$$

Substituting the value of $C_{A,s}$ from equation (III-3) into equation (III-1), one gets

$$r = k_{p,A} \, a_p \left[C_{A,b} - \left(\frac{r}{b_1} \right)^2 \right] \qquad \text{(III-5)}$$

rearranging equation (III-5), a quadratic equation is obtained

$$k_{p,A} \, a_p \, r^2 + b_1^2 \, r - k_{p,A} \, a_p \, b_1^2 \, C_{A,b} = 0 \qquad \text{(III-6)}$$

The value of r is obtained from equation (III-6), taking the positive root,

$$r = -\frac{V_L}{w}\frac{dC_{A,b}}{dt} = \frac{-b_1^2 + \sqrt{b_1^4 + (2 b_1 k_{p,A} a_p)^2 C_{A,b}}}{2 k_{p,A} a_p} \qquad \text{(III-7)}$$

rearranging equation (III-7)

$$\frac{dC_{A,b}}{dt} = \frac{w}{2 k_{p,A} a_p V_L}\left[b_1^2 - \sqrt{b_1^4 + (2 b_1 k_{p,A} a_p)^2 C_{A,b}} \right] \qquad \text{(III-8)}$$

or
$$\frac{dC_{A,b}}{dt} = n - \sqrt{n^2 + m C_{A,b}} \qquad \text{(III-9)}$$

where
$$n = \frac{w b_1^2}{2 k_{p,A} a_p V_L} \qquad \text{(III-10)}$$

and
$$m = \left(\frac{b_1 w}{V_L}\right)^2 \qquad \text{(III-11)}$$

Equation (III-9) is of the form

$$\frac{dx}{dt} = a - \sqrt{a^2 + cx}$$

which on integration gives

$$t = -\frac{a}{c}\left[\ln x + 2\sqrt{1 + \frac{c}{a^2}\,x} + \ln \frac{\sqrt{1 + \frac{c}{a^2}\,x} - 1}{\sqrt{1 + \frac{c}{a^2}\,x} + 1}\right]$$

Thus equation (III-9) upon integration gives

$$t = -\frac{n}{m}\left[\ln C_{A,b} + 2\sqrt{1+\frac{m}{n^2}C_{A,b}} + \ln \frac{\sqrt{1+\frac{m}{n^2}C_{A,b}}-1}{\sqrt{1+\frac{m}{n^2}C_{A,b}}+1}\right] \qquad \text{(III-12)}$$

Defining parameters α and β, using equations (III-10) and (III-11)

$$\frac{1}{\alpha} = \frac{n}{m} = \frac{V_l}{2\,k_{p,A}\,a_p\,w} \qquad \text{(III-13)}$$

and

$$\beta = \frac{m}{n^2} = \left(\frac{2\,k_{p,A}\,a_p}{b_l}\right)^2 \qquad \text{(III-14)}$$

Equation (III-12) now can be written as

$$-\alpha t = \ln C_{A,b} + 2\sqrt{1+\beta C_{A,b}} + \ln \frac{\sqrt{1+\beta C_{A,b}}-1}{\sqrt{1+\beta C_{A,b}}+1} \qquad \text{(III-15)}$$

using the boundary condition

at $t = 0$, $C_{A,b} = C_{A,O}$, one gets

$$\alpha t = \ln \frac{C_{A,O}}{C_{A,b}} + 2\left[\sqrt{1+\beta C_{A,O}} - \sqrt{1+\beta C_{A,b}}\right] + \ln\left[\frac{(\sqrt{1+\beta C_{A,O}}-1)\,(\sqrt{1+\beta C_{A,b}}+1)}{(\sqrt{1+\beta C_{A,O}}+1)\,(\sqrt{1+\beta C_{A,b}}-1)}\right] \qquad \text{(III-16)}$$

Equation (III-16) is the rate equation which was used to fit the experimental data obtained in Run 515. Initially, the allyl alcohol hydrogenation reaction

was zero order in allyl alcohol and was taken through the concentration change in which the transition from zero order to first order occured. The pseudo-zero-order rate constant was obtained from rate measurements in the zero-order region. The particle-liquid mass transfer coefficient $k_{p,A}\, a_p$ was obtained from the data in the first-order region.

Experimental data were plotted in the form $C_{A,b}^{\frac{1}{2}}$ versus t to obtain concentration range of $C_{A,b}$ in which the curve was linear. This portion of data was considered to be in asymptotic region and the rate there was used to calculate first estimate of b_1. In asymptotic region $r = b_1 C_{A,b}^{\frac{1}{2}}$. Value of r is evaluated graphically in the region linear in $C_{A,b}^{\frac{1}{2}}$. Concentration $C_{A,s}$ for that value of t is obtained from the graph of $C_{A,s}/C_{A,b}$, and hence then quantity b_1 is obtained.

In the solution of equation (III-16), the experimental and calculated data agreed for a τ/θ values equal to 6.25 for particles of 16 microns diameter. From the first order region of data the value of $k_{p,A}\, a_p$ was obtained to be 9.48 $cm^3/(g\text{-cat})\,(sec)$, and the zero order region gave the value of constant $k = 3.98 \times 10^{-5}$ moles $/(g\text{-cat})\,(sec)$. These values were used to obtain calculated data. The experimental and calculated data are presented in tables (III-1) and (III-2).

TABLE III-1

Experimental Data of Hydrogenation of Allyl Alcohol in Ethanol

(Run No. 515)

P_H = 687 mm Hg
T = 25°C
w = .0386 g
V_L = 209.5 ml

Time (sec)	V_{H_2} (ml)	$C_{A,b} \times 10^8 \frac{mol}{ml}$
0	0	953.5
61	2.33	912.5
110	4.43	875.4
145	6.01	847.5
183	7.65	818.6
240	10.68	765.1
282	12.36	735.5
325	14.10	704.8
372	15.80	674.8
424	17.70	641.3
515	21.08	581.7
583	23.08	546.4
658	25.28	507.6
732	27.28	472.3
815	29.38	435.2
895	31.31	401.2
983	33.37	364.8
1068	35.11	334.1
1177	37.11	298.8
1310	39.31	259.2

continued

Table III-1 (continued)

Time (sec)	V_{H_2} (ml)	$C_{A,b} \times 10^8$ $\frac{mol}{ml}$
1447	41.64	218.9
1635	44.07	176.1
1813	45.97	142.5
2025	47.98	107.3
2215	49.25	84.7
2390	50.23	67.4
2510	50.86	56.3
2790	51.88	38.3
3125	52.76	22.6
3360	53.23	14.5
3530	53.43	10.9
3900	53.69	6.35
4200	53.90	2.65
4600	54.05	0
5000	54.05	0

TABLE III-2

Calculated Data of Hydrogenation of Allyl Alcohol in Ethanol (Run 515)

Time (sec)	$C_{A,b} \times 10^8$ mol/ml
-10	962.0
131	870.0
281	775.0
443	678.0
618	581.0
806	484.0
1013	390.0
1243	300.0
1400	248.0
1632	182.0
1932	120.0
2213	77.0
2683	37.0
3440	12.0
3730	7.0
4130	3.5

APPENDIX IV

Hydrogen Solubility Data

Hydrogen solubility data in the various solvents and acetone-solvent binary mixtures were needed to calculate concentration driving force for gas absorption and liquid-particle mass transfer.

Experimental data for hydrogen solubility in water, ethanol, benzene, cyclohexane, isopropanol, acetone, and in the binary mixtures of acetone-benzene, acetone-cyclohexane, and acetone-isopropanol were obtained in the laboratory. For the binary solutions, hydrogen solubility was determined at four or five different compoisitions of the liquid phase and was correlated with models for predicting mixed solvent Henry's law constants. The model which represents the data best was then used to interpolate the solubility data at known liquid composition.

IV-1 Experimental

The solubility data were measured at 25°C and approximately one atmosphere total pressure. Solubilities were determined by equilibrium volumetric method which has been discussed earlier in section 4.8.2.

When hydrogen solubilities were measured in the binary liquid mixtures, approximately known volumes of the two liquids were mixed in the solution flask, after the liquids were individually degassed. These solutions were then analyzed by measuring their refractive indicies at 25°C with a Bausch and Lomb Abbe 3-L refractometer. Refractive indicies measured with in $\pm$ 0.00005 for the binary samples of known composition were correlated by the equation

$$\eta_D = x_1 \eta_{D_1} + x_2 \eta_{D_2} + x_1 x_2 (Ax_1 + Bx_2 - Cx_1 x_2)$$

(IV-1)

Here η_{D1} and η_{D2} are the refractive indicies of the pure components. The constants A, B, and C were obtained by the method of least squares. These constants are presented in table IV-1 for the three systems studied. The calibration data were correlated with an average percent deviation of 0.02 for acetone-benzene system, of 0.03 for acetone-cyclohexane system, and of 0.004 for acetone-isopropanol system.

Density data, needed for the binary mixtures to obtain the volume of the liquid, were also correlated by an equation identical to equation (IV-1). The constants of correlation and the percent deviations of the experimental data from the calculated data are presented in table IV-2.

The partial pressure of the liquid vapors in the gas phase were obtained by knowing the composition of the liquid phase, by using equation

$$P_M = P_1 x_1 + P_2 x_2 + x_1 x_2 [C_1 + C_2 (2x_1 - 1) + C_3 (2x_1 - 1)^2 + ...] \quad \text{(IV-2)}$$

where P_1, P_2 and P_M are the vapor pressures of the components 1, 2, and of mixture, respectively. Thermodynamic vapor pressure-composition data were used to obtain constants C_1, C_2, C_3...etc., for the various binary systems. These constants along with the vapor pressures of the pure components are presented in table IV-3.

IV-2 Results and Discussions

Experimental data for hydrogen solubility in pure and mixed solvents are reported as Ostwald coefficients and as Henry's law constants in tables IV-4 and IV-5.

For binary liquid solutions, the Henry's law constants were correlated by the additive excess free energy models for predicting gas solubilities in mixed solvents. Detailed discussion has been presented elsewhere [63]. Of the several models used, four giving the best results are presented here for the situation when $i \neq j$.

(1) Ideal Model: This is the simplest case when the binaries form ideal mixtures. Here, Henry's law constant for mixed solvents is given by the Krischevsky equation [64].

$$\ln H_{1,m} = \sum_{i=2}^{m} x_i \ln H_{1,i} \qquad \text{(IV-3)}$$

(2) One Constant Margules Equation Model:

Here, one constant Margules equation is used to represent binary solvent vapor-liquid equilibrium data

$$\frac{g^E_{ij}}{RT} = B_{ij} x_i x_j \qquad \text{(IV-4)}$$

Using equation (IV-4), Prausnitz and O'Connell[65] derived the following equation

$$\ln H_{1,m} = \sum_{i=2}^{m} x_i \ln H_{1,i} - \tfrac{1}{2} \sum_{i=2}^{m} \sum_{j=2}^{m} B_{ij} x_i x_j \qquad \text{(IV-5)}$$

(3) Two Constant Margules Equation Model:

When excess free energy of the solvent-solvent binaries are expressed with a two constant Margules equation

$$\frac{g^{E}_{ij}}{x_i x_j RT} = B_{ij} + C_{ij}(2x_i - 1) \qquad \text{(IV-6)}$$

The resulting equation for the mixed solvent Henry's law constant was recommended by Boublik and Hala for use with non-electrolyte systems [66].

$$\ln H_{1,m} = \sum_{i=2}^{m} x_i \ln H_{1,i} - \frac{1}{2} \sum_{\substack{i=2 \\ i \neq j}}^{m} \sum_{j=2}^{m} \left[B_{ij} + 2C_{ij}(2x_i - 1) \right] x_i x_j \qquad \text{(IV-7)}$$

(4) Van Laar Model: A further possibility is to express solvent-solvent binary excess free energy by the van Laar equation. In this case only two body interactions are considered, but the effective molar volumes, q_i, are considered as parameters. The result is

$$\ln H_{1,m} = \sum_{i=2}^{m} x_i \ln H_{1,i} - \frac{1}{2} \sum_{\substack{i=2 \\ i \neq j}}^{m} \sum_{j=2}^{m} \frac{x_i}{x_j} \frac{A'_{ij}}{1 + \left(\frac{A'_{ij} x_i}{B'_{ij} x_j} \right)^2} \qquad \text{(IV-8)}$$

Here A'_{ij} and B'_{ij} are the Van Laar constants using the Carlson and Colburn convention [67]

$$\frac{g^{E}_{ij}}{RT} = \frac{A'_{ij} B'_{ij} x_i x_j}{A'_{ij} x_i + B'_{ij} x_j} \qquad \text{(IV-9)}$$

Equation (IV-8) was used for the first time by Puri and Ruether [63].

A comparison of experimental and predicted mixed solvent Henry's constants for the four models is shown in table IV-6. Results of the three systems measured experimentally are also shown in Figure IV-1. Of the models tested, equation (IV-8) based on Van Laar correlation of solvent-solvent non ideality was the best, but was only marginally better than equation (IV-3). Thus, for the present study, Van Laar model was adopted for the interpolation of the gas solubility data for various binaries used.

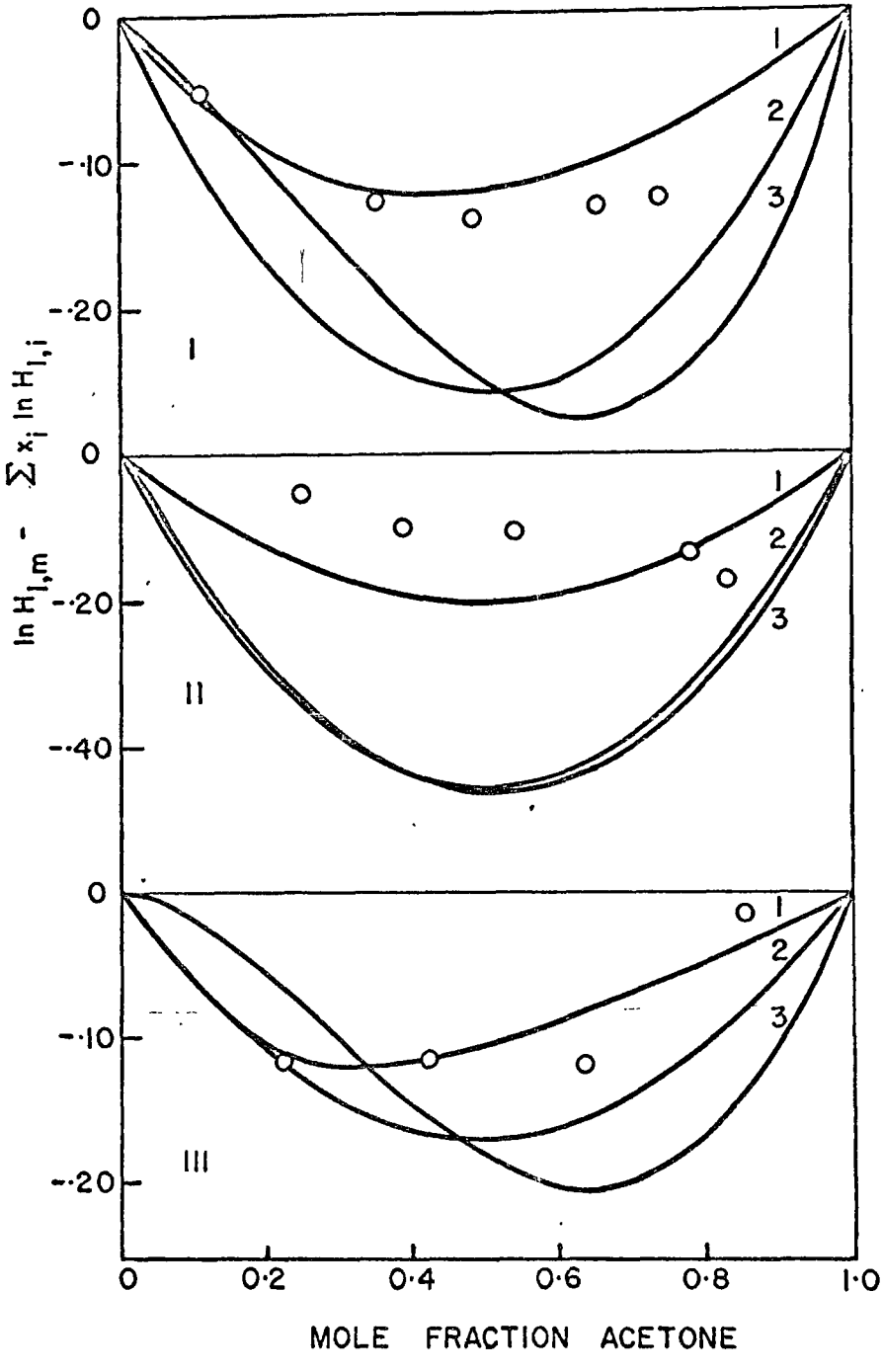

Figure IV-1 Henry's constant for hydrogen in organic binaries at 25°C. Solvents: I acetone-isopropanol; II acetone-cyclohexane; III acetone-benzene. Curves: 1 Equation (IV-8); 2 Equation (IV-5); 3 Equation (IV-7).

TABLE IV-1

Refractive Index - Composition Data Correlation at 25°C

$$\eta_{DM} = x_1 \eta_{D_1} + x_2 \eta_{D_2} + x_1 x_2 (A x_1 + B x_2 - C x_1 x_2)$$

System	η_{D_1}	η_{D_2}	A	B	C	% Dev.
Acetone (1) - benzene (2)	1.3566	1.4979	0.0294546	0.0190779	-0.0080656	0.020
Acetone (1) - cyclohexane (2)	1.3566	1.4233	0.0060214	0.0329934	0.0528160	0.011
Acetone (1) - isopropanol (2)	1.3566	1.3747	-0.0065806	-0.0010431	0.0004512	0.001

TABLE IV-2

Density - Composition Data Correlation at 25°C

$$\rho_M = x_1 \rho_1 + x_2 \rho_2 + x_1 x_2 (A x_1 + B x_2 - C x_1 x_2)$$

System	ρ_1 g/ml	ρ_2 g/ml	A	B	C	% Dev.
Acetone (1) - Benzene (2)	0.7855	0.8735	0.025433	0.012004	-0.011148	0.0910
Acetone (1) - cyclohexane (2)	0.7855	0.7729	-0.058753	-0.039681	-0.030890	0.0039
Acetone (1) - isopropanol (2)	0.7855	0.7809	-0.014116	-0.012597	-0.000856	0.0061

TABLE IV-3

Pressure - Composition Data Correlation at 25°C

$$P_M = P_1 x_1 + P_2 x_2 + x_1 x_2 [C_1 + C_2 (2x_1 - 1) + C_3 (2x_1 - 1)^2 + \ldots]$$

System	P_1 mm Hg	P_2 mm Hg	C_1	C_2	C_3	C_4	C_5	% Dev.
Acetone (1) - benzene (2)	226.50	95.00	113.2077	-68.5211	70.2712	-67.3838	-	0.62
Acetone (1) - cyclohexane (2)	229.55	97.77	373.8838	-182.3288	272.1202	-185.7301	323.7346	0.13
Acetone (1) - isopropanol (2)	229.55	44.02	125.3636	-83.7920	43.0225	-93.7373	-	0.86

TABLE IV-4

Solubility of Hydrogen in Different Solvents at 25°C

Solvent	Bunsen coefficient	
	experimental	literature
water	.0172	.0174 [68]
ethanol	.0783 .0783	.0784 [69]

TABLE IV-5

Solubility of Hydrogen in Pure and Mixed Solvents at 25°C

x mole fr. of acetone	l Ostwald coefficient Experimental	Literature	H^{atm} Henry's Law constant
	Acetone-Benzene		
1.0000	0.0943		2416
0.8536	0.0919		2473
0.6381	0.0952		2366
0.4255	0.0890		2502
0.2233	0.0847		2649
0.0000	0.0756	0.0756 (69) 0.071 (70)	3156
	Acetone-Cyclohexane		
1.0000	0.0943		2416
0.8282	0.0929		1979
0.7769	0.0900		2032
0.5406	0.1028		2014
0.3914	0.1058		1977
0.2466	0.1030		2023
0.0000	0.0953	0.092 (70)	2041
	Acetone-Isopropanol		
1.000	0.0943		2416
0.736	0.1016		2355
0.655	0.1038		2414
0.486	0.1038		2560
0.351	0.1023		2719
0.122	0.0920		3201
0.000	0.0845		3539

TABLE IV-6

Measured and Predicted Values of Henry's Constants in Mixed Solvents

System	No. of data points	Average Absolute Deviation [a]			
		Eqn (II-3)	Eqn (II-5)	Eqn (II-7)	Eqn (II-8)
Hydrogen-Acetone-Benzene	4	-9.6	+4.1	7.5	1.5
Hydrogen-Acetone-Cyclohexane	5	-11.9	21.7	22.0	6.6
Hydrogen-Acetone-isopropanol	5	-12.4	+8.9	+8.3	2.3

a $\text{Deviation} = \dfrac{H_{exp} - H_{cal}}{H_{exp}} \times 100$

\+ indicates positive deviation

\- indicates negative deviation

No sign indicates both positive and negative deviations

APPENDIX V

Experimental and Calculated Data for Allyl Alcohol and Fumaric Acid Hydrogenation

TABLE V-I

Reaction Order with Respect to Substrate Concentration at 25° C

P_H mm Hg	$C_{A,O} \times 10^5$ $\frac{mol}{ml}$	$r \times 10^5 \frac{mol}{(sec)(g\text{-}cat)}$
Allyl Alcohol in Water (Run No. 212)		
713.6	0.673	3.506
714.0	2.018	3.299
714.3	3.368	3.219
714.8	6.055	3.136
714.2	8.746	2.757
Allyl Alcohol in Ethanol (Run No. 504)		
685.5	6.700	3.695
685.5	13.400	4.171
685.5	20.100	4.354
Fumaric Acid in Ethanol (Run No. 306)		
707.5	11.48	0.657
707.5	7.74	0.657
707.5	4.01	0.657

TABLE V-2

Reaction Order with Respect to Hydrogen Partial Pressure at 25° C

P_H mm Hg	$C_{H,b} \times 10^8$ $\frac{mol}{ml}$	$P_{H,b}$ mm Hg	$r \times 10^6$ $\frac{mol}{(g\text{-cat})(sec)}$
Allyl Alcohol in Water (Run No. 205)			
714.5	49.51	480.8	30.30
607.5	42.03	408.1	25.85
512.5	35.53	345.0	21.71
423.8	29.13	282.8	18.27
Fumaric Acid in Ethanol (Run No. 307)			
683.7	305.7	664.3	6.35
436.7	194.1	429.8	4.85
287.6	126.9	275.7	3.94
138.2	59.9	130.2	2.66
Allyl Alcohol in Ethanol (Run No. 514)			
692.0	316.5	687.7	38.12
458.5	209.4	455.0	33.48
307.3	140.1	304.4	28.20
221.5	100.7	218.8	24.60

TABLE V-3

Reaction Rates with Linear Dependence on Bulk Concentration at 25°C

P_H mm Hg	$(P_{H,b})^{-0.5} \times 10$ $(mm\ Hg)^{0.5}$	$\frac{C_{A,b}}{r}$ $\frac{(g\text{-}cat)\ (sec)}{ml}$
Allyl Alcohol in Water (Run No. 210)		
731.4	0.3698	0.05615
671.6	0.3859	0.05555
628.8	0.3988	0.05437
594.4	0.4101	0.04491
427.5	0.4838	0.04963
277.9	0.5999	0.05140
251.1	0.6309	0.04668
337.0	0.5446	0.04963
149.0	0.8190	0.04728
182.9	0.7396	0.04963
Allyl Alcohol in Ethanol (Run No. 506)		
677.1	0.3843	0.08867
488.3	0.4525	0.08509
372.9	0.5178	0.07151
292.2	0.5851	0.06932
206.0	0.6968	0.07236
108.1	0.9615	0.06655
Fumaric Acid in Ethanol (Run No. 302)		
705.7	0.3765	0.4993
655.5	0.3906	0.5053
531.4	0.4338	0.5366
379.7	0.5133	0.6324
261.9	0.6181	0.7989

TABLE V-4

Data for Apparent Activation Energy for Allyl Alcohol in Ethanol

t° C	$\frac{1}{T} \times 10^3$ (°K) $^{-1}$	ln k_o or ln $k_{p,A}{}^{a}{}_{p}$
(Run No. 528)		
Zero order region		
24.5	3.359	3.19
28.6	3.314	3.67
32.2	3.275	4.04
35.3	3.242	4.31
First order region		
24.5	3.359	2.68
28.6	3.314	2.34
32.2	3.275	2.53
35.3	3.242	2.27

TABLE V-5

Experimental Rate Data

Allyl Alcohol in Water (Run No. 212)

C_{AO} = 11.44 x 10^{-5} mol/ml

V_l = 218.5 ml

w = 6.23 x 10^{-3} g.

t = 25°C

$P_{H,mm\ Hg}$	$C_{A,b}$ $\frac{mol}{ml}$ x 10^5	$C_{H,b}$ $\frac{mol}{ml}$ x 10^8	r $\frac{mol}{g\text{-}sec}$ x 10^6	$\frac{C_{AO} - C_A}{C_{AO}}$	$\mathcal{J}_A = \frac{C_{A,s}}{C_{A,b}}$	$f(\theta)^a_A$	$\mathcal{J}_H = \frac{C_{H,s}}{C_{H,b}}$	$f(\theta)^a_H$
713.6	0.673	60.8	35.06	0.941	0.739	1.06	0.238	9.65
714.0	2.018	61.3	32.99	0.824	0.918	0.27	0.292	7.34
714.3	3.368	61.9	32.20	0.706	0.952	0.15	0.313	6.62
714.8	6.055	62.3	31.36	0.471	0.974	0.08	0.324	6.19
714.2	8.746	63.6	27.57	0.235	0.984	0.05	0.427	4.04
714.4	11.440	64.4	25.36	0.0	0.989	0.03	0.479	3.27

a: Defined by equation II-7.1

Allyl Alcohol in Water (Run No. 206)

C_{AO} = 11.44 x 10^{-5} mol/ml
V_l = 229.0 ml
w = 3.48 x 10^{-3} g
t = 25°C

P_H mm Hg	$C_{A,b}$ $\frac{mol}{ml}$ x 10^6	$C_{H,b}$ $\frac{mol}{ml}$ x 10^8	r $\frac{mol}{g\text{-}sec}$ x 10^6	$\frac{C_{AO} - C_A}{C_{AO}}$	$\mathcal{J}_A = \frac{C_{A,s}}{C_{A,b}}$	$f(\theta)_A$	$\mathcal{J}_H = \frac{C_{H,s}}{C_{H,b}}$	$f(\theta)_H$
704.7	2.68	67.8	24.40	0.9766	0.545	2.52	0.524	2.73
	2.13	67.9	24.40	0.9814				
	1.63	69.1	17.76	0.9858	0.455	3.61	0.660	1.55
	1.14	69.8	14.49	0.9900	0.363	5.27	0.725	1.14
	0.51	71.0	7.89	0.9955	0.222	10.5	0.853	0.52

Allyl Alcohol in Water (Run No. 210 A)

$C_{A,O}$ = 11.44 x 10^{-5} mol/ml

V_l = 220.0 ml

w = 13.0 x 10^{-3} g

t = 25°C

P_H mm Hg	$C_{A,b}$ $\frac{mol}{ml}$ x 10^6	$C_{H,b}$ $\frac{mol}{ml}$ x 10^8	r $\frac{mol}{g\text{-}sec}$ x 10^6	$\frac{C_{AO} - C_A}{C_{AO}}$	$\mathcal{J}_A = \frac{C_{A,s}}{C_{A,b}}$	$f(\theta)_A$	$\mathcal{J}_H = \frac{C_{H,s}}{C_{H,b}}$	$f(\theta)_H$
731.4	0.966	66.5	19.32	0.9916	0.00	∞	0.603	1.15
	0.637	69.5	12.73	0.9944	-0.001	-3010	0.738	0.73
	0.420	71.5	8.41	0.9963	-0.001	-2510	0.827	0.47
	0.225	73.3	4.51	0.9980	-0.002	-1372	0.907	0.25
	0.075	74.6	1.50	0.9993	0.00	∞	0.969	0.08

Fumaric Acid in Ethanol (Run No. 306)

C_{AO} = 11.48 x 10^{-5} mol/ml
V_l = 211.5 ml
w = 38.4 x 10^{-3} g
t = 25°C

P_H mm Hg	$C_{A,b}$ $\frac{mol}{ml}$ x 10^5	$C_{H,b}$ $\frac{mol}{ml}$ x 10^8	r $\frac{mol}{g\text{-}sec}$ x 10^6	$\frac{C_{AO} - C_A}{C_{AO}}$	$\mathcal{J}_A = \frac{C_{A,s}}{C_{A,b}}$	$f(\theta)_A \mathcal{J}_H = \frac{C_{H,s}}{C_{H,b}}$	$f(\theta)_H$	
680.1	4.01	303.8	6.57	0.651	0.988	.0306	0.990	.025
	7.74	303.8	6.57	0.326	0.994	.0159	0.990	.025
	11.48	303.8	6.57	0.00	0.996	.0107	0.990	.025

Fumaric Acid in Ethanol (Run No. 309)

C_{AO} = 11.48 x 10^{-5} mol/ml
V_l = 228.0 ml
w = 53.7 x 10^{-3} g

697.4	0.275	319.6	0.670	0.9760	0.981	.0463	0.999	.0025
	0.178	319.8	0.566	0.9845	0.976	.0607	0.999	.0021
	0.073	320.1	0.379	0.9936	0.957	.1012	0.999	.0014
	0.114	319.9	0.461	0.9901	0.969	.0781	0.999	.0017
	0.024	320.5	0.180	0.9980	0.944	.1487	0.999	.0007

Fumaric Acid in Ethanol (Run No. 307)

$C_{AO} = 11.48 \times 10^{-5}$ mol/ml

$V_l = 229.6$ ml

$w = 41.6 \times 10^{-3}$ g

$t = 25°C$

P_H mm Hg	$C_{A,b}$ $\frac{mol}{ml}$ $\times 10^5$	$C_{H,b}$ $\frac{mol}{ml}$ $\times 10^8$	r $\frac{mol}{g\text{-}sec}$ $\times 10^5$	$\frac{C_{AO} - C_A}{C_{AO}}$	$\mathcal{J}_A = \frac{C_{A,s}}{C_{A,b}}$	$f(\theta)_A$	$\mathcal{J}_H = \frac{C_{H,s}}{C_{H,b}}$	$f(\theta)_H$
683.7	3.65	305.7	6.315	0.682	.991	.0326	.991	.0247

Fumaric Acid in Ethanol (Run No. 315)

$C_{AO} = 11.48 \times 10^{-5}$ mol/ml

$V_l = 206.3$ ml

$w = 21.6 \times 10^{-3}$ g

$t = 25°C$

684.0	2.08	311.4	4.258	.820	.994	.0385	.994	.0163

Allyl Alcohol in Ethanol (Run No. 504)

$C_{AO} = 20.1 \times 10^{-5}$ mol/ml

$V_l = 219.3$ ml

$w = 2.52 \times 10^{-3}$ g

$t = 25°C$

P_H mm Hg	$C_{A,b}$ $\frac{mol}{ml}$ $\times 10^5$	$C_{H,b}$ $\frac{mol}{ml}$ $\times 10^8$	r $\frac{mol}{g\text{-}sec}$ $\times 10^6$	$\frac{C_{AO} - C_A}{C_{AO}}$	$\mathcal{J}_A = \frac{C_{A,s}}{C_{A,b}}$	$f(\theta)_A$	$\mathcal{J}_H = \frac{C_{H,s}}{C_{H,b}}$	$f(\theta)_H$
685.5	6.70	312.5	36.95	0.667	0.958	.119	0.947	.148
	13.40	311.8	41.71	0.330	0.977	.066	0.0940	.169
	20.10	311.6	43.54	0.00	0.984	.046	0.931	.177

Allyl Alcohol in Ethanol (Run No. 506 A)

$C_{AO} = 20.10 \times 10^{-5}$ mol/ml

$V_l = 217.2$ ml

$w = 15.2 \times 10^{-3}$ g

$t = 25°C$

P_H mm Hg	$C_{A,b}$ $\frac{mol}{ml}$ $\times 10^5$	$C_{H,b}$ $\frac{mol}{ml}$ $\times 10^8$	r $\frac{mol}{g\text{-}sec}$	$\frac{C_{AO} - C_A}{C_{AO}}$	$\mathcal{J}_A = \frac{C_{A,s}}{C_{A,b}}$	$f(\theta)_A$	$\mathcal{J}_H = \frac{C_{H,s}}{C_{H,b}}$	$f(\theta)_H$
677.1	0.1370	301.8	18.25	0.9932	-.0001	∞	.973	.074
	0.0746	306.2	9.92	0.9963	-.0002	∞	.986	.039
	0.0612	307.2	8.40	0.9969	-.0320	∞	.988	.037
	0.0357	309.0	4.75	0.9982	-.0004	∞	.993	.018
	0.0149	310.5	1.98	0.9992	-.0008	∞	.997	.003

Allyl Alcohol in Ethanol (Run No. 511)

$C_{AO} = 20.10 \times 10^{-5}$ mol/ml

$V_l = 219.3$ ml

$w = 10.0 \times 10^{-3}$ g

$t = 25°C$

P_H mm Hg	$C_{A,b}$ $\frac{mol}{ml}$ $\times 10^5$	$C_{H,b}$ $\frac{mol}{ml}$ $\times 10^8$	r $\frac{mol}{g\text{-}sec}$ $\times 10^6$	$\frac{C_{AO} - C_A}{C_{AO}}$	$\mathcal{J}_A = \frac{C_{A,s}}{C_{A,b}}$	$f(\theta)_A$	$\mathcal{J}_H = \frac{C_{H,s}}{C_{H,b}}$	$f(\theta)_H$
678.3	0.954	300.4	33.23	0.9525	0.738	0.98	0.951	.138
	0.585	300.4	33.23	0.9708	0.573	2.07	0.951	.138
	0.425	302.7	26.64	0.9788	0.529	2.47	0.961	.108
	0.326	304.7	20.98	0.9838	0.516	2.60	0.969	.084
	0.271	305.8	17.99	0.9865	0.501	2.75	0.974	.072
	0.147	308.9	9.12	0.9925	0.534	2.43	0.987	.035
	0.058	310.3	5.07	0.9970	0.343	5.28	0.993	.019

APPENDIX VI

Experimental and Calculated Data for Acetone Hydrogenation

TABLE VI-1

Hydrogenation Reaction Rate Data of Acetone at 25°C

Run No.	$C_{A,b}$ $\frac{mol}{l}$	$\frac{r}{P_H} \times 10^5 \frac{mol}{(min)(g)(atm)}$	$\left(\frac{C_{A,b} P_H^{\frac{1}{2}}}{r}\right)$	$\left(\frac{C_{A,b} P_H^{\frac{1}{2}}}{r}\right)^{\frac{1}{2}}$
System: Acetone-Benzene				
1-2-E	0.06	3.85	39.5	41.6
1-3-R	3.63	15.03	155.0	166.0
1-5-R	6.41	13.12	221.0	238.7
1-7-R	9.29	12.89	268.0	291.0
1-10-R	13.89	17.42	311.0	342.3
1-11-R	2.87	12.42	152.0	162.0
1-12-R	1.47	10.10	120.6	127.0
1-13-R	5.58	13.06	207.0	222.0
1-14-R	8.33	12.67	256.0	278.0
System: Acetone-Cyclohexane				
2-1-E	0.06	9.30	25.4	26.8
2-5-R	6.73	20.15	183.0	203.9
2-6-R	7.78	14.32	233.0	260.0
2-7-R	9.51	12.51	275.0	307.6
2-8-R	11.26	14.24	281.0	313.8
2-10-R	10.59	10.68	315.0	351.0
2-11-R	12.24	13.76	298.0	333.0
2-12-R	13.89	16.69	288.0	316.0
2-14-R	2.05	17.30	108.8	119.6
2-16-R	4.92	19.11	160.0	178.3
System: Acetone-Isopropanol				
3-1-E	0.06	14.20	20.5	21.7
3-2-R	2.18	8.81	157.0	163.0
3-3-R	4.63	13.50	185.0	196.0
3-5-R	6.77	18.60	191.0	204.0

continued

Run No.	$C_{A,b}$ $\frac{mol}{l}$	$\frac{r}{P_H} \times 10^5$ $\frac{mol}{(min)(g)(atm)}$	$\left(\frac{C_{A,b} P_H}{r}\right)^{\frac{1}{2}}$	$\left(\frac{C_{A,b} P_H^{\frac{1}{2}}}{r}\right)^{\frac{1}{2}}$
System: Acetone Isopropanol				
3-6-R	8.73	18.98	214.0	231.1
3-7-R	10.11	18.78	232.0	251.4
3-8-R	11.78	19.60	245.0	267.3
3-9-R	13.89	20.37	261.1	286.9

TABLE VI-2

Data for Reaction Order with Respect to Hydrogen Pressure at 25°C

Acetone concentration = 0.015 mol/l

P_H mm Hg	$C_{H,b}$ $\frac{mol}{l}$ x 10^3	r $\frac{mol}{(sec)\ (g\text{-}cat)}$ x 10^8
System: Acetone-Benzene (Run No. 1-2-E)		
652.0	3.04	55.13
566.0	2.64	54.27
419.0	1.95	42.74
System: Acetone-Cyclohexane (Run No. 2-1-E)		
652.0	3.86	133.7
567.0	3.36	116.2
431.0	2.55	93.7
276.0	1.63	92.5
System: Acetone-Isopropanol (Run No. 3-1-E)		
746.0	3.41	220.3
623.0	3.01	194.3
422.0	2.04	157.0
299.5	1.45	130.0

TABLE VI-3

Data for Apparent Energy of Activation for Hydrogenation of Acetone

Run No.	T°K	$-\ln k$ $\frac{\text{mol}}{(\text{min})\ (\text{g-cat})\ (\text{mm Hg})^{\frac{1}{2}}}$
System: Acetone-Benzene		
1-1-E	298.15	13.843
1-3-E	300.65	13.792
1-4-E	303.15	13.692
1-5-E	307.15	13.606
System: Acetone-Cyclohexane		
2-1-E	298.15	12.661
2-2-E	300.65	12.601
2-3-E	303.15	12.524
2-4-E	307.15	12.545
System: Acetone-Isopropanol		
3-2-E	298.15	13.268
3-3-E	300.65	13.227
3-4-E	303.15	13.081
3-5-E	307.15	13.054

TABLE VI -4

Data for Effect of Hydrogen Pressure on Rate in the Linear Region at 25° C

$\left(-\frac{1}{\text{slope}}\right)^{*}$	$\frac{C_{A,b}}{r}$	$P_H^{-0.5}$
System: Acetone-Benzene (Run No. 1-1-RA)		
	V_L = 180 ml	
	w = 0.85 g	
5400	25.5	.039
6410	30.3	.047
8240	38.9	.064
System: Acetone-Cyclohexane (Run No. 2-3-RA)		
	V_L = 198 ml	
	w = 0.18 g	
5700	5.18	.039
6372	5.79	.047
8655	7.87	.060
System: Acetone-Isopropanol (Run No. 3-2-RA)		
	V_L = 207 ml	
	w = 0.75 g	
27190	98.5	.038
31129	113.0	.044

* $-\frac{1}{\text{slope}}$ is the reciprocal of slope of the line on a semi-log plot of $V^f - V$ versus t.

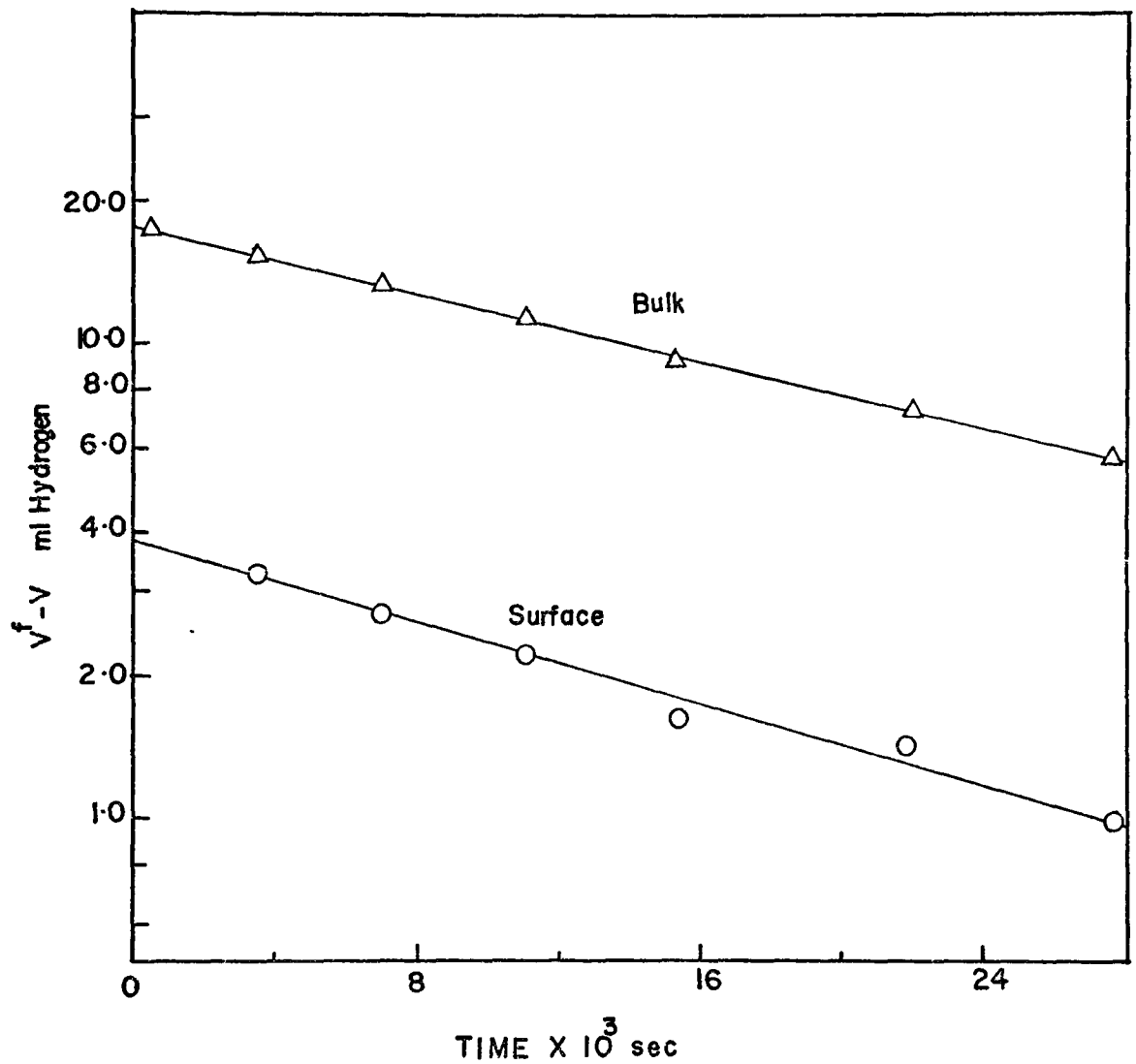

Figure VI-1 First order plot for bulk and surface concentration for acetone-benzene system at 25°C.

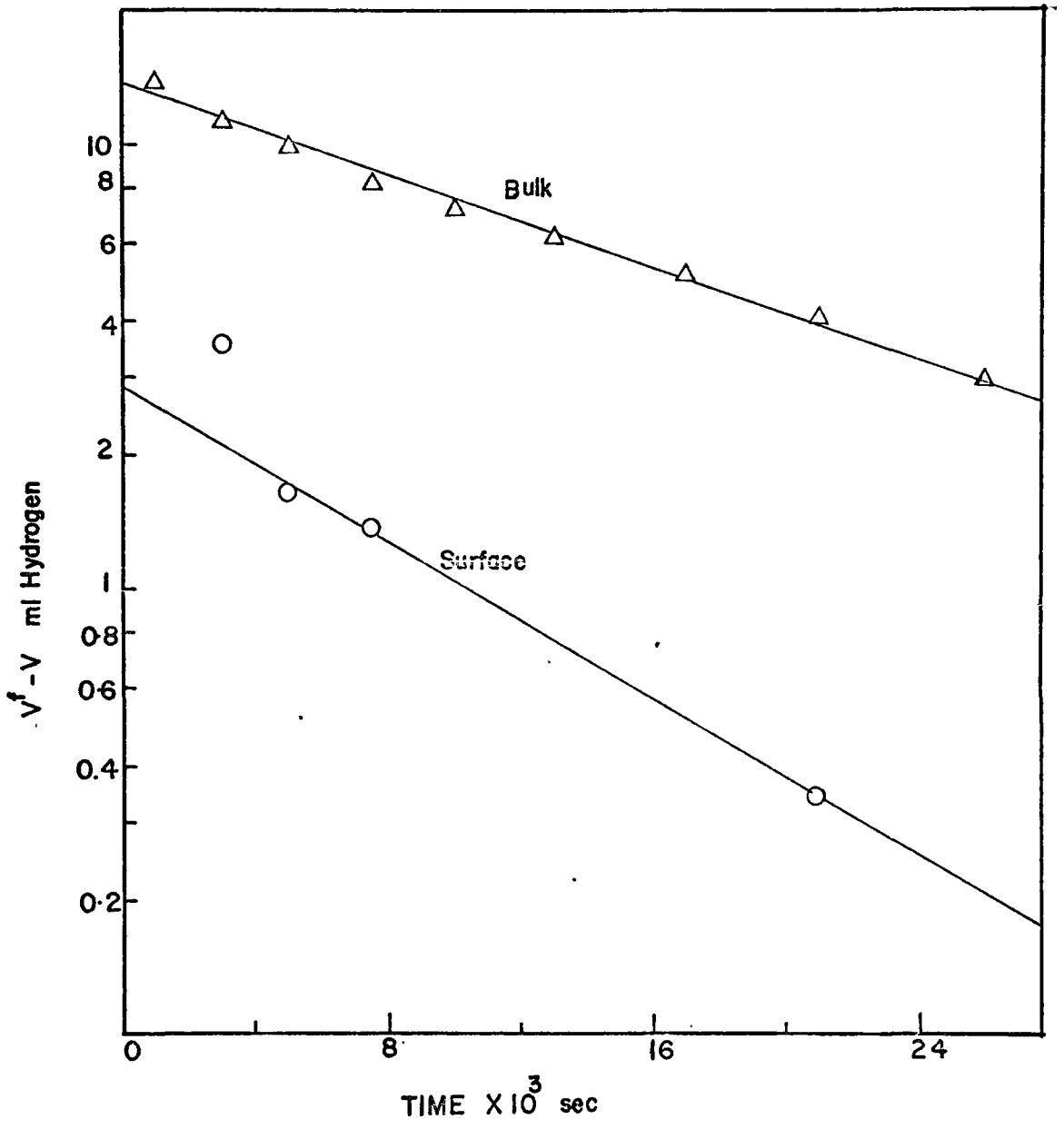

Figure VI-2 First order plot for bulk and surface concentration for acetone-cyclohexane system at 25°C.

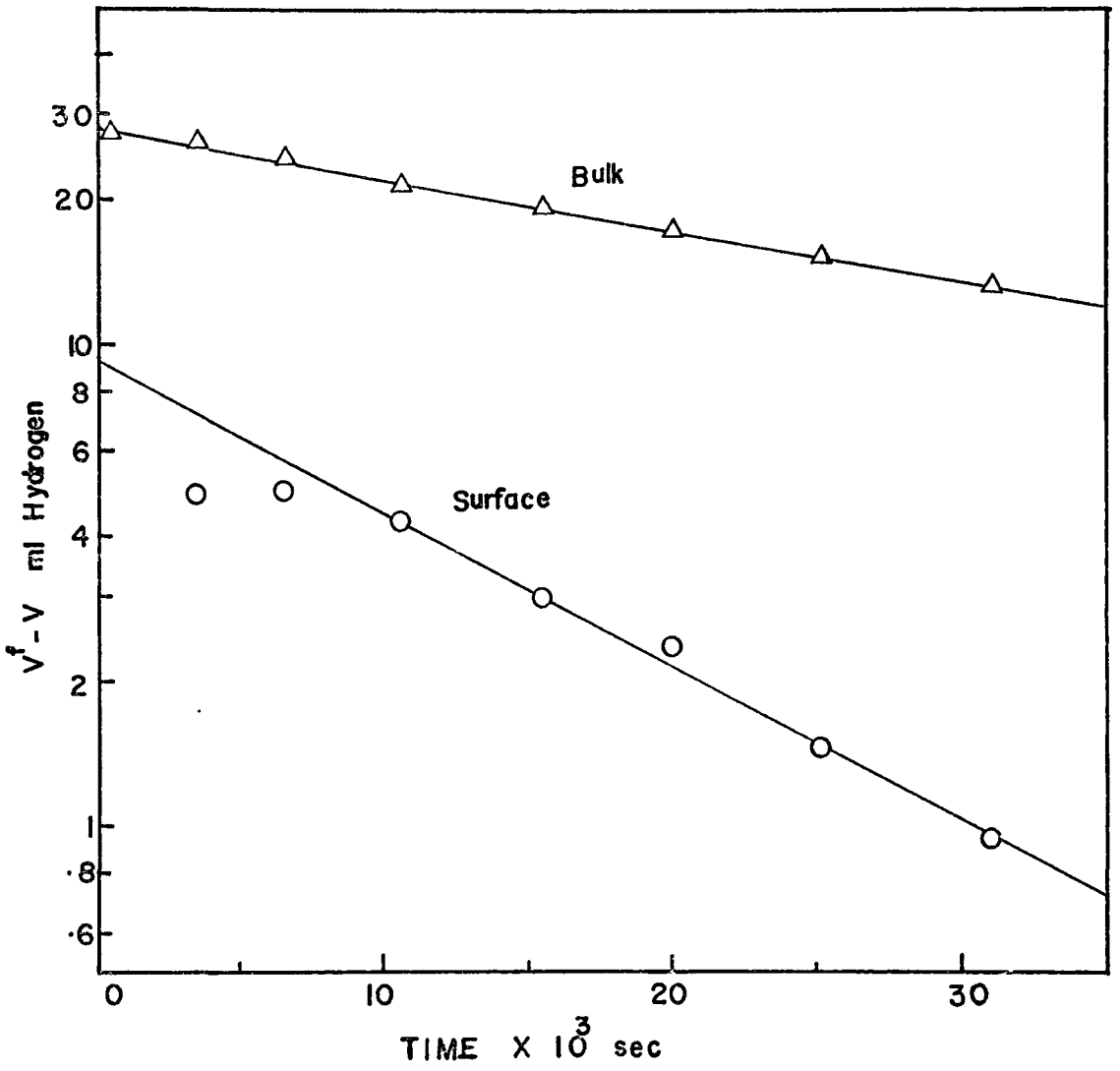

Figure VI-3 First order plot for bulk and surface concentration for acetone-isopropanol system at 25°C.

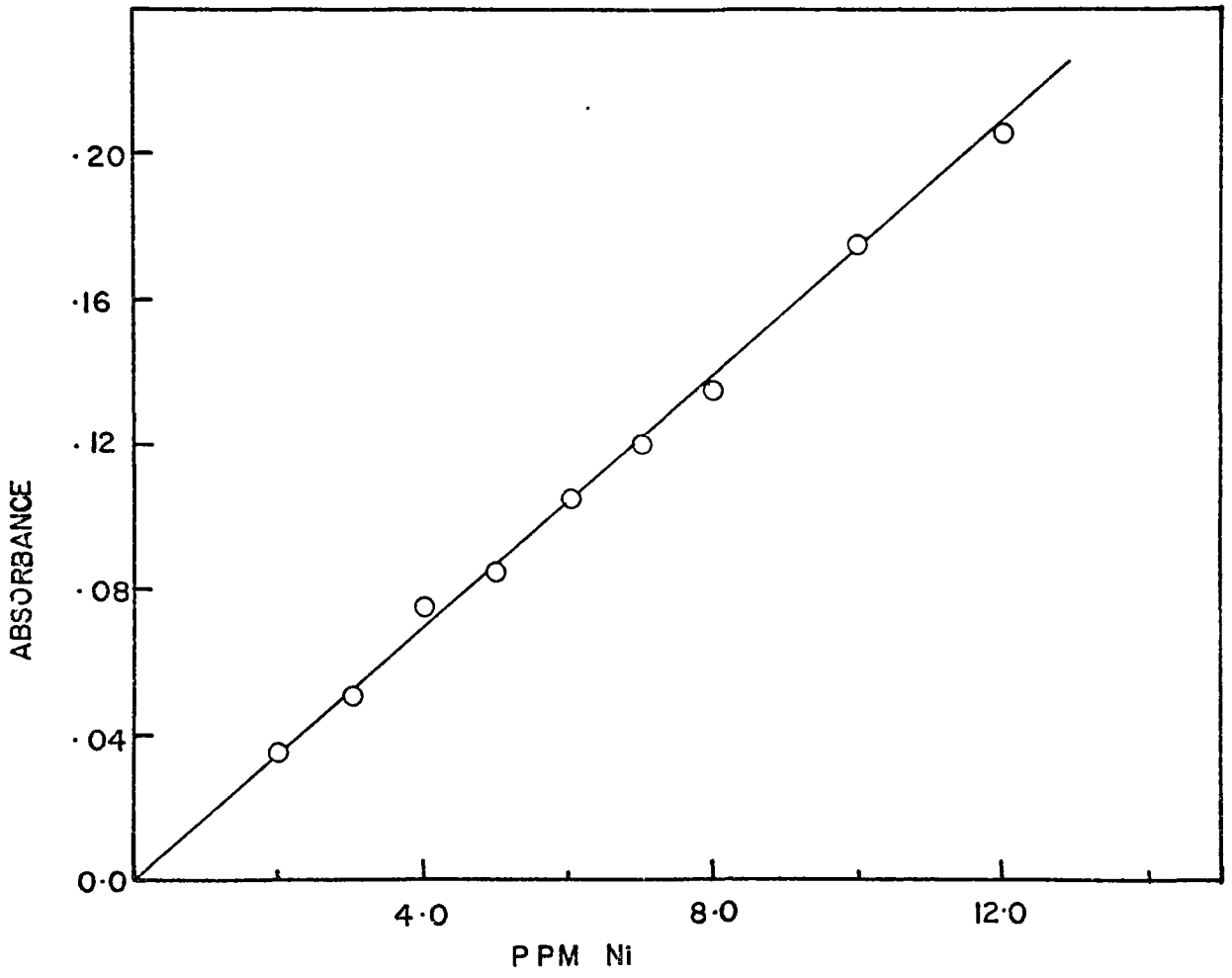

Figure VI-4 Absorbance versus nickel concentration in solution.

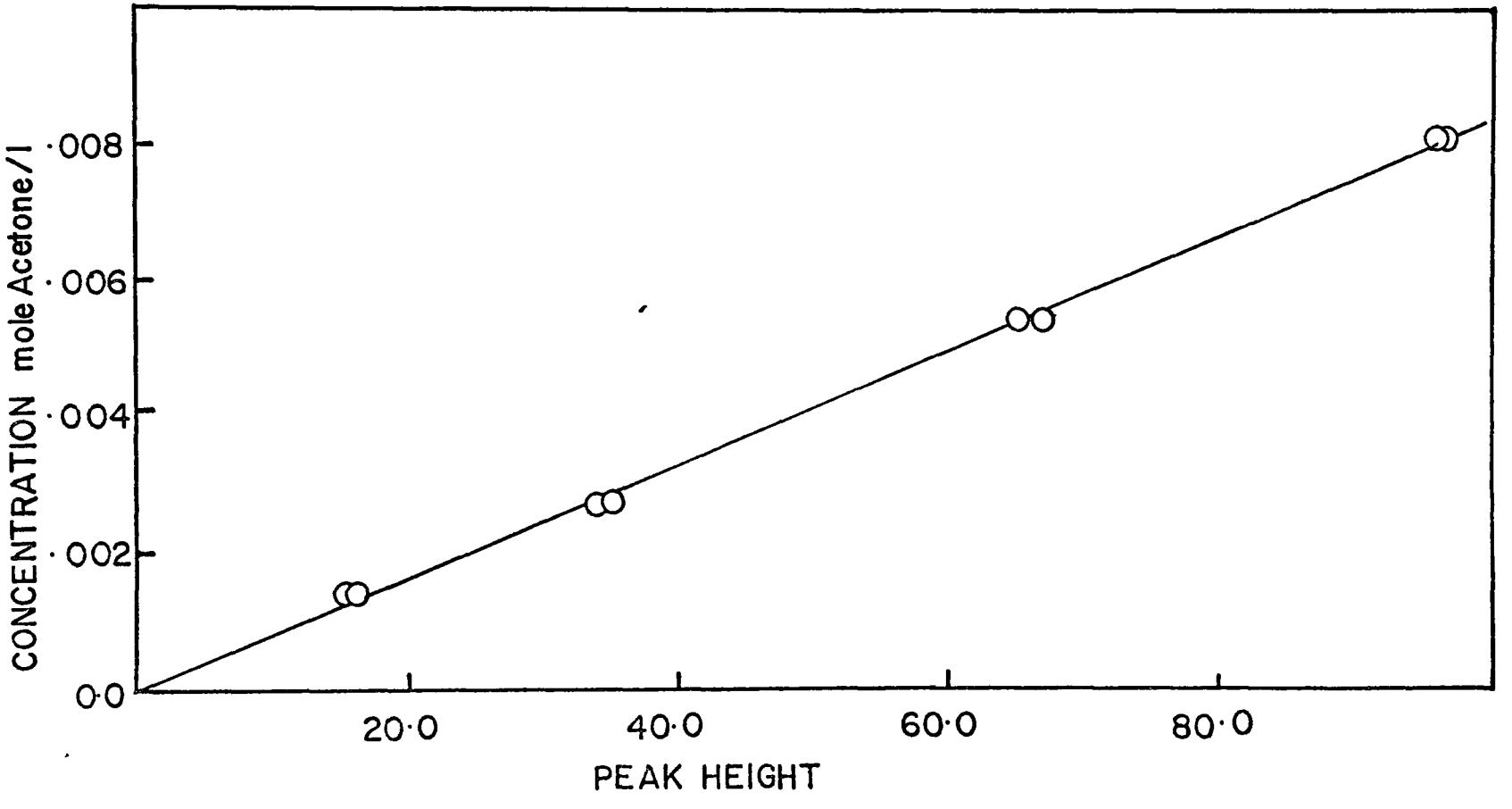

Figure VI-5 Concentration versus peak height for acetone-benzene system.. Attenuation = 64.

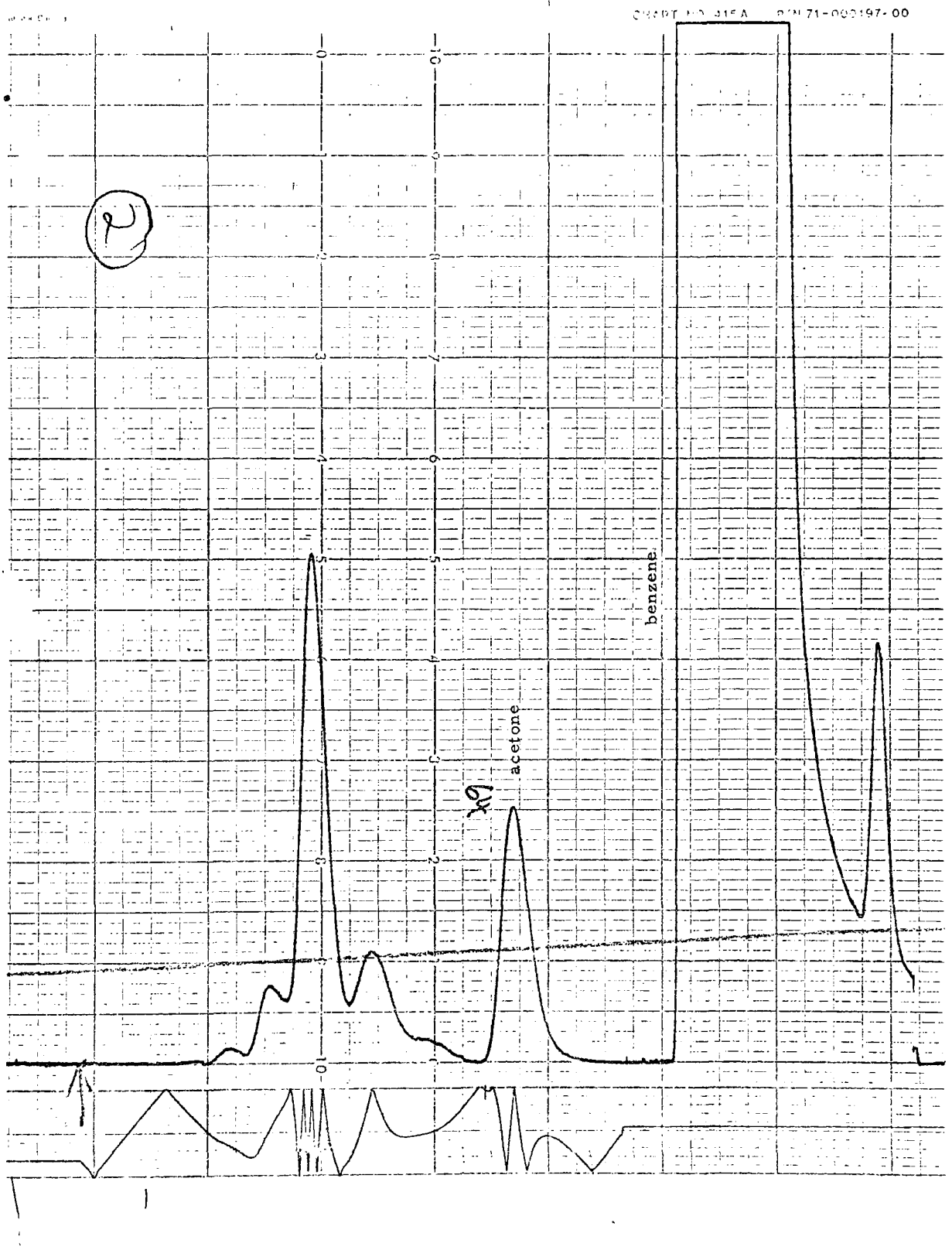

Figure VI-6 A typical acetone-benzene chromatogram. Run 1-1-SE, sample 2, concentration of acetone ≈ 2.05 x 10^{-3} mol/l.

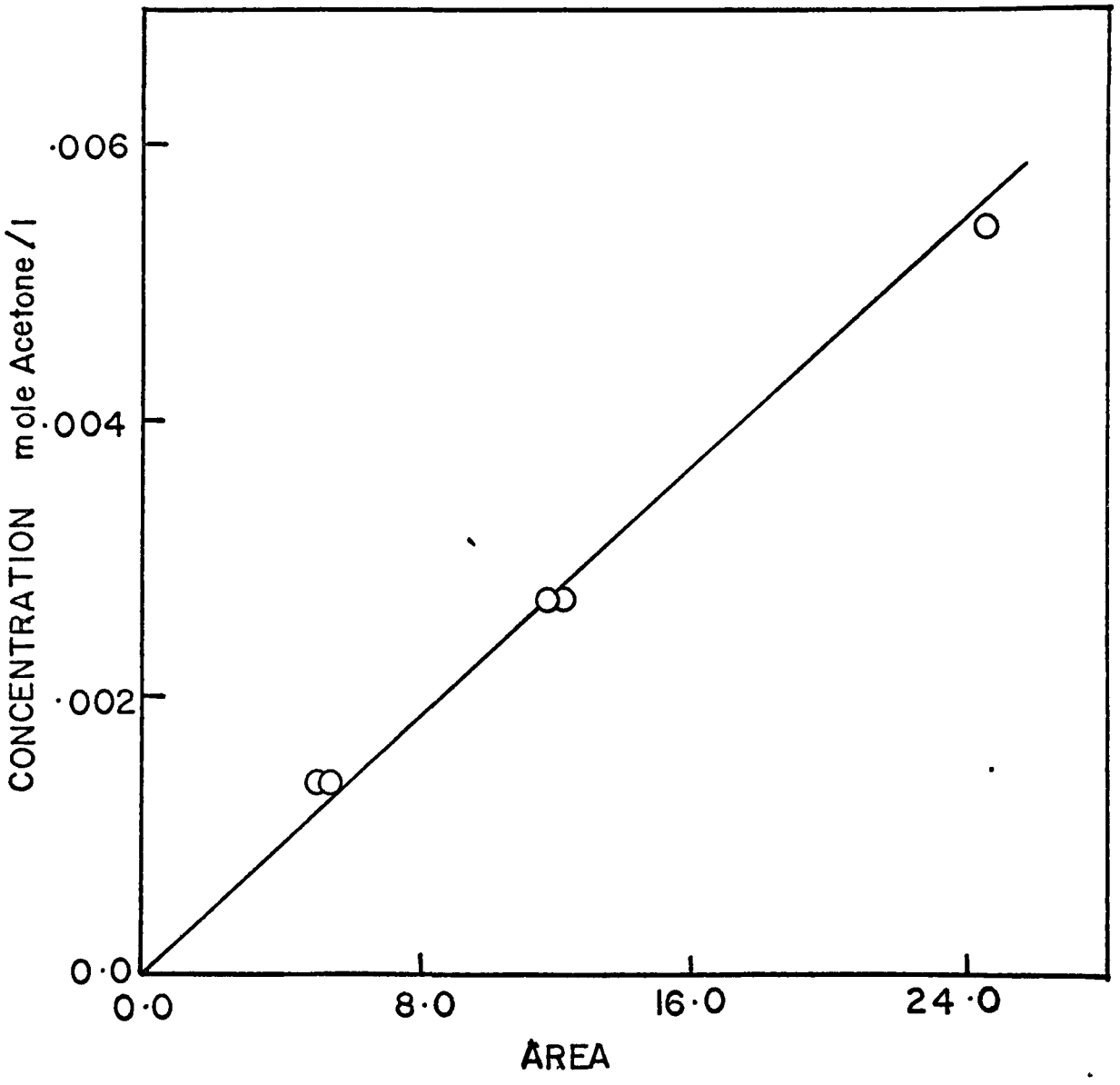

Figure VI-7 Concentration versus peak area for acetone-cyclohexane system. Attenuation = 16.

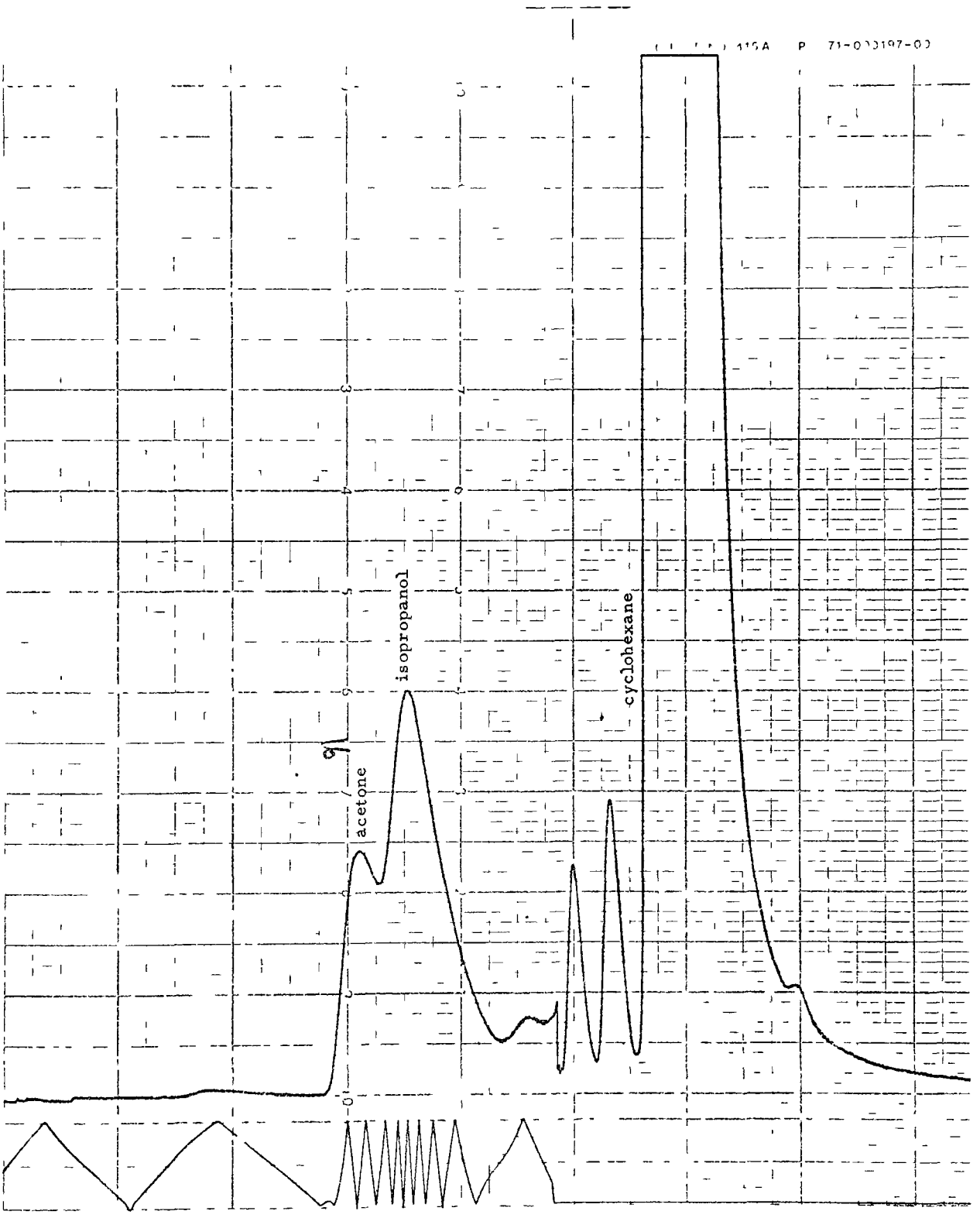

Figure VI-8 A typical acetone-cyclohexane chromatogram. Run 2-3-SE, sample 3, concentration of acetone = 1.41×10^{-3} mol/l.

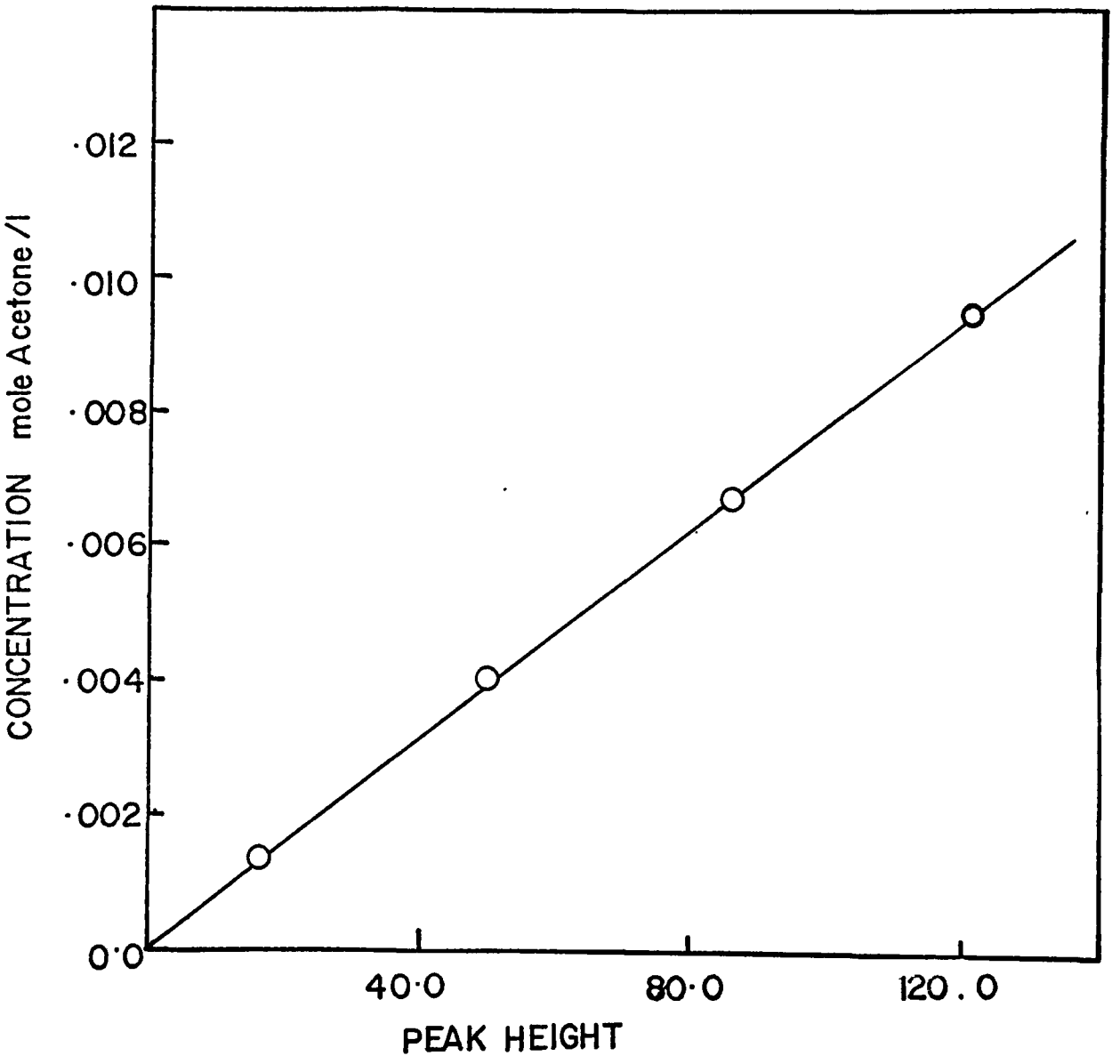

Figure VI-9 Concentration versus peak height for acetone-isopropanol system. Attenuation = 64.

Figure VI-10 A typical acetone-isopropanol chromatogram. Run 3-1-SE, sample 6, concentration of acetone = 2.90×10^{-3} mol/l.

TABLE VI-5

Surface Concentration Data in First Order Region at 25° C

Sample number	Time sec	Hydrogen reacted ml	$C_A \times 10^4$ mol/l		$C_{A,s} \times 10^4$	Volume of H_2
			Solution	Surface	mol/g.cat	Equivalent to surface conc.
System: Acetone-Benzene (Run No. 1-1-SE); P_H = 654 mm Hg						
1	500	17.59	-	-	-	-
2	3500	15.48	20.5	5.44	2.48	3.25
3	7000	13.32	17.8	4.52	2.06	2.70
4	11000	11.39	15.4	3.69	1.68	2.20
5	15400	9.38	13.0	2.72	1.24	1.62
6	21800	7.26	9.8	2.37	1.08	1.41
7	27600	5.68	8.0	1.52	0.69	0.91
8	33600	4.45	6.5	0.96	0.44	0.57
9	38000	3.79	5.6	0.75	0.34	0.45
System: Acetone-Cyclohexane (Run No. 2-3-SE); P_H = 645 mm Hg						
1	1000	13.69	-	-	-	-
2	3000	11.42	13.5	6.01	12.38	3.52
3	5000	9.90	14.1	2.81	5.79	1.64
4	7500	8.23	11.7	2.36	4.86	1.38
5	10000	7.12	12.0	0.16	0.33	0.09
6	13000	6.17	11.2	~ 0	~ 0	~ 0
7	17000	5.09	8.6	~ 0	~ 0	~ 0
8	21000	4.03	6.3	0.58	1.19	0.34
9	26000	2.74	5.5	~ 0	~ 0	~ 0
10	31000	2.12	5.3	~ 0	~ 0	~ 0
11	36000	1.36	4.2	~ 0	~ 0	~ 0

Sample number	Time sec	Hydrogen reacted ml	$C_A \times 10^4$ mol/l Solution	$C_A \times 10^4$ mol/l Surface	$C_{A,s} \times 10^4$ mol/g. cat	Volume of H_2 Equivalent to surface conc.
System: Acetone-Isopropanol (Run No. 3-1-SE); P_H = 706 mm Hg						
1	0	28.44	-	-	-	-
2	500	27.87	50.0	0.0	-	-
3	3500	26.21	38.0	8.81	3.35	4.93
4	6500	24.59	35.0	8.92	3.39	4.99
5	10000	21.82	31.2	7.77	2.96	4.35
6	15400	19.21	29.0	5.31	2.02	2.97
7	20000	17.18	26.5	4.19	1.59	2.35
8	25200	15.18	24.5	2.61	0.99	0.46
9	31000	13.26	22.0	1.68	0.64	0.94
10	42800	9.91	17.0	0.70	0.27	0.39

APPENDIX VII

Catalyst Particle Temperature Calculations

Heat and mass are transferred between solid and fluid by similar mechanisms, and data for heat transfer in fixed beds are correlated in the same way as data on mass transfer (4). For particles in stirred tanks both heat and mass transfer coefficients to particles were measured by Brian, Hales and Sherwood (24). They equated the function $j_H N_{Re}$ to $j_D N_{Re}$ by plotting $N_{Nu} N_{Pr}^{-1/3}$ and $N_{Sh} N_{Sc}^{-1/3}$ as a function of a dimensionless power dissipation factor.

For heat and mass transfer, Chilton and Colburn suggested the following relationship:

$$\frac{k_p \rho}{G} N_{Sc}^{2/3} = f(N_{Re}) \qquad (1)$$

Where G is the mass flow rate. The group on the left hand side is usually symbolized by j_D.

A similar relation can be written for the heat transfer, usually symbolized as j_H:

$$\frac{h}{Cp\ G} N_{Pr}^{2/3} = f(N_{Re}) \qquad (2)$$

where

$$h = \frac{q}{T_s - T_o} \qquad (3)$$

and

$$N_{Pr} = \frac{C_p \mu}{k} \tag{4}$$

Here h is the heat transfer coefficient, q is the heat flux per unit pellet surface area, Cp is the heat capacity per unit mass of fluid, T_s is the particle surface temperature and T_o is the fluid stream temperature.

For many geometries, jH is approximately equal to jD (4, p83). Therefore from equations (1), (2) and (4)

$$h = k_p \rho C_p \left(\frac{k}{C_p \rho D} \right)^{2/3} \tag{5}$$

To obtain the temperature of the catalyst particles in the slurry, a typical system of acetone hydrogenation in isopropanol is considered. The data for this system are:

$k_p, A a_p$ (for acetone in isopropanol as reported in table II-3)
= 16.8 $cm^3/(sec)(g)$, giving k_p = 0.01881 cm/sec.

ρ = 0.7809 g/cm^3

C_p = 0.625 cal/g-°C

k = 4.12×10^{-4} cal/(cm)(sec)(°C)

D Hydrogen in isopropanol = 7.7×10^{-5} cm^2/sec (table II-2)

The surface area of the catalyst was reported earlier to be 58.12 m^2/g.

The heat of this hydrogenation reaction is obtained from the heat of formation data obtained from Chemical Engineers Handbook (5th ed.).

Heat of formation of hydrogen = 0.0 Kcal

Heat of formation of acetone = -74.32 Kcal

Heat of formation of isopropanol = -59.32 Kcal

Therefore, heat of hydrogenation reaction is obtained as = 15.0 Kcal.

The highest temperature which a catalyst particle may attain during the reaction would correspond to the highest reaction rate encountered during this study.

The highest reaction rate was $= 6.31 \times 10^{-5}$ moles/(sec)(g cat.)

$= 5.69 \times 10^{-13}$ moles/(sec)(particle)

Heat flux $q = 5.69 \times 10^{-13} \times 15000$

$= 8.54 \times 10^{-9}$ cal/(sec)(particle)

From equation (5):

$$h = 0.01881 \times .7809 \times .625 \left(\frac{4.12 \times 10^{-4}}{0.625 \times .9809 \times 7.7 \times 10^{-5}} \right)^{2/3}$$

$= 0.0389$ cal/(sec)(cm^2)(°C)

$= 2.04 \times 10^{-4}$ cal/(sec)(particle)(°C)

From equation (3), the temperature difference between particles and solution is given by:

$$T_s - T_o = \frac{q}{h} = \frac{8.54 \times 10^{-9}}{2.04 \times 10^{-4}} = 4.2 \times 10^{-5} \text{ °C}$$

Hence the temperature difference between the catalyst particles and solution was negligible. Since the plysical properties of the various systems studied in this work were of the same order, it is assumed that the temperature difference between catalyst surface and solution was negligible in all the cases.